Cannabinoid signaling mechanisms

in the central nervous system

Wayne Anderson

B.Biomed Sci (Hons)

A Thesis submitted in fulfilment of the requirements for a

Degree of

Doctor of Philosophy

The School of Biomedical Sciences

Faculty of Health

University of Newcastle

April, 2009

Declaration of Originality

This thesis contains no material which has been accepted for the award of any other degree or diploma in any university or other tertiary institution and, to the best of my knowledge and belief, contains no material previously published or written by another person, except where due reference has been made in the text. I give consent to this copy of my thesis, when deposited in the University Library**, being made available for loan and photocopying subject to the provisions of the Copyright Act 1968.

**Unless an Embargo has been approved for a determined period.

(Signed): …….

ACKNOWLEDGEMENTS

Firstly, I would like to thank my principal supervisor Bob Callister. He has shown great patience and understanding during my scientific training and I will be forever indebted to him. Thanks Bob!

To my co-supervisor Paul Tooney I say thanks for all the years “Toons”. We have known each other quite a while now and I consider you a true friend.

Many other people have helped me throughout the years, and I would not have made it without them. Brett Graham, Alan Brichta, Melissa Walsh, Rebecca Lim, Angela Kindig, Belinda Harris, Aaron Camp, Amanda Brown, David Pow, Robert Sullivan, Susan Sullivan, Lauren Macnab, Liz Lamont and Sophie Percival just to name a few. Thanks guys!

I would also like to thank the faculty and staff of the School of Biomedical Sciences. I have interacted with each and every one of you over the years and have enjoyed it immensely. I shall miss you all.

Finally to my family and friends who have stuck by me during these long and sometimes difficult years. What can I say but I love you all, you are truly irreplaceable.

Table of Contents

ABSTRACT

A group of substances, known as cannabinoids, exist in the cannabis plant and have recently shown great promise as therapeutics for a wide range of conditions. A structurally related group of compounds known as endocannabinoids have also been found in the body. These compounds act at the same receptor as cannabis and exert their effects within defined areas of the CNS. Most notably amongst these areas is the spinal cord dorsal horn, which plays a key role in the processing of nociceptive (painful) signals.

In this thesis I examined several aspects of cannabinoid signaling that may play a role in spinal cord pain processing mechanisms. The first series of experiments asked whether the cannabinoid and serotonergic systems interact via the phenomenon of G protein-coupled receptor (GPCR) dimerization (or oligomerization). This mechanism may be important in controlling the ultimate action of ligands that bind to GPCRs. The type 1 cannabinoid receptor (CB_1) and the type 2A serotonin receptor ($5HT_{2A}$) subtypes were chosen because both are GPCRs and play roles in nociceptive processing. Each receptor was isolated from total human brain RNA, cloned, amplified in *E.* coli, and expressed in Baby Hamster Kidney (BHK) cells. Fluorescent resonance energy transfer (FRET) analysis, which measures the proximity of two fluorescent molecules according to the transfer of resonance energy from a fluorescent donor protein to an acceptor fluorophore, was used to determine whether the CB_1 and $5HT_{2A}$ receptors formed complexes with themselves and/or each other.

This series of experiments showed that the CB_1 and $5HT_{2A}$ receptors could form homo- and heterodimers, and were thus capable of interacting and indeed influencing one another's signaling pathways. The link between dimerization and cellular physiology is currently not clear, however the phenomenon is reasonably prevalent and has both basic science and applied implications. At the basic sciences level proteins that dimerize often have related functions or are involved in the same physiological processes (Woolf & Linderman, 2004). Thus, dimerization needs to be considered in future quests for discovery of novel classes of dimerization-regulating drugs.

The ultimate aim of a second set of experiments, was to examine the action of a synthetic cannabinoid (methanandamide) on the two ligand-gated ion channels (glycine and $GABA_A$ receptors) that are important for inhibitory signaling in the dorsal horn of the spinal cord. These experiments were driven by three considerations: both receptor types have been implicated in the onset and maintenance of various pain states; reports of a specific or unique type of glycine receptor (GlyR) in the superficial laminae of the spinal cord; and recent evidence for a direct (allosteric) action of cannabinoids on GlyRs in oocytes and dissociated neurons.

I first carried out an extensive characterization of fast inhibitory neurotransmission in the superficial (SDH; laminae I-II) and deep laminae (DDH: laminae IV-VI) of the mouse spinal cord dorsal horn. These two spinal cord regions have well established, although largely separate, roles in processing sensory inputs arising in skin, muscle, joints and viscera. Whole cell patch clamp electrophysiology was used to compare the properties of GlyRs and $GABA_A$Rs on SDH and DDH neurons in transverse spinal cord slices.

Several important properties of the two receptors differed in the SDH and DDH. Specifically, glycinergic mIPSC amplitude was smaller, decay time was slower, and frequency was lower in SDH versus DDH neurons. In contrast, $GABA_A$ergic mIPSCs had similar amplitudes and frequencies, but their decay times were faster in DDH neurons. These data suggest GlyR-mediated inhibition is more important in deep regions of the dorsal horn, which preferentially receives peripheral inputs from axons with high conduction velocities. The existence of large and fast inhibitory inputs in the DDH would be well suited to modulate the effect of such inputs. In contrast, smaller and slower $GABA_A$R-mediated inhibition appears to be equally important in both superficial and deep regions of the spinal cord dorsal horn. These features suggest $GABA_A$R-mediated inhibition is more important for fine-tuning the effects of a functionally wider range of peripheral inputs.

I next tested whether physiologically relevant concentrations of the endogenous cannabinoid, methanandamide (methAEA - 5 μM), had any direct effects on synaptically located GlyRs and $GABA_A$Rs. For GlyRs, methAEA reduced mIPSC frequency in the SDH and DDH but had no significant effect on mIPSC amplitude, rise time, or decay time constant. These observations are consistent with the well-documented presynaptic action of cannabanoids via CB_1 receptor-mediated mechanisms. Because methAEA had no effect on mIPSC amplitude or kinetics I conclude there is no evidence for a ***direct*** effect of methAEA on synaptically located glycine receptors in either SDH or DDH neurons. For $GABA_A$Rs, methAEA significantly reduced mIPSC frequency and slowed rise time in the SDH and DDH but had no significant effect on mIPSC amplitude, or decay time. This suggests that

methAEA may have a direct effect or modulatory action on $GABA_A$Rs, specifically their kinetics, in SDH and DDH neurons.

Because glycinergic and $GABA_A$ergic mIPSC properties differed in the SDH and DDH, I also compared the subunit expression of GlyR and $GABA_A$Rs, and the CB_1 receptor using real-time RT-PCR (qPCR) in each spinal cord region. In the SDH, the α1 subunit of the GlyR was the most highly expressed, followed by β, α2 and α3. In the DDH α1 and β were highly expressed followed by α2 and α3. The expression of both α1 and α2 GlyR genes was higher in the DDH. Comparison of $GABA_A$R subunit expression showed levels of α1 and β2 genes differed in the two regions, again with higher expression detected in the DDH. In contrast to previous reports, using immunohistochemistry, I found CB_1 receptor expression to be significantly higher in the DDH. When combined with the mIPSC data, my qPCR data are consistent with the dominance of fast GlyR-mediated inhibition in the DDH. Finally, my qPCR data provide no support for a higher concentration of CB_1Rs existing in the pain processing (lamina I-II) regions of the spinal cord.

CHAPTER 1

General Introduction

General Introduction

The cannabis plant (*Cannabis sativa*) is one of the earliest crops cultivated by man (*Figure 1.1*), with the Chinese using its fibre and pulp for strings, ropes, textiles and paper since 4,000 B.C. (Li, 1974). Around the first century B.C., the world's oldest pharmacopeia, the *pen ts'ao ching*, reported the use of cannabis as a medicine (Hou, 1977). This ancient text also documents the first use of cannabis as a psychoactive drug.

Figure 1.1 - Cannabis Sativa. *The cannabis plant has been used for centuries by numerous cultures and societies for it's practical and medicinal properties.*

In India, around 1,000 B.C., cannabis was used widely as both a medicine and recreational drug and was closely aligned with religious beliefs in the region. In fact, sacred virtues were bestowed upon the plant as evidenced in a collection of sacred texts known as the *Atharva Veda*. Many medicinal actions were assigned to cannabis, including those of an analgesic, anticonvulsive, anaesthetic, hypnotic, tranquilizer, anti-inflammatory, appetite stimulant and expectorant (Mikuriya & Aldrich, 1988).

The use of cannabis continued to grow in India, the Middle East and Africa until the 18th century A.D. It was introduced to the Western world during the 19th century by William O'Shaughnessy, an Irish physician, and Jacques-Joseph Moreau, a French psychiatrist (Frankhauser, 2002). The work of these two men continued to contribute to our knowledge of the therapeutic and psychoactive effects of cannabis during the 19th century, when over 100 scientific articles were published on its medicinal value (Grinspoon, 1999). The popularity of cannabis as a medicine peaked in the late 19th to early 20th century with the marketing of cannabis extracts by drug companies including Merck, Wellcome and Eli-Lilly (Mikuriya & Aldrich, 1988). The popularity of cannabis waned during the early to mid 20th century because of the advent of vaccines and other drugs like aspirin, injectable morphine and barbiturates. These new drugs directly rivalled the indications for which cannabis was prescribed, particularly its analgesic properties. Another reason for the decline in cannabis use as a medicine was due to the variable efficacy of preparations made from the cannabis plant (Zuardi, 2006).

The scientific/medical interest in cannabis increased once again after the main active ingredient in cannabis, delta-9-Tetrahydrocannabinol (Δ^9-THC), was isolated in 1964 by Gaoni and Mechoulam (Gaoni & Mechoulam, 1964). Later, its chemical structure was

determined and Δ^9-THC was synthesized by the same researchers (Mechoulam & Gaoni, 1965). The interest in Δ^9-THC chemistry peaked during the 1970's, then steadily declined until the early 1990's when the first cannabinoid receptor was cloned in the rat nervous system by Matsuda (Matsuda *et al.*, 1990). Further work showed that the receptor for Δ^9-THC was a G protein-coupled receptor (GPCR) and that the receptor was widely distributed in the mammalian brain and spinal cord (Devane *et al.*, 1988; Herkenham *et al.*, 1991; Tsou *et al.*, 1998). Not long after the isolation of the receptor in the nervous system, an endogenous ligand was discovered. This endogenous compound was called anandamide, after the Sanskrit word for 'bliss' (Devane *et al.*, 1992). This discovery was closely followed by isolation and cloning of a second cannabinoid receptor in macrophages (Munro *et al.*, 1993). These discoveries opened up exciting possibilities for research on the biology and effects of the body's own natural cannabinoids or 'endocannabinoids'.

Cannabinoid research is now enjoying a 'golden age' in both basic science and clinical medicine, because cannabinoids are known to have powerful effects on nervous system function. Cannabinoid research encompasses research fields as diverse as emesis, glaucoma, epilepsy and analgesia. Despite these potentially beneficial research directions, cannabis use has also been linked to cognitive deficits (Pope *et al.*, 2003), and mental illnesses such as psychosis (Arseneault *et al.*, 2004) and schizophrenia (Andreasson *et al.*, 1987, 1988; Bersani *et al.*, 2002; Krebs *et al.*, 2005). These issues are important to consider when espousing the use of cannabinoids as therapeutics.

The Cannabinoids

The term cannabinoid was originally used to describe a number of compounds found in the cannabis plant. This term has now been extended to include the endogenous cannabinoids (or 'endocannabinoids'), as well as a number of synthetic compounds. The main criteria for classifying a compound as a cannabinoid, is that it activates a membrane-bound cannabinoid receptor. The two best-characterized cannabinoid receptors are both G-protein-coupled receptors (GPCRs) and are termed CB_1 and CB_2. There is also recent evidence for a third cannabinoid receptor known as GPR55, which has signaling properties distinct from the CB_1 and CB_2 receptors (Begg *et al.*, 2005; Lauckner *et al.*, 2008).

'Endocannabinoids' (*Figure 1.2*) are synthesized, released and degraded by the body and include compounds such as arachidonoylethanolamine (anandamide; AEA) (Devane *et al.*, 1992), 2-arachidonylglycerol (2-AG) (Mechoulam *et al.*, 1995; Sugiura *et al.*, 1995), palmitoylethanolamide (PEA) (Facci *et al.*, 1995), Virodhamine (Porter *et al.*, 2002), Noladin (Fezza *et al.*, 2002) and *N*-arachidonoyldopamine (NADA) (Bisogno *et al.*, 2000). Some synthetic cannabinoids have also been made in recent years and include WIN-55,212-2, HU-210, Nabilone and CP-55,940.

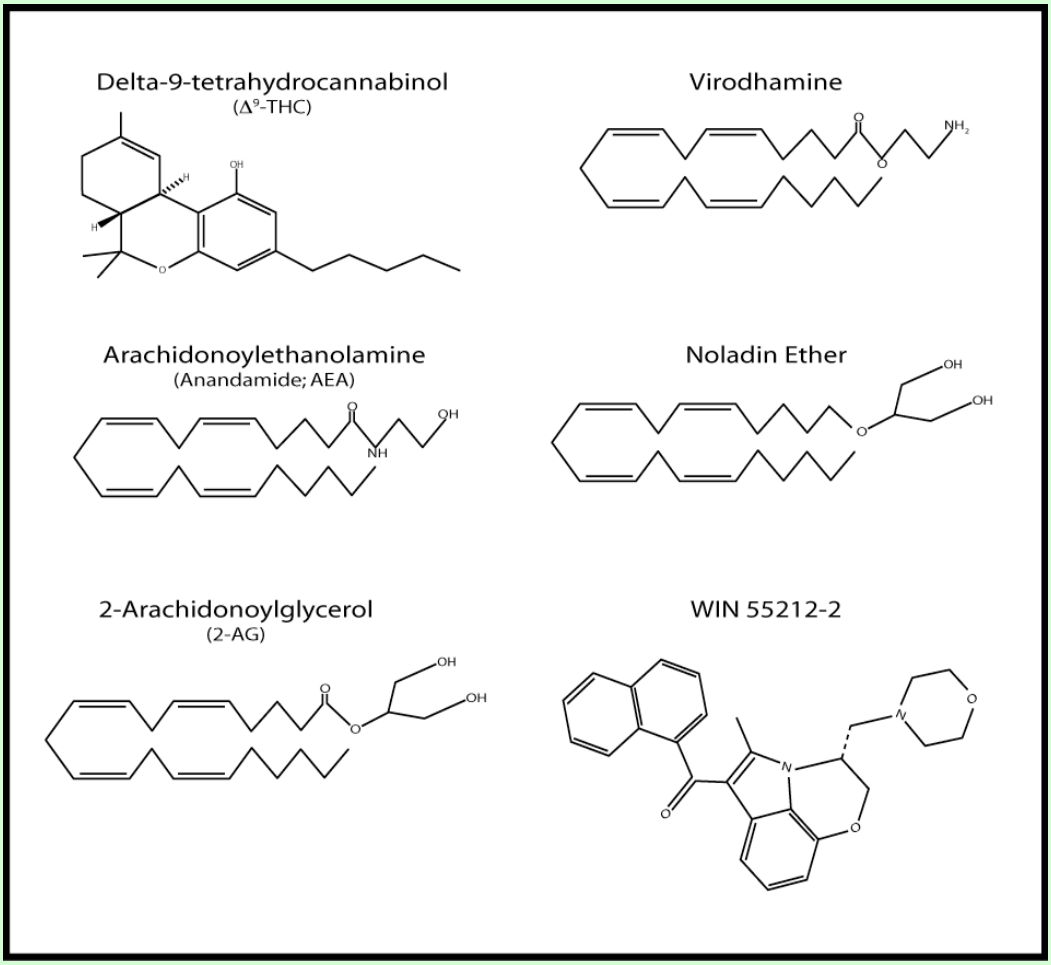

Figure 1.2 - Cannabinoid receptor agonists. *(Top Left), Δ^9-tetrahydrocannabinol (THC) the major biologically active compound in the cannabis plant (Cannabis sativa), and the two best characterized endocannabinoids, (Middle Left) AEA and (Bottom Left) 2-AG. (Right) two less commonly studied endocannabinoids. (Top) Virodhamine and (Middle) Noladin Ether are both CB_1/CB_2 agonists, whereas WIN-55,212-2 (Bottom) is a synthetic agonist at the same receptors.*

Endocannabinoid Biosynthesis

Anandamide Biosynthesis

The two best known and characterized endocannabinoids to date are anandamide (AEA) and 2-AG. The biosynthesis of anandamide begins with the enzyme *N*-acyltransferase (NAT). This enzyme catalyzes the transfer of arachidonic acid from phosphotidylcholine to the head group of phosphotidylethanolamine and results in the production of *N*-arachidonoylphosphatidyl-ethanolamine (NAPE). NAPE is a phospholipid precursor which results in the production of anandamide after cleavage by a newly discovered and specific phospholipase D (PLD) (Okamoto *et al.*, 2004). NAT requires calcium and is also regulated by cAMP via protein kinase A (PKA) (*Figure 1.3*) (Cadas *et al.*, 1996; Piomelli, 2003). It is generally accepted that an increase in intracellular calcium levels in nerve cells is required for the synthesis and release of anandamide. The original hypothesis proposed that influx of extracellular Ca^{2+} was responsible for these events, but more recent evidence implicates the release of calcium from intracellular stores as the most likely mechanism (Isokawa & Alger, 2005; Straiker & Mackie, 2005; Isokawa & Alger, 2006).

Although anandamide can diffuse passively into and out of cells, the process is greatly accelerated in both neurons and glia, by the presence of a rapid and selective carrier system (Beltramo *et al.*, 1997; Hillard & Campbell, 1997). Most researchers agree that cannabinoids require the assistance of the molecularly elusive anandamide membrane transporter (AMT) (or endocannabinoid membrane transporter; EMT) for both release and re-uptake (Beltramo *et al.*, 1997; Bisogno *et al.*, 1997; Hillard & Campbell, 1997; Ligresti *et al.*, 2004). It appears that this system involves facilitated diffusion (a passive form of transport across biological membranes via specialized proteins), because AEA

transport occurs in both directions, and intracellular accumulation of AEA depends upon its concentration gradient across the cellular membrane (Hillard *et al.*, 1997).

Termination of Endocannabinoid Signaling

To be effective, any physiological signaling mechanism must be capable of rapidly and effectively terminating its actions, using mechanisms such as enzymatic degradation or re-uptake. In the case of anandamide and 2-AG, these processes occur via distinct pathways. Long before anandamide was discovered, Schmid *et al*. (1985) (Schmid *et al.*, 1985) identified a membrane-associated enzyme that broke down fatty acid ethanolamides. It is now known that this enzyme was fatty acid amide hydrolase (FAAH). This enzyme is widely distributed throughout the body, with high concentrations in brain and liver. After the completion of its signaling actions, anandamide is thought to be transported into cells by its membrane transporter, and then rapidly broken down into arachidonic acid and ethanolamine by FAAH (Schmid *et al.*, 1985; Hillard *et al.*, 1995; Cravatt *et al.*, 1996) (*Figure 1.3*).

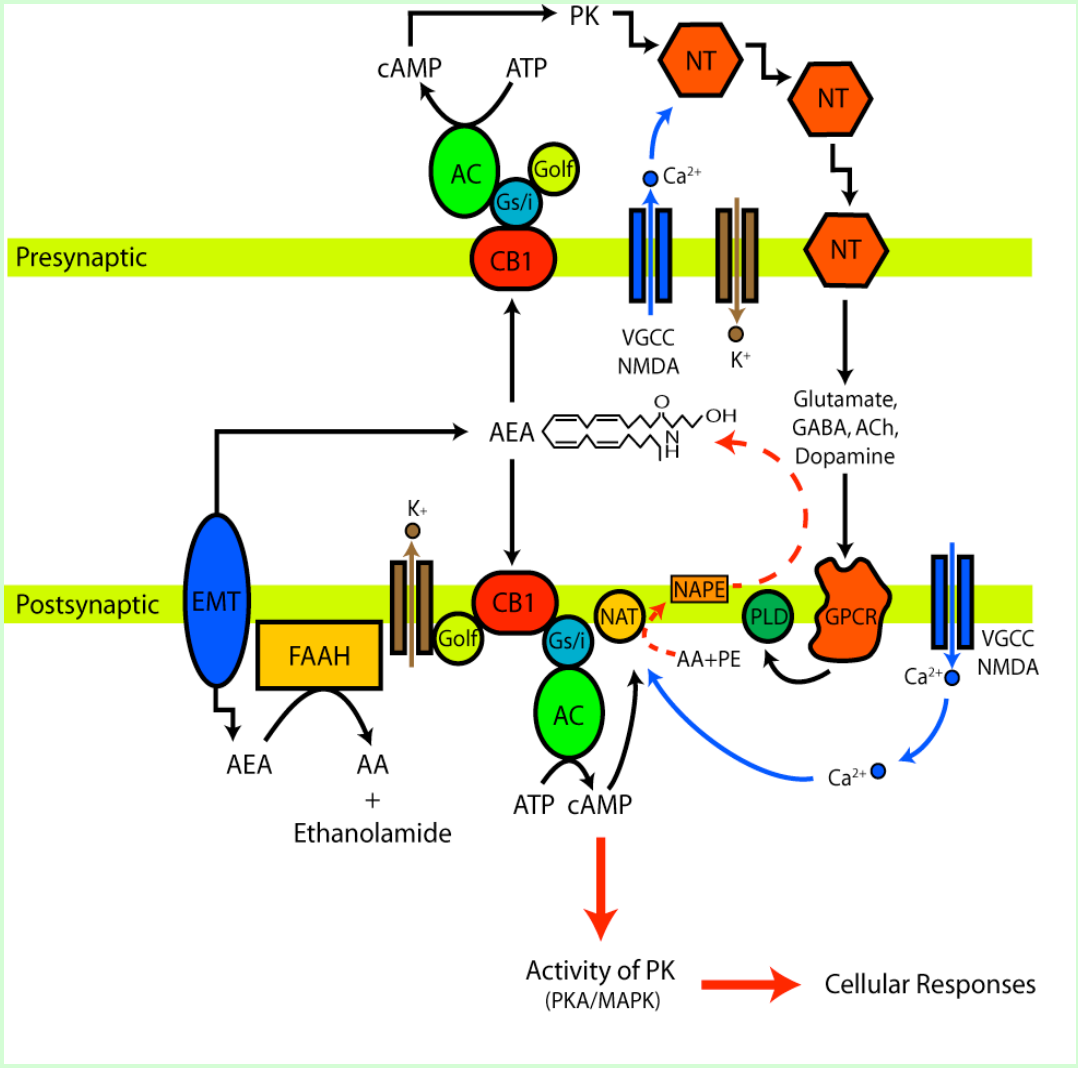

(Adapted from de Fonseca, 2005)

Figure 1.3 - Overview of the biochemical pathways for synthesis, degradation and cellular actions of the endogenous cannabinoid anandamide in the nervous system. *N-arachidonoyl-phosphatidylethanolamine (NAPE), a phospholipid precursor consisting of arachidonic acid (AA) and phosphatidylethanolamine (PE), is biosynthesized by a membrane bound enzyme, N-acyltransferase (NAT), after activation by calcium (Ca^{2+}) and cAMP. Anandamide is then released from NAPE by the action of a specific phospholipase D (PLD) which itself is activated by depolarization or G-protein-coupled receptor (GPCR) stimulation in neurons. Once released, anandamide acts as a retrograde messenger at presynaptic cannabinoid receptors (CB_1), where it regulates neurotransmitter release (NT) through its second messenger transduction systems, consisting mainly of Ca^{2+} incorporation through voltage-gated calcium channels (VGCC) or glutamate NMDA (N-methyl-D-aspartate) receptors. Anandamide also acts as a neuromodulator of major transmitter systems, including dopamine, at postsynaptic cells, where it regulates excitability and synaptic plasticity through its modulation of potassium (K^+) channels, and the regulation of a broad spectrum of protein kinases (PK) including protein kinase A (PKA) and mitogen-activated protein kinases (MAPK). Anandamide action is terminated via a two-step process, which includes firstly, its cellular uptake through an as yet molecularly characterized specific endocannabinoid transporter (EMT) and secondly, degradation by enzymatic cleavage to arachidonic acid (AA) and ethanolamide by the membrane-bound enzyme fatty acid amide hydrolase (FAAH).*

Cannabinoid Mechanism of Action

Most of the central and peripheral effects of cannabinoids are mediated through two cell membrane bound receptors termed CB_1 and CB_2, respectively. Both receptors belong to the superfamily of GPCRs. The characteristic feature of all known GPCRs is their seven α-helical transmembrane-spanning domains (Foord *et al.*, 2005). Following activation by their ligand, a conformational change takes place causing the intracellular loops to associate with a nearby membrane-bound heterotrimeric G protein complex containing α, β and γ subunits (Maudsley *et al.*, 2005) (*Figure 1.4*). Once activated, the subunits dissociate into α and β/γ entities, both of which can interact with various second messenger systems and effector molecules such as enzymes, ion channels and proteins (Gilman, 1987).

Once activated by cannabinoid ligands, both types of cannabinoid receptors utilize a similar transduction pathway. Briefly, the cannabinoid receptors associate with $G\alpha_{i/o}$ and β/γ and subsequently decrease the catalytic activity of adenylate cyclase, cAMP and PKA-mediated phosphorylation events (Devane *et al.*, 1988; Howlett *et al.*, 1990).

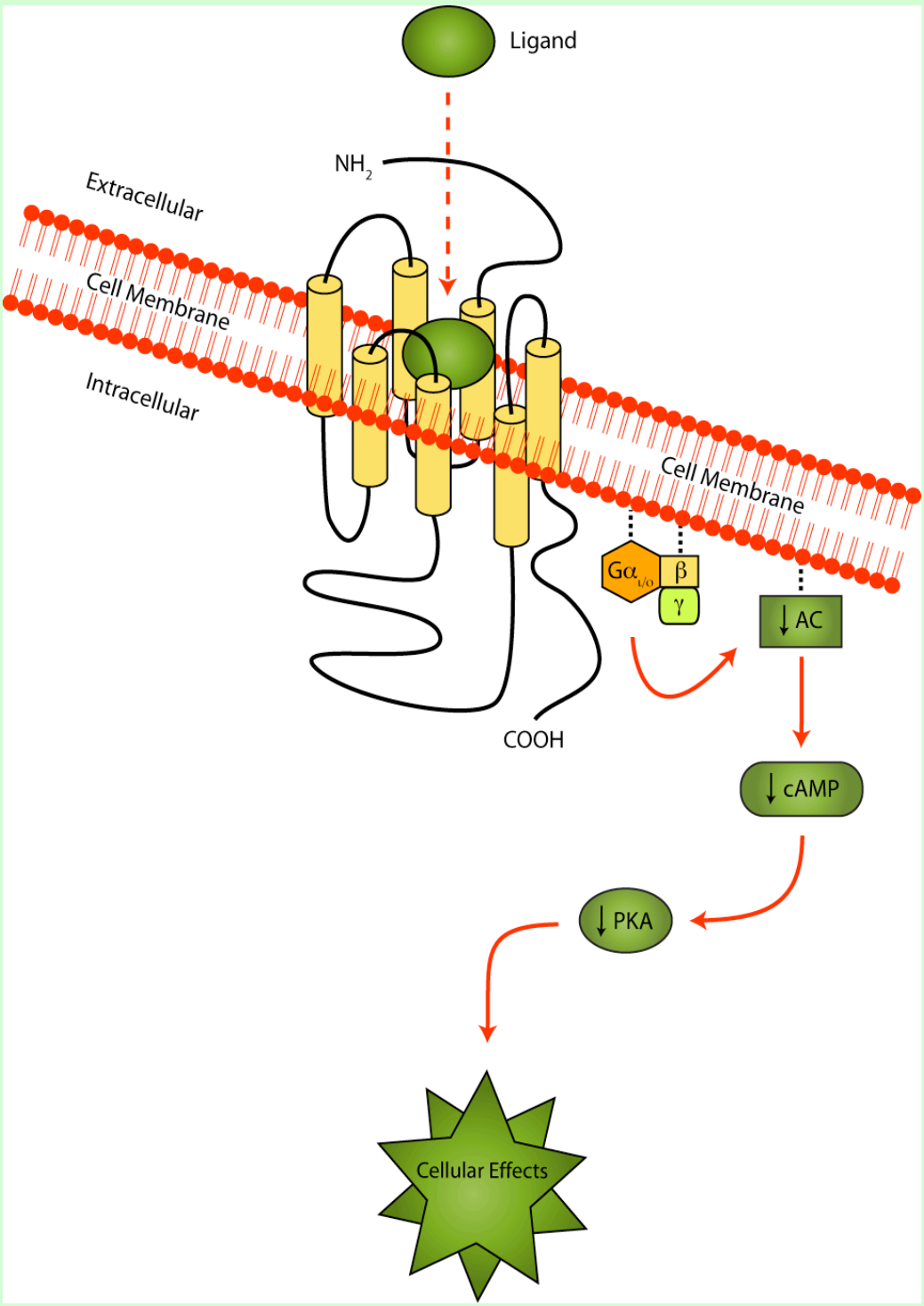

Figure 1.4 - GPCR signaling pathway. *Following activation by a ligand, the heptahelical-structured GPCR is able to associate with excitatory or inhibitory trimeric G protein complexes (Gα/β/γ) and thus drive cell signaling events. In the case of the CB_1 GPCR, association with Gαi/o leads to a decrease in the catalytic activity of adenylate cyclase (AC) and therefore cAMP, leading to a reduction in PKA-mediated phosphorylation and altered cell function.*

A number of groups have shown that cannabinoid receptors are negatively coupled to ion channels through the Golf protein (*Figure 1.3*). This inhibits N-, P/Q-, L- and R-type Ca^{2+} channels, and activation of inwardly rectifying potassium (K^+) channels (Mackie & Hille, 1992; Mackie *et al.*, 1995; Childers & Deadwyler, 1996; Twitchell *et al.*, 1997; Gebremedhin *et al.*, 1999; Brown *et al.*, 2003). The CB_1 receptor also activates second messengers in the MAPK pathway such as IP_3, focal adhesion kinase and nitric oxide. The overall effect of these events, with some exceptions (Felder *et al.*, 1998), is one of cellular inhibition.

It is noteworthy, that the CB_1 receptor exhibits the greatest density of any GPCR in the mammalian brain and spinal cord (Herkenham *et al.*, 1990; Herkenham *et al.*, 1991; Ong & Mackie, 1999b), and is highly conserved across species. For example, CB_1 receptors in human, rat and mouse, share 97-99% sequence homology (McPartland & Glass, 2003), suggesting they play similar roles in these species. This supports the notion that mouse and rat models are excellent experimental candidates for cannabinoid receptor research. Indeed, when coupled with evidence from other vertebrates and invertebrates, it strongly supports an important role for endocannabinoid signaling throughout the entire animal kingdom.

A somewhat surprising observation is that endocannabinoids have vastly different binding affinities and activity at the different cannabinoid receptors. For example, anandamide is a partial agonist at both CB_1 and CB_2 receptors but has a higher affinity for the CB_1 receptor (Hillard *et al.*, 1999; Howlett, 2002). The intrinsic activity of anandamide, however, is 4-30 times greater at the CB_1 receptor than at the CB_2 receptor. 2-AG on the other hand, is a complete agonist at both the CB_1 and CB_2

receptors. It is possible given the above situation, that anandamide may actually function as an antagonist or inverse agonist in certain situations, thus adding to its pharmacological promiscuity.

Cannabinoid receptor distribution in the nervous system

The CB_1 Receptor

In 1991, Herkenham *et al.* (1991) conducted a landmark study of CB_1 receptor localization in the brain. A synthetic radioactive cannabinoid, [^{3}H]CP55,940, was used to visualize the distribution of CB_1 receptors in brain sections of rat, guinea pig, dog, rhesus monkey, and humans. Using autoradiography, the results showed a unique and conserved distribution across species with binding being most dense in the neocortex, basal ganglia, hippocampus and cerebellum. Together, these findings suggested a role for cannabinoids in cognition, memory, and movement. Herkenham also suggested that sparse CB_1 receptor distribution in the lower brainstem region, which contains the important cardiovascular and respiratory centres, may explain why high doses of cannabinoids like Δ^9-THC are not lethal.

In contrast to Herkenham *et al*., Ong & Mackie (1999a) used immunohistochemistry to determine the distribution and subcellular localization of the CB_1 receptor in the primate brain. They also noted high levels of the receptor in rat cortex, hippocampus, cerebellum and amygdala, but also found some significant differences to previous studies (Herkenham *et al.*, 1991; Tsou *et al.*, 1998). For example, few CB_1 positive cells were found in some regions of the basal ganglia complex (globus pallidus or substantia nigra pars reticulata).

Cannabinoid receptor localization in the spinal cord

As noted above, it is important to determine the distribution of cannabinoid receptors within the nervous system before any physiological actions can be ascribed to them. In relation to nociception (activation of peripheral receptors that can signal pain), it is imperative that cannabinoid receptors and/or their ligands be located in relevant pain pathways and regions before analgesic actions can be considered to have arisen from their actions on the nervous system. It is well known that the spinal cord dorsal horn represents a region in the important ascending pain pathway where incoming nociceptive (potentially painful) signals can be modified. It is also known that there are large numbers of CB_1 receptors in this region (Farquhar-Smith *et al*., 2000), suggesting a role for the endocannabinoid system in nociception.

The CB_2 Receptor

The CB_2 receptor was originally cloned by Munro *et al.* (1993) from macrophages in the spleen. Unlike the CB_1 receptor it was not detectable in the CNS. Following this initial characterization, Galiegue *et al.* (1995), using reverse transcription polymerase chain reaction (RT-PCR), reported that the level of CB_2 expression in the periphery was of similar magnitude to CB_1 expression levels in the CNS. This study also showed that among human blood cells, the distribution pattern of CB_2 mRNA displayed important variations. The rank order of CB_2 mRNA was B-cells > natural killer cells > monocytes > polymorphonuclear neutrophil cells > T8 cells > T4 cells. Together, these findings suggest that cannabinoids may also be important in immune function, via the CB_2 receptor.

Other studies have confirmed a mostly peripheral distribution of CB_2 receptors. The current dogma is that CB_2 receptors are absent from the CNS, although the localization and distribution of CB_2 receptors in the CNS has not been investigated as thoroughly as the CB_1 receptor. Until recently, a number of laboratories had been unable to detect CB_2 receptors in brain (Derocq *et al.*, 1995; Galiegue *et al.*, 1995; Griffin *et al.*, 1999; Carlisle *et al.*, 2002). Recently however, CB_2 receptors have been detected in rat microglial cells (Carrier *et al.*, 2004) and in the rat retina (Lu *et al.*, 2000). In fact these recent studies have raised some intriguing possibilities for the CB_2 receptor in nervous system function (Gong *et al.*, 2006; Onaivi *et al.*, 2006). For example, although their levels in the CNS are less than that of CB_1 receptors, some regions within the rat brain, such as neuronal and glial processes, hippocampal pyramidal cells and cerebellar Purkinje cells do exhibit significant density of CB_2 receptors. Even though the presence of CB_2 receptors has been established in the CNS, the cell types and subcellular localization remain to be determined. Gong *et al*. (2006) suggests that given the evidence above, a rethink on the role of CB_2 receptors in nervous system function may be needed.

GPCR Oligomerization

As mentioned previously, the known cannabinoid receptors are GPCRs with seven α-helical transmembrane-spanning domains linked by three intra- and three extra-cellular loops. In the classic model of GPCR function, when a ligand binds to a single (monomeric) GPCR on the extra-cellular side, a conformational change takes place causing the intra-cellular loops to associate in a stoichiometric ratio of 1:1 with a heterotrimeric G protein complex and activate second messenger cascades (Gether & Kobilka, 1998) (*Figure 1.4*).

Recently, this classic model of GPCR functioning has been challenged as being overly simplistic and a new field of research based on GPCR dimerization or oligomerization has emerged. This concept postulates that two or more similar or dissimilar GPCRs can couple together to form a unique signaling complex. Indeed, it has been shown that if two different GPCRs dimerize, their individual signaling properties are altered. In particular, dimerization can effect intrinsic GPCR properties such as trafficking (Couve *et al.*, 1998), second messenger systems (White *et al.*, 1998; Kuner *et al.*, 1999), internalization (Jordan & Devi, 1999) and transactivation (Pfeiffer *et al.*, 2002).

One point of contention in this field is whether dimerization is generally a constitutive process (the normal state), and as such, cannot be influenced at a point distant from intracellular organelles (e.g. endoplasmic reticulum - ER), or whether receptor activation at the plasma membrane level by a ligand is necessary for the formation or destruction of GPCR complexes. Difficulties in understanding these processes have been brought about by the diverse range of techniques used to address this question and subsequent interpretations.

In an attempt to answer some of these questions, in Chapter two I carry out a series of dimerization experiments to determine whether the cannabinoid CB_1 receptor is capable of forming complexes with itself, and/or other members of the GPCR superfamily.

Effects of cannabinoids not mediated by CB_1 & CB_2 receptors

Neuronal

Even though the majority of cannabinoid signaling events are thought to be mediated via CB_1 and CB_2 receptors, several studies have shown the existence of cannabinoid receptor-independent signaling. These include effects on the vanilloid TRPV1 receptors (Zygmunt *et al.*, 1999; Malinowska *et al.*, 2001), potassium (K^+) channels (Poling *et al.*, 1996; Maingret *et al.*, 2001) and T-type calcium channels (Chemin *et al.*, 2001). These observations have led some to propose a new cannabinoid receptor known as GPR55 (or tentatively as the CB_3 receptor) (Di Marzo *et al.*, 2000; Breivogel *et al.*, 2001).

Studies using the CB_1-receptor knockout mouse ($CB_1^{-/-}$) support the existence of another G protein-coupled cannabinoid receptor in the brain (Breivogel *et al.*, 2001). The results were based on the method whereby receptor activation of G-proteins can be measured using agonist-stimulated binding of the non-hydrolyzable GTP analogue, [^{35}S]guanosine-5'-*O*-(3-thiotriphosphate) ([^{35}S]GTPαS) to membranes (Breivogel *et al.*, 1997). Breivogel *et al*. showed that anandamide and WIN-55,212-2 had activity in $CB_1^{-/-}$ mouse brain membranes via a common G protein-coupled receptor which is only found in the CNS. Furthermore, this novel receptor was shown to be pharmacologically distinct from CB_1 or CB_2 because it could be stimulated by WIN-55,212-2 and anandamide, but not by the synthetic cannabinoids, CP55,940 and HU210, or by the phytocannabinoid, Δ^9-THC, and was only weakly antagonized by a cannabinoid antagonist (SR141716A). A very surprising finding in the above experiments was that compounds derived from cannabis did not activate this receptor.

Other studies using $CB_1^{-/-}$ mice (Hajos *et al.*, 2001; Rouach & Nicoll, 2003) showed the presence of similar non-CB_1/CB_2-mediated signaling mechanism in the hippocampus, while others have reported this mechanism in the amygdala (Pistis *et al.*, 2004). Moreover, Welch *et al.* (1998) and Houser *et al.* (2000) conducted studies assessing the analgesic efficacy of Δ^9-THC in the mouse spinal cord and found that there were differences in the ability of the cannabinoid antagonist, SR141716A, to attenuate analgesia produced by either Δ^9-THC, anandamide, or the synthetic cannabinoid, CP55,940. The authors concluded, either anandamide acted differently than the classic cannabinoids at the CB_1 receptor, or that subtypes of cannabinoid receptors existed.

TRPV1-mediated Anandamide Signaling

The vanilloid receptor (TRPV1; formally known as VR1) is a non-selective ligand-gated ion channel belonging to the transient receptor potential (TRP) superfamily (Lam *et al.*, 2005). The classic agonist for the TRPV1 receptor is capsaicin, the major vanilloid component in chilli peppers. TRPV1 is located mainly on C-fibre terminals and more sparingly on those of Aδ fibres. Depolarization of the nerve terminal causes sodium and calcium influx leading to generation of an action potential, and increased pain perception (Lam *et al.*, 2005).

Anandamide has been suggested as an endogenous ligand for the TRPV1 receptor channel due to its structural similarity to capsaicin. Furthermore, vasodilation caused by AEA acting within the classic “axon reflex” pathway, was found to be sensitive to the TRPV1 antagonist capsazepine and not to the CB_1 antagonist SR141716A (Zygmunt *et al.*, 1999). It has also been shown that AEA activates TRPV1 in recombinant and endogenous systems, which strengthens the case for it having an ‘endovanilloid’ role

(Di Marzo *et al.*, 2002). In support of these findings, Lam *et al.* (2005), conducted a series of experiments to determine the effect of both exo- and endocannabinoids on the TRPV1 receptor ion channel. They found that capsaicin activated TRPV1, Δ^9-THC activated CB_1, and AEA activated both receptors. They concluded that both CB_1 and TRPV1 might be metabotropic and ionotropic members of a unique family of endocannabinoid receptors.

Allosterism and the Cannabinoids

Another putative method by which cannabinoids may activate signaling systems independent of CB_1/CB_2 receptors, is by allosteric interactions with ion channels or GPCRs. Allosterism literally means a change in the activity and conformation of a protein by binding of a compound at a site other than its 'normal ligand' binding site. This phenomenon has been suggested to occur between cannabinoids and several members of the cys-loop ligand gated ion channel (LGIC) family. Specifically, the serotonin $5HT_{3A}$ (Fan, 1995; Barann *et al.*, 2002) and glycine receptor (GlyR) (Lozovaya *et al.*, 2005; Hejazi *et al.*, 2006). Importantly, both of these receptor systems play a role in the control of emesis and pain (Yaksh, 1989; Karim *et al.*, 1996; Simpson *et al.*, 2000; Voog *et al.*, 2000; Tramer *et al.*, 2001; Harvey *et al.*, 2004; Zeilhofer, 2005).

Cannabinoid regulation of serotonin-activated ion channels ($5HT_{3A}$)

From studies employing electrophysiology on outside-out patches of recombinant $5HT_{3A}$ receptors in Human Embryonic Kidney (HEK) 293 cells, Barann *et al.* (2002) showed that cannabinoids can inhibit 5HT induced currents independently of CB_1 receptors. They suggested that the $5HT_{3A}$ receptor may contain a motif that recognizes

both cannabinoid agonists and antagonists, but with much greater preference for phyto- and endocannabinoids (Δ^9-THC and anandamide) versus synthetic cannabinoids. Furthermore, due to the high affinity of anandamide for a modulatory site on the $5HT_{3A}$ receptor, they suggest that tonic activation of the receptor by endocannabinoids may play an important physiological role in mediating the effects of serotonin ion channels in emesis and pain and thus may represent a new drug target.

Cannabinoid regulation of glycine-activated chloride ion channels (GlyR)

The glycine receptor is an integral lipid membrane protein that when activated by glycine, opens a selective chloride ion (Cl^-) pore and allows passive diffusion of Cl^- across the membrane (Legendre, 2001; Lynch, 2004). It is intimately involved in fast inhibitory synaptic transmission in both the brain stem and spinal cord. This ligand-gated ion channel belongs to the cys-loop LGIC superfamily, and has a pentameric structure consisting of 2 α and 3 β subunits (Grudzinska *et al.*, 2005). To date, four α-subunits (α_{1-4}) and one β-subunit (β_1) have been identified. The α subunits contain the glycine binding site, and the β-subunit is responsible for anchoring GlyRs at subsynaptic locations via the cytoskeletal protein gephyrin (Lynch, 2004) (*Figure 1.5*). There is also good evidence that the β subunit participates in glycine binding in α/β heteromeric receptors (Grudzinska *et al.*, 2005).

Functional glycine receptors may consist of α homomers or α/β heteromers. In the spinal cord, regional diversity exists amongst α-subunits with immunohistochemical methods showing that α_1 is predominately found in the dorsal and ventral horn, whilst α_3 is only found in the outer layers of the dorsal horn where nociceptive fibres terminate (Harvey *et al.*, 2004). This recent finding of a unique GlyR subtype in a region of the

spinal cord known to be important for pain processing has generated great excitement regarding the development of new pain therapies. In the rat, a developmental switch from α_2 homomers to α_1/β heteromers takes place around postnatal day 14 (Becker *et al.*, 1992; Singer *et al.*, 1998). Evidence also exists for functional glycine receptors in the retina, spinal cord motor reflex pathways, spinal cord pain sensory pathways and brainstem nuclei (Lynch, 2004).

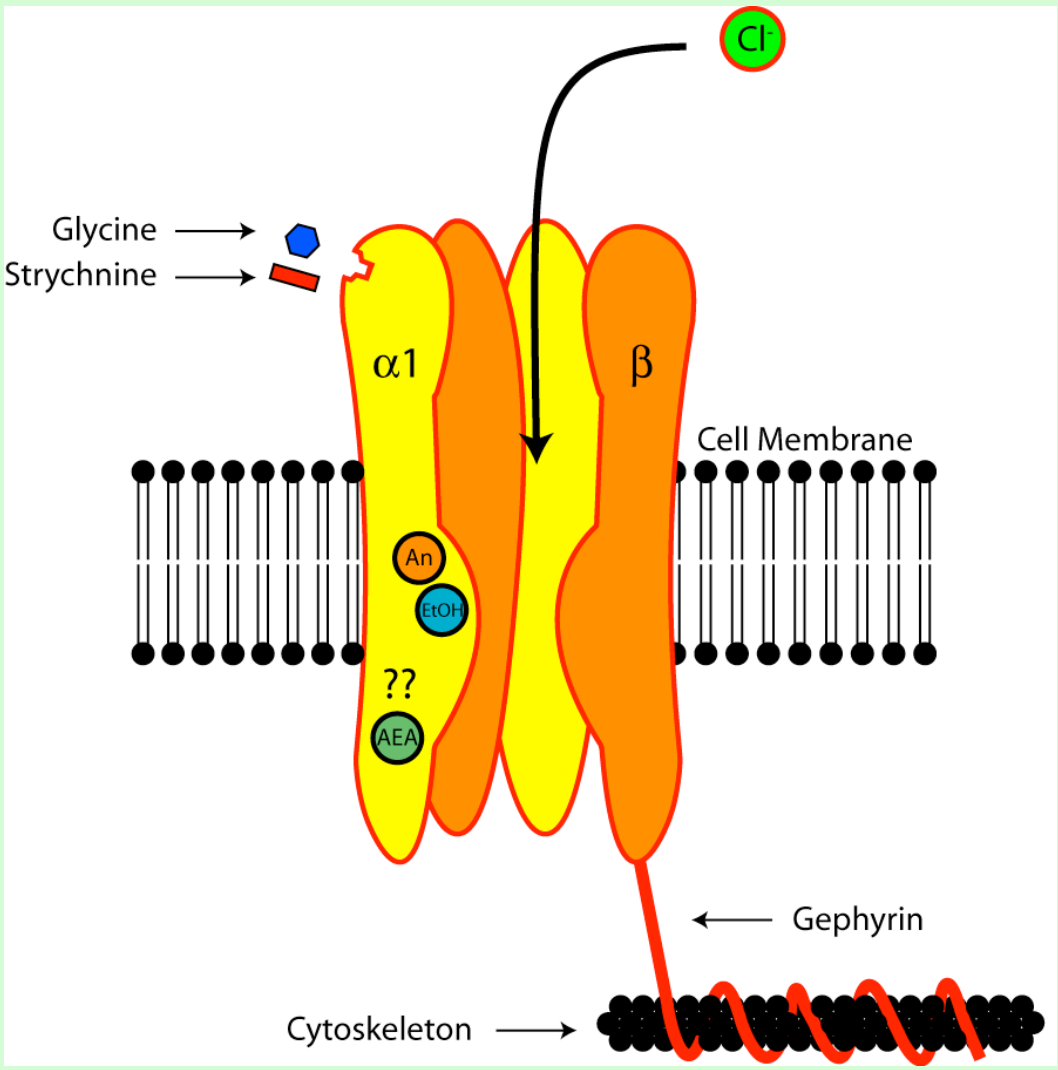

Figure 1.5 - The glycine receptor *is a chloride ion selective ion channel with a pentameric structure composed of various combinations of α (α_{1-4}) and β (β_1) subunits. The receptor is anchored under synapses via the association of gephyrin with the β subunit and cytoskeletal proteins. Strychnine acts as an antagonist at these receptors. The most dominant form of the GlyR in the adult nervous system contains 2 α and 3 β subunits. A new form containing α3 subunits has recently been localized to the outer layers of the spinal cord dorsal horn. There are also binding sites for anaesthetics (An) and ethanol (EtOH).*

Reports have implicated cannabinoids (at physiologically relevant concentrations) in the regulation of GlyR signaling. Two of the most recent investigations using electrophysiological techniques suggest that cannabinoids can allosterically modulate GlyRs, however, they differ on the proposed nature of this interaction. Lozavaya *et al.* (2005) studied the effects of the endocannabinoids, AEA and 2-AG, on the functioning of glycine receptor channels in ***dissociated*** hippocampal and cerebellar neurons. They showed that these cannabinoids ***attenuated*** the amplitude and altered the kinetics of the glycine-activated current (I_{Gly}) in a concentration-dependent manner (*Figure 1.6A-B*).

In contrast to the study above, Hejazi *et al*. (2006) investigated the effects of Δ^9-THC and AEA on the properties of GlyRs in isolated ventral tegmental area (VTA) neurons and in *Xenopis laevis* oocytes expressing both homo- (α_1) and heteromeric ($\alpha_1\beta$) forms of the GlyR. Again, they provided evidence of an allosteric interaction between the exo- and endocannabinoids and GlyRs. In this case however, it was one of ***potentiation*** rather than attenuation (*Figure 1.6C-D*). Importantly, both studies suggest that cannabinoids act ***directly*** on GlyRs and alter levels of inhibition and consequently impact on biological functions such as analgesia, drug addiction and memory. Both studies, however, have some limitations when it comes to physiological relevance especially in relation to pain, as 1) the experiments were undertaken on non-native GlyRs; and 2) the recordings were made in regions of the nervous system not overly involved in pain perception.

In Chapter three of this thesis, I test the hypothesis that cannabinoids can allosterically modulate the strychnine-sensitive glycine receptor in the mouse spinal cord.

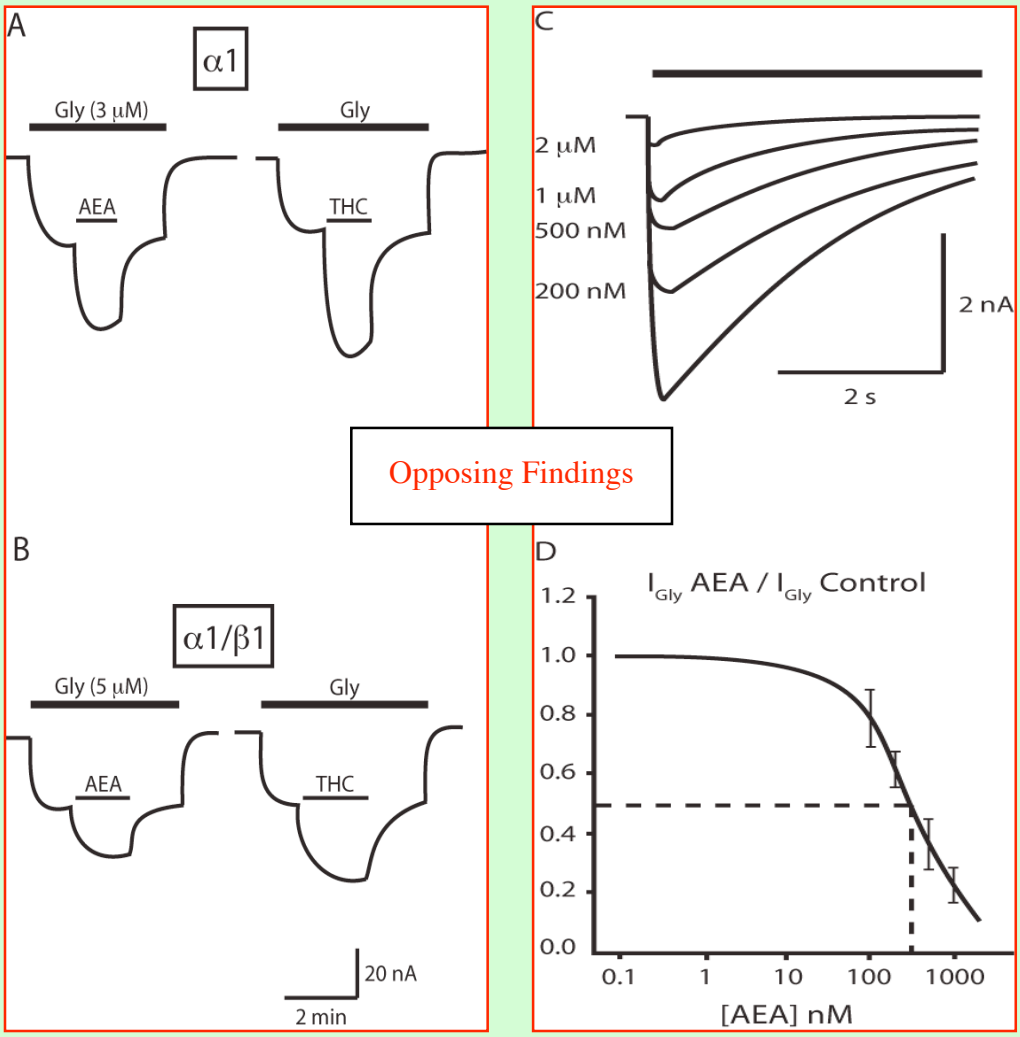

Hejazi et al. 2006 ***Lozovaya et al. 2005***

Figure 1.6 - Modulation of glycinergic currents by endogenous cannabinoids. *Traces showing THC (300 nM) and AEA (300 nM) enhancement of steady-state currents activated by glycine in oocytes expressing the α1 subunit (A) and in oocytes expressing the α1/β1 subunits (B). (C). Representative traces showing the inhibitory effect of various concentrations of AEA on glycinergic-mediated currents (200 nM to 2 μM). (D). Summary plot showing the inhibitory effect of increasing concentrations of AEA on the amplitude of glycine-induced currents.*

Clinical implications of cannabinoid biology

Schizophrenia

Schizophrenia is a chronic and severe mental disorder with individuals having a 1% lifetime risk of developing the disease. Symptoms normally present during adolescence or early adulthood. The disease is normally associated with a number of positive and negative symptoms. Positive symptoms include hallucinations and delusions, whereas negative symptoms include withdrawal, loss of motivation, ambivalence and poverty of speech (First & Pincus, 2002). A number of encouraging treatments have been developed using typical and atypical antipsychotics or neuroleptics, but a satisfactory treatment and etiology of schizophrenia remains frustratingly elusive.

Numerous hypotheses have been put forward to explain the etiology of schizophrenia. Among them is the "dopamine hypothesis" which postulates that an overproduction of dopamine in the mesolimbic pathway (i.e. from the ventral tegmentum in the midbrain to the nucleus accumbens in the limbic system) leads to the positive symptoms (such as delusions and hallucinations) associated with schizophrenia, whereas problems with dopamine function in the mesocortical pathway (i.e. from the ventral tegmentum to the neocortex) leads to the negative symptoms (such as loss of motivation) associated with this disease (Snyder, 1976). Another hypothesis implicates a dysfunction in NMDA receptor signaling, possibly due to low glycine levels, for both positive and negative symptoms (Olney & Farber, 1995). Currently, the best accepted hypothesis is the neurodevelopmental hypothesis first proposed in 1987 (Murray & Lewis, 1987). According to this hypothesis, cannabinoids are thought to be one of the pharmacological mediators in the precipitation of schizophrenia.

A great deal of work has been completed on the link between the localization and expression of CB_1 receptors and schizophrenia. Glass *et al.* (1997) showed high levels of CB_1 receptors in brain areas associated with schizophrenia such as the prefrontal cortex, basal ganglia and hippocampus. Further, it has been shown that there is an increase in CB_1 expression levels in the dorsolateral prefrontal cortex in post-mortem tissue from patients with schizophrenia who have never abused cannabis (Dean *et al.*, 2001). Indeed, in support of these observations, Zavitsanou *et al.* (2004) showed a 64% increase in binding of the CB_1 receptor antagonist, [^{3}H]SR141716A, in the anterior cingulate cortex (ACC), an intrinsic part of the brain that also receives inputs from nociceptive pathways (Apkarian et *al*., 2005; Tracey *et al*., 2000). They suggest that changes in the endogenous cannabinoid system in the ACC may be involved in the pathology of schizophrenia particularly in relation to negative symptoms.

Many psychological studies espouse the notion of cannabis as an instigator of psychosis and a precipitator of schizophrenia. Andreasson *et al.* (1987) showed that cannabis likely plays a role in the development of schizophrenia. In one study, over 50,000 Swedish army conscripts aged between eighteen and twenty years were recruited for investigation. This study showed that those who abused cannabis before the age of eighteen were six times more likely to develop schizophrenia than those who never used the drug. In a follow up study, the same researchers showed that the progression of mental deterioration in schizophrenics who used cannabis, versus those that did not, was more abrupt (Andreasson *et al.*, 1989).

More support for cannabis as a factor in the development of schizophrenia came from the work of Jentsch and colleagues (Jentsch *et al.*, 1998). They showed that longer term

administration of Δ^9-THC reduced dopaminergic transmission (via the dopaminergic D_2 receptor, a member of the GPCR superfamily) in the rat medial prefrontal cortex. This suggests a role for drug-induced alterations in cortical dopaminergic transmission in schizophrenics, and supports the dopamine hypothesis of schizophrenia.

A more recent study showed that cannabis abuse can increase the incidence of psychosis in both psychosis-free and psychosis-predisposed individuals in a dose-dependent manner (van Os *et al.*, 2002). In contrast to these studies showing a causal relationship between cannabis abuse and schizophrenia, Degenhardt *et al.* (2003) reported that cannabis use does not appear to be causally related to the incidence of schizophrenia; rather, cannabis may precipitate disorders in persons who are vulnerable to developing psychosis and exacerbate the disorder in those who have already developed the disease. All of these studies suggest a role for cannabinoids in the precipitation and/or maintenance of schizophrenia, but the mechanism remains elusive.

Dysregulation of serotonergic signaling has also been implicated in the pathophysiology of schizophrenia. Quantitative data showing a decrease in $5HT_{2A}$ receptor density and mRNA have been found in schizophrenics by many investigators (Arora & Meltzer, 1991; Burnet *et al.*, 1996). Neuroendocrine challenge studies are consistent with an altered sensitivity of serotonergic $5HT_{2A}$ receptors (yet another member of the GPCR superfamily), and many typical and atypical antipsychotic agents bind with high affinity to this receptor. Alterations in serotonergic systems have been correlated with specific symptoms of schizophrenia, and novel antipsychotic agents which function as $5HT_{2A}$ antagonists appear superior to neuroleptics in the treatment of negative symptoms and in treatment-resistant schizophrenia (Roth *et al.*, 1998).

In Chapter two of this thesis, I will test the hypothesis that cannabinoid and serotonergic GPCRs can form complexes, therefore making it possible to alter the signaling properties of these two neurotransmitter systems.

Cannabinoids and Pain

The International Association for the Study of Pain® (IASP®) defines pain as "an unpleasant sensory and emotional experience associated with actual or potential tissue damage, or described in terms of such damage" (Loeser & Treede, 2008). Painful stimuli are detected and processed by primary afferent nociceptors, which deliver noxious information via the dorsal roots to the spinal cord and subsequently to the brain (*Figure 1.7*). The pain system comprises both ascending pathways such as the spinothalamic and spinoparabrachial tracts, and descending pathways arising in the periaqueductal grey (PAG) and rostral ventromedial medulla (RVM). The ascending systems encode, whereas, the descending systems modulate pain signals respectively (D'Mello & Dickenson, 2008) (*Figure 1.7*).

A number of specific pain states have been identified. These include acute, persistent somatic (Calignano *et al.*, 1998; Jaggar *et al.*, 1998), persistent visceral (Jaggar *et al.*, 1998; Farquhar-Smith & Rice, 2001) and neuropathic pain (Herzberg *et al.*, 1997; Bridges *et al.*, 2001) to name a few. Thus, the existence of multiple neural pathways associated with pain, and evidence that pain with somatic, neural or visceral origins is processed differently means pain and its treatment becomes very complicated in the clinical setting.

There is now considerable evidence that cannabinoid receptors are expressed on

neurons in various parts of the pain pathway, including descending neurons in the brainstem, local interneurons in the spinal cord and on the central terminals of primary afferents (Farquhar-Smith *et al.*, 2000; Monhemius *et al.*, 2001). In behavioural studies, cannabinoids have been shown to influence whole-body functions/physiology such as antinociception, hypothermia, hypomotility and catalepsy. At the cellular level, the synthetic cannabinoid agonist, WIN-55,212-2, has selective effects on the firing of nociceptive neurons in the spinal cord and thalamus during noxious-stimulation. These data are taken as evidence for the antinociceptive action of cannabinoids (Martin *et al.*, 1996; Hohmann *et al.*, 1999).

In addition, administration of cannabinoids to 'normal' animals produces antinociception mediated by spinal and supraspinal sites (Gilbert, 1981; Smith & Martin, 1992). At the level of the spinal cord, cannabinoids can inhibit both capsaicin-sensitive fibres and wide dynamic range (WDR) neurons (Hohmann *et al.*, 1998; Richardson *et al.*, 1998a) and modulate the activity of the glutamatergic (Shen *et al.*, 1996; Richardson *et al.*, 1998b), noradrenergic (Lichtman & Martin, 1991) and opioidergic systems (Welch, 1993; Smith *et al.*, 1994; Pugh *et al.*, 1995; Pugh *et al.*, 1996; Reche *et al.*, 1996; Reche *et al.*, 1998). Furthermore, WIN-55,212-2 reduced formalin-mediated expression of *c-Fos* in the nociceptive laminae I-II (SDH) and laminae V-VI (DDH) of the spinal cord, but not in the non-nociceptive laminae III-IV (Tsou *et al.*, 1996).

At the supraspinal level, cannabinoids have also been shown to mediate several effects involving the opioid system (Reche *et al.*, 1996; Reche *et al.*, 1998) and the PAG-RVM pathway (Martin *et al.*, 1996; Martin *et al.*, 1998). Indeed, by a similar

mechanism to opioids, cannabinoids can activate the descending PAG-RVM pathway via GABA-mediated disinhibition and produce analgesia (Vaughan, 2006).

A new role for endocannabinoids in stress-induced analgesia (SIA) has recently been described (Hohmann *et al.*, 2005). It was shown that during stressful stimuli, levels of AEA and 2-AG are elevated within the PAG, producing analgesia in rats. These effects were blocked by the CB_1 antagonist, SR141716A, but not by the CB_2-selective antagonist, SR144528, or the opioid non-selective antagonist, naloxone.

Taken together, with the previously mentioned analgesic synergy that exists between cannabinoids and opioids (Smith *et al.*, 1994; Pugh *et al.*, 1996; Cichewicz, 2004), the cannabinoid system seems to be important in pain processing, and thus may represent a potential therapeutic target for the treatment of various pain states.

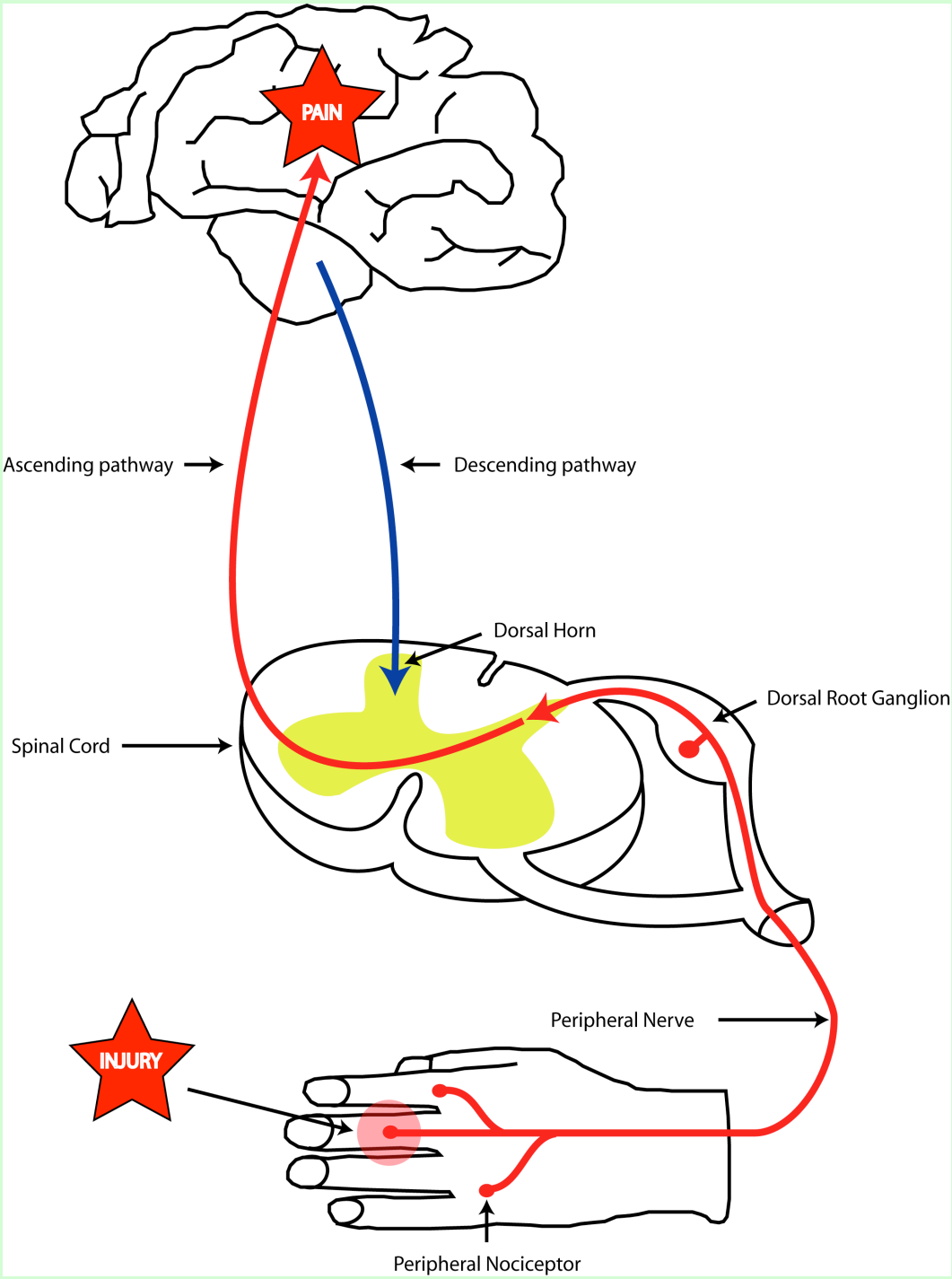

Figure 1.7 - The perception of pain and the ascending pain pathway. *The central processes of peripheral nociceptors project through the dorsal root ganglion into the dorsal horn of the spinal cord. Here, the signal is processed and the output is transmitted along ascending pathways such as the spinothalamic & spinoparabrachial tracts to various higher brain centres. Descending pathways from the medulla, including the periaqueductal grey (PAG) and rostral ventromedial medulla (RVM) play an important role in modulating pain processing in the spinal cord. Neurons in both the descending pathway, and dorsal horn interneurons express cannabinoid CB_1 receptors.*

Summary

In summary, the available evidence suggests that cannabinoid receptors, either alone or via their direct or indirect interaction with other neurotransmitter systems, are important for pain and analgesia. This thesis will attempt to reconcile some of those interactions, and determine firstly, if cannabinoid type 1 receptors (CB_1R) can form homo- and heterodimers with $5HT_{2A}$ receptors, and secondly, if cannabinoids can directly affect the inhibitory signaling system in the spinal cord dorsal horn.

CHAPTER 2

G Protein-Coupled Receptor Oligomerization

Introduction

As mentioned previously, the concept of GPCR dimerization or oligomerization postulates that two or more similar or dissimilar GPCRs couple together to form a unique signaling entity. This coupling of receptors is further distinguished as homo- or hetero- depending on whether the receptors in the complex are the same or different. This coupling phenomenon can directly affect cellular functions such as trafficking (Couve *et al.*, 1998), internalization (Jordan & Devi, 1999), and intracellular signal transduction events (White *et al.*, 1998; Kuner *et al.*, 1999).

It has been reported that the cannabinoid and serotonergic (5HT) systems are capable of interaction and modulation of signaling pathways in the CNS (Cheer *et al.*, 1999; Devlin & Christopoulos, 2002). Furthermore, these experiments show that the interactions are complex and likely involve crosstalk mechanisms such as GPCR dimerization. Recent evidence also suggests that cannabinoids and serotonergic systems within the spinal cord and supraspinal regions can interact, producing analgesia (Hogestatt *et al.*, 2005; Mallet *et al.*, 2008; Radhakrishnan *et al.*, 2003; Solomon & Gebhart, 1988; Danzebrink & Gebhart, 1991; Obata *et al.*, 2001). For example, studies have shown that cannabinoid and 5HT levels are increased in animal models of neuropathic pain (Hohmann *et al*., 2005; Palazzo *et al*., 2006), and both cannabinoid agonists and some 5HTR antagonists have analgesic effects (Honda *et al*., 2006). Indeed, one form of the 5HTR, the $5HT_{2A}R$, is involved in the peripheral sensitization of nociceptors as well as the central sensitization of dorsal horn neurons (Van Steenwinckel et al., 2008). Therefore, if cannabinoid receptors can couple with 5HTR's, this may lead to changes in the signal transduction pathways of the 5HT system, thus promoting analgesia.

G Protein-Coupled Receptors (GPCRs)

A characteristic feature of all known G protein-coupled receptors (GPCRs) is their seven α-helical transmembrane (TM) - spanning domains (Foord *et al.*, 2005; *Figure 2.1*). These receptors include several thousand distinct but related proteins whose ligands include diverse entities such as peptides, small molecules and even light. GPCRs have an amino terminus (NH_2) located extracellularly that contains several glycosylation sites. The carboxy terminus (COOH) is located intracellularly and contains phosphorylation sites, which are involved in receptor desensitization and internalization events (Perez & Karnik, 2005). The seven transmembrane domains are linked by three intracellular and three extracellular loops. Most GPCRs have *at least* one highly conserved disulphide bond between cysteines in the extracellular loops, which is/are important for determining binding affinity and correct folding of the receptor (Karnik & Khorana, 1990).

GPCRs bind ligands on the extracellular side and following activation by the ligand, a conformational change takes place causing the intracellular loops to associate with a heterotrimeric G protein complex containing α, β and γ subunits (Maudsley *et al.*, 2005). Once activated, the subunits of this complex dissociate into α and β/γ entities that can interact with various second messenger systems and effector molecules such as enzymes, ion channels and proteins (Gilman, 1987). Several types of α subunit have been identified, each with different functions. For instance, the G protein known as $G\alpha_{i/o}$ is known to be negatively coupled to adenylate cyclase resulting in the inhibition or modulation of such intracellular mediators as cAMP and PKA. In contrast, $G\alpha_s$ is positively coupled to these systems (Simon *et al.*, 1991).

Other intracellular signaling systems can also be utilized. For example, $G\alpha_{q/11}$ can stimulate formation of the second messenger inositol-1,4,5-trisphosphate (IP_3) via activation of the mitogen-associated protein kinase (MAPK) cascade (Maudsley *et al.*, 2005). A final group of G proteins known as $G_{12/13}$ couple GPCRs to activation of the small monomeric GTPase RhoA (Needham & Rozengurt, 1998). Activation of RhoA modulates various downstream effector systems that are known to be important in diseases such as hypertension, artherosclerosis, asthma and cancer.

GPCR Dimerization

As mentioned previously, the best characterized cannabinoid receptors (CB_1 and CB_2) are GPCRs. Although most GPCRs are thought to be capable of homodimerization, a significant literature is now emerging that proposes a number of heterodimerization partners as well (*Table 1*). Dimerization is thought to take place early in the GPCR 'life cycle' with reports of 'coupling' taking place at the level of the ER. Here, GPCR partners are released from the golgi apparatus and trafficked to the plasma membrane where other processes such as ligand-promoted regulation and internalization can occur (*Figure 2.2*). In some cases, dimerization has been shown to have a primary role in receptor maturation and for transport of GPCRs from the ER to the cell surface (Bouvier, 2001).

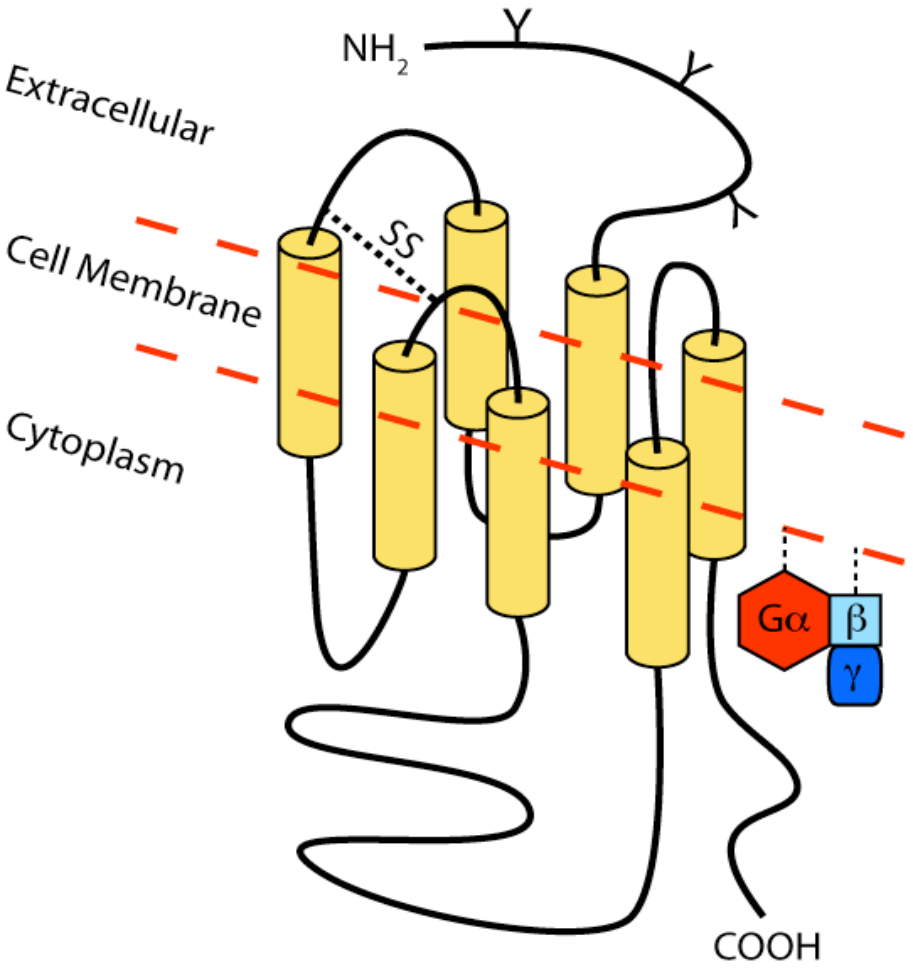

Figure 2.1 - GPCR structure. Receptors that belong to the *GPCR superfamily have an amino terminus (NH_2) located extracellularly that contains several glycosylation sites (Y). The carboxy terminus (COOH) is located intracellularly and contains phosphorylation sites involved in receptor desensitization and internalization events. The seven transmembrane domains are linked by three intra- and three extra-cellular loops, which interact with the G protein complex. Most GPCRs have at least one highly conserved disulphide bond (SS) between cysteines in the extra-cellular loops, which is/are involved in the correct folding and binding affinity of the receptor.*

Once at the plasma membrane, dimers can become a target for dynamic regulation, leading to potentiation or attenuation of signaling, or even a change in G protein selectivity (*Table 1*). For example, heterodimerization can promote the co-internalization of two receptors after the stimulation of only one monomer in the complex (Jordan *et al.*, 2001). Alternatively, the presence of a GPCR that is resistant to agonist-promoted endocytosis within a heterodimer complex, can inhibit the internalization of that complex regardless of the partner receptor's endocytotic ability (Jordan & Devi, 1999).

The metabotropic $GABA_B$ receptor represents a well-characterized and functional example of heterodimerization. This receptor complex requires the co-expression and heterodimerization of the $GABA_B$ R1 and $GABA_B$ R2 isoforms for the receptor to function appropriately (White *et al.*, 1998; Kuner *et al.*, 1999). When the R1 isoform is expressed alone, an ER retention signal present in the carboxyl tail confines the immature glycoprotein to the ER (Couve *et al.*, 1998). In contrast, when the R2 isoform is expressed alone it is able to fold correctly, transfer and insert into the cell membrane, but is incapable of binding GABA (White *et al.*, 1998). When the R1 and R2 isoforms are co-expressed, both proteins fold correctly and dimerization occurs in the ER. Subsequently, the $GABA_B$ R2 isoform masks the $GABA_B$ R1 ER retention signal and chaperones the complex to the cell surface where it becomes a functional GPCR, capable of binding the GABA ligand (White *et al.*, 1998; Kuner *et al.*, 1999). This process whereby one subunit binds the ligand while the other subunit mediates subsequent signal transduction is known as ***transactivation*** (George *et al.*, 2002; Carrillo *et al.*, 2003; *Figure 2.3*).

GPCRs known to exhibit heterodimerization

Receptors	Properties	References
	Ligand Binding: changes in ligand binding	
$GABA_BR1$-$GABA_BR2$	Required for agonist binding	White et al., 1998
μ-δ Opioid	Decreased agonist affinity	George et al., 2000
μ-δ Opioid	Co-operative binding	Gomes et al., 2000
κ-δ Opioid	Decreased selective agonist affinity	Jordan & Devi., 1999
κ-δ Opioid	Co-operative binding	Jordan & Devi., 1999
A2A adenosine-D_1 dopamine	Increased agonist affinity	Franco et al., 2000
SSTR5-D_2 dopamine	Increased agonist affinity	Rocheville et al., 2000a
SSTR5-D_2 dopamine	Increased dimer level	Rocheville et al., 2000a
	Signaling: changes due to dimerization	
$GABA_BR1$-$GABA_BR2$	Required for function	Jones et al., 1998
μ-δ Opioid	Increased potency and efficacy	Gomes et al., 2000
κ-δ Opioid	Increase in potency via synergy	Jordan & Devi., 1999
A1 adenosine-D_1 dopamine	Decreased signaling	Gines et al., 2000
SSTR5-D_2 dopamine	Increased potency	Rocheville et al., 2000a
SSTR5-SSTR1	Increased potency and efficacy	Rocheville et al., 2000b
ATII AT-B2 bradykinin	Modulation of agonist efficacy	Abdalla et al., 2000
	Receptor Trafficking: changes in properties	
$GABA_BR1$-$GABA_BR2$	Required for cell surface expression	Kuner et al., 1999
κ-δ Opioid	Decreased agonist-mediated endocytosis	Jordan & Devi, 1999
κ Opioid-β_2 Adrenergic	Decreased agonist-mediated endocytosis	Jordan et al., 2001
δ Opioid-β_2 Adrenergic	Increased agonist-mediated endocytosis	Jordan et al., 2001
A1 adenosine-D_1 dopamine	Decreased clustering with ligands	Gines et al., 2000
SSTR5-SSTR1	Change in agonist-mediated endocytosis	Rocheville et al., 2000b

Adapted from Rios *et al.*, 2001

Table 1 - GPCR heterodimers. *This Table lists the GPCRs that can heterodimerize and the implications dimerization has on their various functions. The methods used in the above studies include co-immunoprecipitation, fluorescence resonance energy transfer (FRET), and/or bioluminescence resonance energy transfer (BRET). These techniques have been described in detail in a number of reviews (Jordan et al., 2000; Marshall, 2001; George et al., 2002; Kroeger et al., 2003; Milligan et al., 2003; Terrillon & Bouvier, 2004).*

Dimerization of Cannabinoid Receptors

Several studies using techniques such as immunoprecipitation, immunohistochemistry, Western blotting, resonance energy transfer (FRET & BRET) and functional assays, have shown that the CB_1 receptor can participate in both homo- and hetero-dimerization (Glass & Felder, 1997; Hajos *et al.*, 2000; Wager-Miller *et al.*, 2002; Kearn *et al.*, 2005). The best-characterized heterodimer partners for the CB_1 receptor in the brain, are the dopamine D_2 receptor (Kearn *et al.*, 2005), the $5HT_2$ class of receptors (Kapur *et al.*, 1999; Herrick-Davis *et al.*, 2004; Herrick-Davis *et al.*, 2005; Herrick-Davis *et al.*, 2006) and members of the opioid receptor family (Rios *et al.*, 2006). Both the CB_1 (Leroy *et al.*, 2001; Zavitsanou *et al.*, 2004) and D_2 (Kapur *et al.*, 1999; Tsai, 2005; de Haan *et al.*, 2006; Takahashi *et al.*, 2006) receptors have been implicated in schizophrenia. Thus, heterodimerization between CB_1 and D_2 receptors may be important in the signaling dysfunctions that characterize this disease.

Similarly, synergistic actions have been shown to occur between cannabinoids and opioid analgesics in the spinal cord. For example, Cichewicz (2004), showed that Δ^9-THC enhanced the actions of morphine and vice versa. It is entirely possible in this case that dimerization of CB_1 and mu opioid receptors is responsible for these observations, since these receptors co-localize in a subpopulation of spinal cord dorsal horn neurons (Salio *et al.*, 2001). Indeed, recent data suggests a direct receptor/receptor interaction between these two GPCRs (Rios *et al.*, 2006).

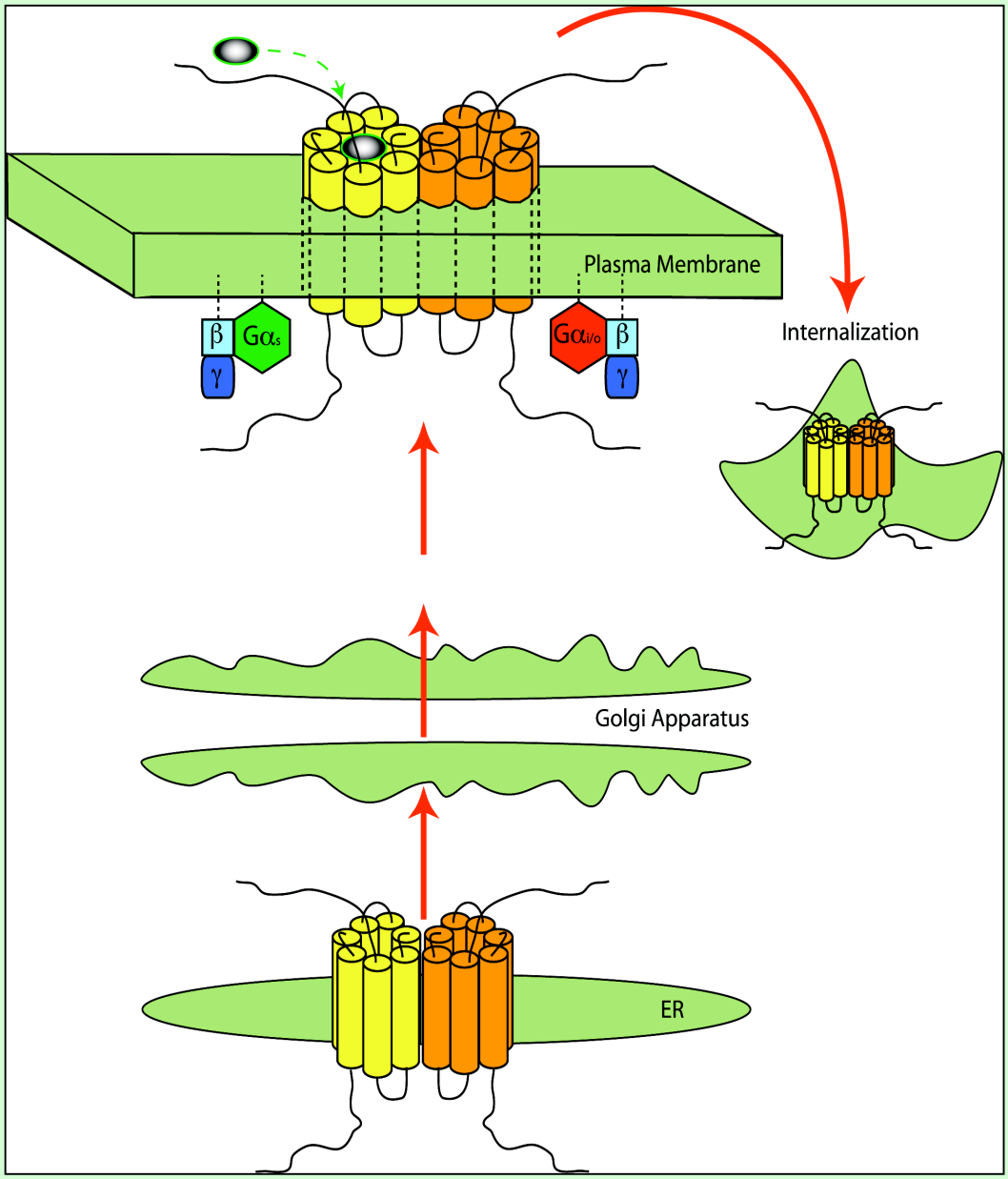

Figure 2.2 – The life cycle of a GPCR. *In some cases, dimerization has been shown to have a primary role in receptor formation and targeting to the cell membrane, and allows the correct transport of GPCRs from the endoplasmic reticulum (ER) to the cell surface. It has been proposed that GPCR heterodimerization leads to both positive and negative ligand binding cooperativity, as well as potentiating/attenuating signaling or changing G protein selectivity. Heterodimerization can promote the co-internalization of two receptors after the stimulation of only one GPCR monomer in the complex. Alternatively, the presence of a monomer that is resistant to agonist-promoted endocytosis, within a heterodimer, can inhibit the internalization of the complex.*

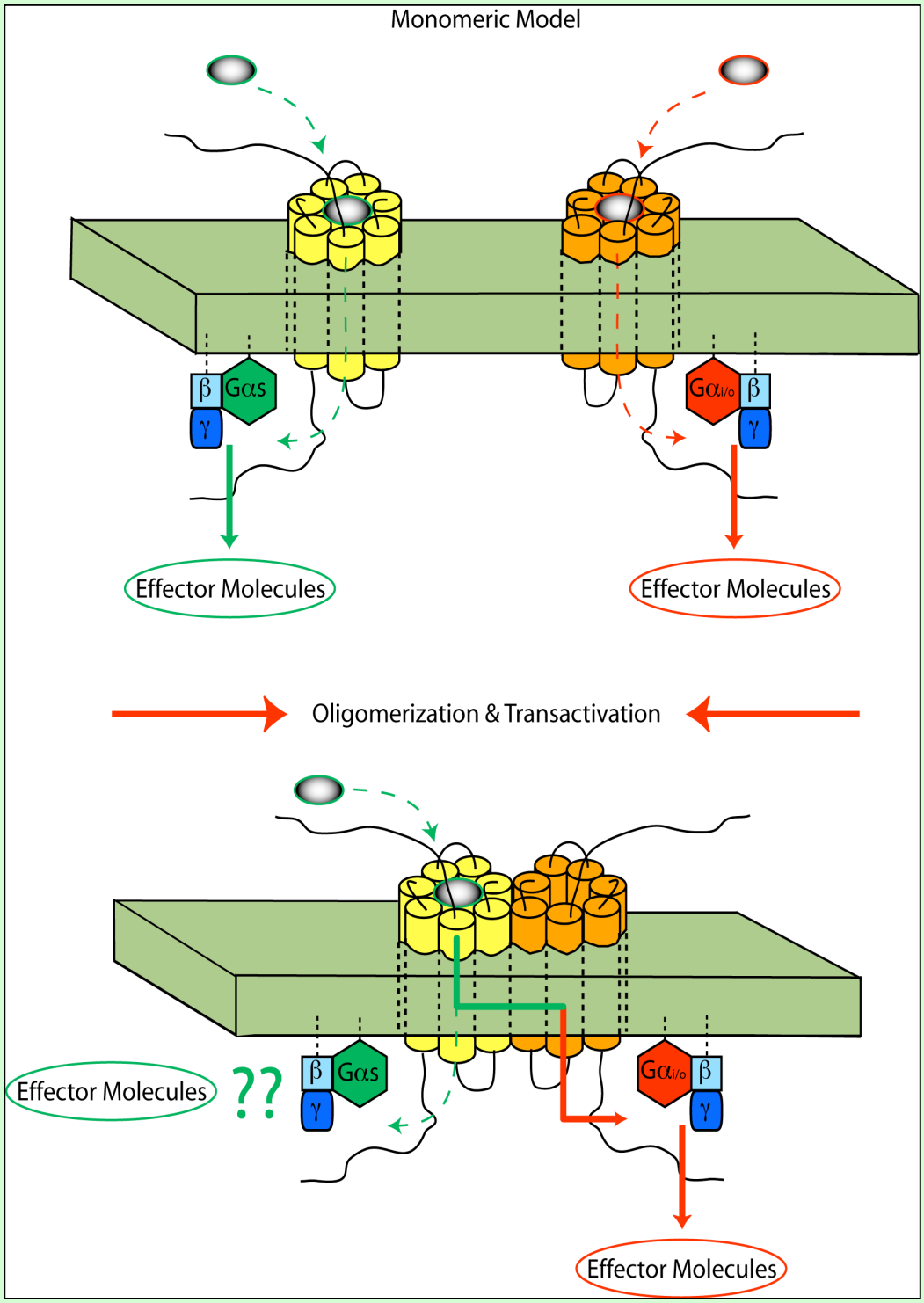

Figure 2.3 - GPCR Transactivation. *Traditionally, it was thought that GPCRs only operated in isolation as monomeric entities. It has now been shown that some GPCRs can only signal when they are coupled to their heterodimeric partner. When this occurs, binding of a specific ligand for one receptor activates the signaling cascade of the partner receptor (eg. $GABA_B$ R1 and $GABA_B$ R2, somatostatin sst_{2A} and mu opioid receptor).*

Although there is evidence for these multimeric interactions between GPCRs, the dimerization interface has yet to be resolved. Some researchers have suggested that dimerization or oligomerization involves the TM4/TM5 domains and the 2nd intracellular loop, whereas the TM1/TM2 domains and the 3rd intracellular loop seems to be critical for constructing highly organized rows of dimers (Guo *et al.*, 2003; Guo *et al.*, 2005; Kota *et al.*, 2006).

Whatever the case, there is clearly a need for more research into the functional interactions of the cannabinoid receptors with other GPCRs. Such interactions could prove to be important for human health. Indeed, the implications of using cannabinoids or cannabinoid antagonists (or inverse agonists) as medicines is only just beginning to be realized, with these drugs being used for conditions as diverse as obesity (Van Gaal *et al.*, 2005), smoking cessation (Cohen *et al.*, 2005), Parkinson's disease (van der Stelt *et al.*, 2005) and analgesia (Ware *et al.*, 2003).

Detection of GPCR dimers

Fluorescence Resonance Energy Transfer (FRET)

In contrast to the previously mentioned immunological techniques, the biophysical methods underpinning Fluorescence Resonance Energy Transfer (FRET) and Bioluminescence Resonance Energy Transfer (BRET) detect complexation of GPCRs in living cells by the transfer of resonance energy from a fluorescent or luminescent donor respectively, to an acceptor fluorophore (Selvin, 2000). Both methods are sensitive to the distance between their donor and acceptor components, as the non-radiative transfer of resonance energy will only take place if they are within 10-100 Angstrom (Å; 100 x 10^{-10} m; or 10 nm) of one another (Boute *et al.*, 2002). The efficiency (E) of this transfer

was described by Foster (1959) according to the FRET efficiency equation; $E=1/1+(R/R_o)^6$ (where R is the distance between the donor and acceptor fluorophores and R_o equals the distance where transfer of half of the energy occurs). This equation shows that the transfer of energy is inversely dependent upon the distance between donor and acceptor to the sixth power. An increase in the emission of the acceptor fluorophore indicates that the acceptor and donor fluorophores are in very close proximity, and complexation of the receptors has most likely occurred (Selvin, 2000; Eidne *et al.*, 2002; *Figure 2.4*).

The fluorophores primarily used for biophysical assays are the enhanced (e) spectral variants of green fluorescent protein (GFP). This protein was originally described in the jellyfish *Aequorea Victoria* (Morise *et al.*, 1974), and its genetic cloning 18 years later (Prasher *et al.*, 1992), started a new era in biotechnology techniques. For example, variants of these fluorescent proteins, eGFP (green), eCFP (cyan), and eYFP (yellow) have been used as protein expression tags to identify and follow, in real-time, both the interaction and subcellular localization of tagged proteins in living cells (Matz *et al.*, 2002; Zeilhofer *et al*., 2005).

For transfer of resonance energy to occur, the emission and absorption spectrum of the donor and acceptor fluorescent proteins need to overlap sufficiently. After consideration of these issues, it was found that the best fluorophore pairing to use for FRET is the cyan (CFP) and yellow (YFP) spectral variants (Boute *et al.*, 2002; *Figure 2.5*).

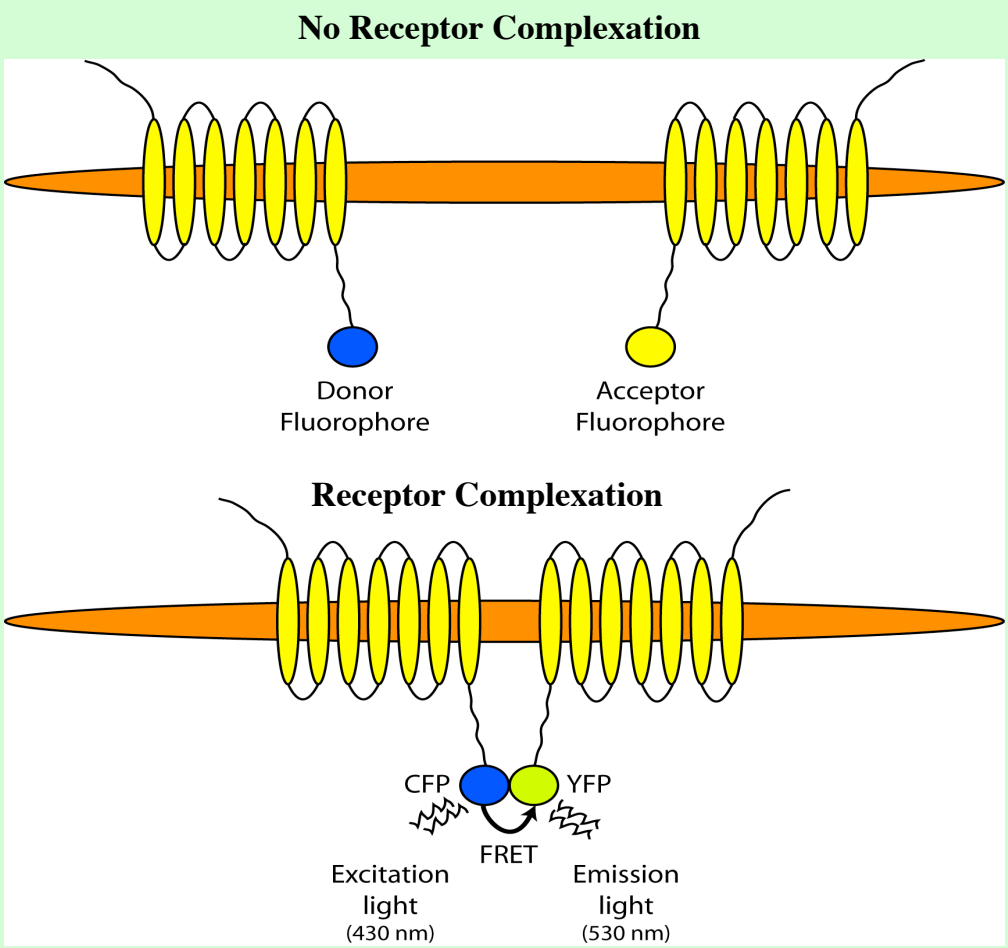

Adapted from Eidne et al., 2002

Figure 2.4: Schematic representation of receptor complexation using FRET*. Receptors of interest are tagged with a fluorescent protein. If these receptors are between 10 and 100 Angstroms apart, FRET can take place. After excitation of the donor fluorophore (eCFP, enhanced cyan fluorescent protein), energy is transferred to the acceptor fluorophore (eYFP, enhanced yellow fluorescent protein), and fluorescent light is emitted at the corresponding wavelength of the eYFP. This can be detected and measured by a FLUOstar multifunctional microplate reader system.*

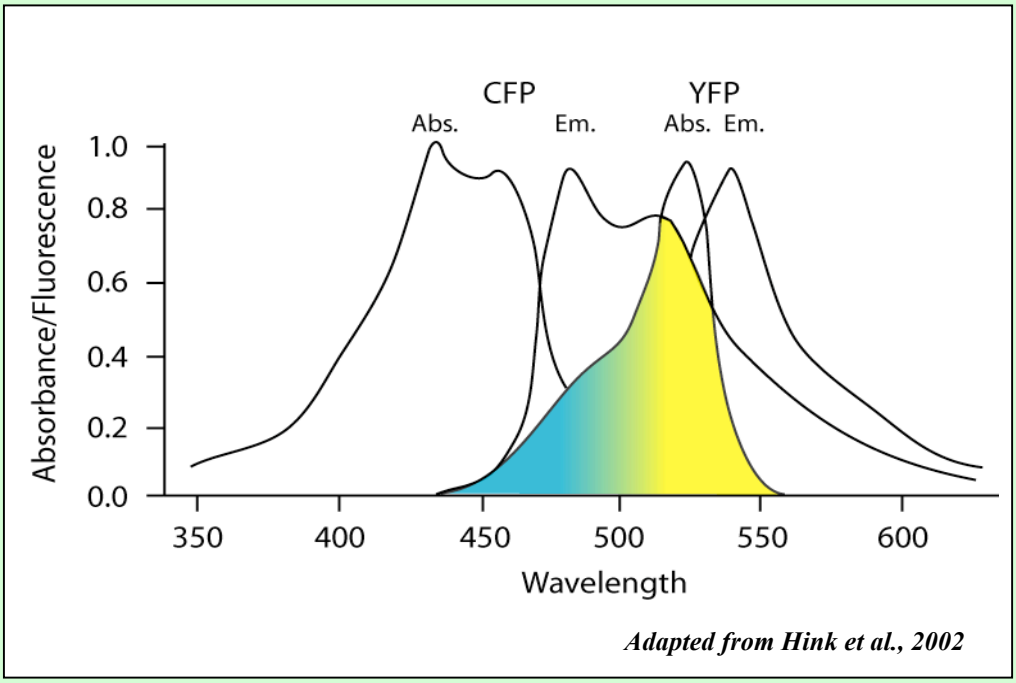

Figure 2.5 - Emission and Absorption Spectrum of CFP and YFP Fluorescent Proteins used in FRET studies*. FRET studies are only possible if the emission (Em.) and absorbance (Abs.) spectra of the fluorophore pair used overlap, and if the distance between the proteins is very small (10-100 Angstrom). Note the sufficient spectral overlap of the fluorescent proteins CFP and YFP, making them the most suitable for use in FRET studies (Boute et al., 2002).*

General Research Plan

The major aim of this series of experiments was to determine whether the CB_1 and $5HT_{2A}$ receptors were capable firstly, of forming homodimers, and subsequently, of forming heterodimers. I used a series of molecular techniques and cell culture protocols to answer these questions. The flow chart below provides an overview of the work carried out in this chapter. The materials and methods section which follows, contains more detailed accounts of each step.

General Research Plan

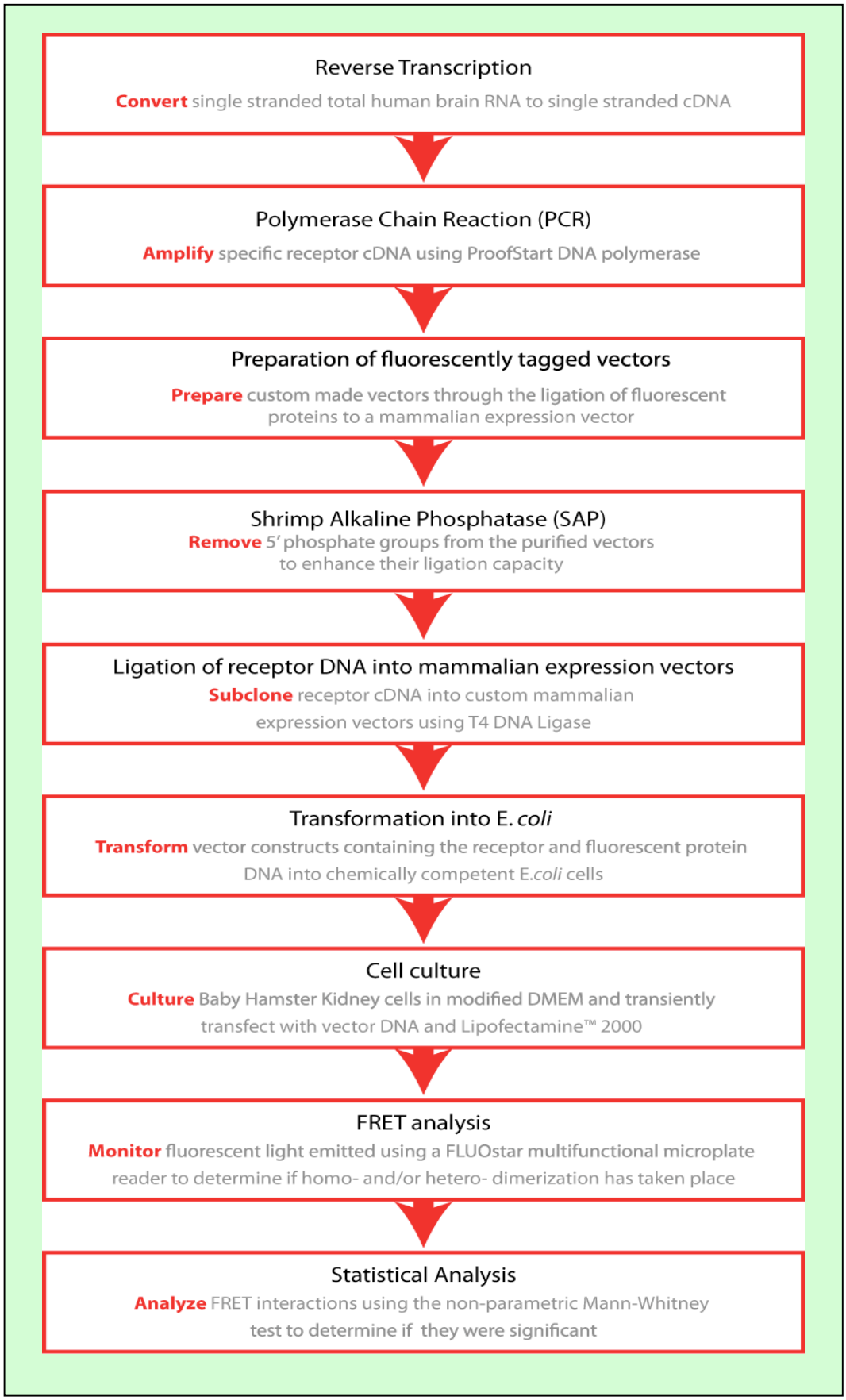

Materials and Methods

Generation of G protein-coupled receptors

Reverse Transcription

Reverse Transcription (RT) was performed to convert single stranded total human brain RNA to single stranded cDNA. RNA was obtained from Applied Biosystems (Melbourne, Australia) and stored in 2 μL aliquots at -80^{o}C until required. The cDNA was produced using a random primer RT-PCR protocol and reagents obtained from Invitrogen (Melbourne, Australia). The RT reaction mixture consisted of 300 ng of random primers (Invitrogen), 1 μL of 10 mM deoxynucleotide triphosphate (dNTP) mix (Invitrogen), 1 μL of total human brain RNA, and RNAse free water made up to a final volume of 12.5 μL. This solution was then heated at 65^{o}C for 5 min then immediately chilled on ice. While on ice, 4 μL of 5x Buffer, 2 μL of 100mM DTT, and 1 μL of 40U/μL RNaseOUT (Invitrogen) was prepared in a separate tube and added to the tubes containing the RNA. Following incubation at 25^{o}C for 10 min and a further incubation for 2 min at 42^{o}C, 200 units of SuperScriptII™ Reverse Transcriptase (Invitrogen) was added and the reaction mixture heated at 42^{o}C for 50 min. A final 15 min incubation at 70^{o}C was carried out before cooling the resultant cDNA on ice. The cDNA was then stored at -20^{o}C until required.

Oligonucleotide RT-PCR Primers

Primers for the amplification of the human cannabinoid CB_1 receptor cDNA (Genebank accession number NM_016083) and the serotonin $5HT_{2A}$ receptor (Genebank accession number NM_000621), were custom designed using the Primer Premier Version 5 software program (Premier Biosoft International, Palo Alto, CA, USA), and obtained from Sigma-Aldrich (Sydney, Australia). All primers amplified the full length of the

Open Reading Frame (ORF) of receptor cDNA and also contained sequences for specific enzyme restriction sites to facilitate the subcloning of receptor cDNA into custom-made mammalian expression vectors. All primers were reconstituted at a concentration of 10 μM in TE buffer (10 mM Tris HCl, 1 mM EDTA, pH 8.0).

Polymerase Chain Reaction (PCR)

Specific cDNA for the CB_1 and $5HT_{2A}$ receptors was amplified using ProofStart DNA polymerase (Qiagen, Melbourne, Australia). ProofStart is a hot-start proofreading polymerase uniquely modified to prevent primer degradation during PCR setup, and provides robust high-fidelity PCR. The PCR reaction was carried out in a total volume of 25 μL and contained 2.5μL of 10x ProofStart PCR buffer, 2.5 μL each of 1.0 μM forward and reverse primers, 300 nM of mixed dNTPs (Eppendorf, Sydney, Australia), 2.0 μL of cDNA template, 1 unit of ProofStart DNA polymerase and DNAse free water (Invitrogen) to 25 μL. Amplification of cDNA was performed using an iCycler PCR Thermocycler (Bio-Rad Laboratories, Sydney, Australia). The heating protocol for the thermocycler included 5 min incubation at 95^{o}C to activate the ProofStart DNA polymerase, followed by 40 cycles of denaturing (30 s, 95^{o}C), annealing (30 s, 60^{o}C), and extension (2 min, 72^{o}C). A final extension and polishing step was programmed for 8 min at 72^{o}C.

Analysis and Purification of PCR Products

PCR products were run on a 1% agarose gel to determine whether amplification was successful. The amplification was considered successful if a band corresponding to the required receptor cDNA fragment length could be identified by comparison with a DNA molecular weight (DMW) 200bp ladder (Geneworks, Adelaide, Australia). The

correctly amplified PCR product was then run on a preparative 1% agarose gel and the corresponding band was excised and purified using the PerfectPrep Gel Clean up kit (Eppendorf) according to manufacturer's instructions.

Preparation of Fluorescently Tagged Vectors

Attachment of Fluorescent Proteins and Production of Cohesive Ends

Following gel purification, each PCR product was incubated with the appropriate restriction enzymes for 6 h at 37^{o}C. The CB_1 receptor DNA was incubated with the restriction enzymes *BamHI and HindIII*, whereas the $5HT_{2A}$ receptor DNA was incubated with *BamHI and XhoI* to enable directional insertion into expression vectors. The restriction enzyme digest reaction mixture consisted of 4 µL 10x Buffer B (Promega, Sydney, Australia), 4 µL of 10x acetylated bovine serum albumin (αBSA, Promega), 30 µL of purified PCR product and 1 µL of the appropriate restriction enzymes (as mentioned previously). The addition of 1 µL aliquots of fresh restriction enzymes every 2 h ensured the quality and integrity of the reaction. The products were ligated into mammalian expression vectors (described below) which had been digested with the same restriction enzymes, to produce complementary and cohesive ends.

Custom made vectors (CFPzeo, YFPzeo, and CFP-YFPzeo) were prepared through the ligation of the fluorescent protein cDNAs for eCFP and/or eYFP, to the mammalian expression vector, pcDNA3.1zeo, which also contained the ampicillin resistance gene (Invitrogen, Australia). CFP and YFP cDNA was obtained from the pECFP-C1 vector and the pEYFP-C1 vector respectively (Clontech Laboratories Inc. Melbourne, Australia). To produce the N-terminal vectors, CFPzeo and YFPzeo, the fluorescent

proteins were inserted into the expression vector between the NheI/HindIII restriction enzyme sites.

The reaction mixture consisted of 4μL of the appropriate 10x Buffer (Promega), 4 μL of 10x acetylated BSA, 30 μL of purified fluorescently tagged product and 1 μL of each restriction enzyme. To prepare these vectors for ligation with the various receptor cDNA inserts, the fluorescently tagged vectors were digested at 37^{o}C for 2 h with the appropriate restriction enzymes to produce complementary cohesive ends. Following incubation, the vectors were purified using the Perfectprep Gel Clean up kit (Eppendorf) according to the manufacturer's instructions, followed by dephosphorylation using Shrimp Alkaline Phosphatase (described below).

Shrimp Alkaline Phosphatase (SAP) Procedure

To enhance the ligation capacity of the fluorescently tagged vectors and the receptor cDNA, the 5' phosphate groups were removed from the purified vectors using SAP. The SAP reaction mixture consisted of 5 μL of 10x SAP Buffer (Promega), 30 μL purified vector DNA, 1 μL Shrimp Alkaline Phosphatase (SAP) enzyme (Promega) and water to a final volume of 50μL. After incubation of the reaction mixture at 37°C for 15 min, an additional 1 μL of SAP enzyme was added and the mixture was then incubated for an additional 15 min at 37°C. The reaction mixture was then purified using the PerfectPrep Gel Clean up kit (Eppendorf).

Ligation and Transformation

Ligation

Receptor cDNA, with cohesive ends produced through restriction enzyme digestion, were subcloned into custom mammalian expression vectors using T4 DNA Ligase. The reaction mixture consisted of 5 μL of 2x Rapid Ligation Buffer (Promega), a 3:1 ratio of receptor cDNA to vector, and 1 μL of T4 DNA ligase. The reaction mixture was incubated at room temperature for 25 min to produce fluorescently tagged vectors with the appropriate receptor cDNA inserts. These inserts were subsequently transformed into chemically competent E. *coli* cells (Note: Chemically competent cells are treated with a buffer that contains $CaCl_2$ and other salts that disrupt the cell membrane creating "holes" that allow the plasmids to pass into the cell).

Chemical Transformation

To produce large numbers of the vector constructs containing the relevant receptor and fluorescent protein DNA, the constructs were inserted into E.*coli* cells. A 100 μL volume of chemically competent E.*coli* cells (Promega) were thawed gently on ice and added together with 10 μL of the ligation product to a pre-chilled polypropylene tube and left on ice for 10 min. The E.*coli* cells were then heat shocked at 42°C for 50 s and then placed back on ice for a further 2 min. Following this step, 900 μL of SOC medium (tryptone 2% (w/v), yeast extract 0.5% (w/v), NaCl 8.6 mM, KCl 2.5 mM, $MgSO_4$ 20 mM, Glucose 20 mM) was added and the mixture incubated with shaking for 60 min at 37°C.

Colonies containing the ligation product were produced by plating the E.*coli* cells on agar plates containing ampicillin (100 mg/mL) and incubated overnight at 37°C. The

isolated colonies were removed and grown in 5 mL of terrific broth (Sigma-Aldrich) for 8 h with shaking at 260 rpm. Prior to pelleting the E.*coli* cells (4000 rpm for 5 min) for purification and restriction enzyme analysis, glycerol stocks consisting of 650 μL of terrific broth containing the grown colonies and 350 μL of 80% glycerol were made and stored at -80°C until required.

Plasmid DNA Purification

Standard/Plasmid Mini-prep Purification

The fluorescent vector-receptor DNA constructs required for restriction enzyme analysis (described below) or cloning were purified using the GenElute Plasmid Miniprep kit (Sigma-Aldrich). Prior to purification, all DNA constructs were grown for 8-12 h in 5 mL of bacterial culture, centrifuged (4000 rpm for 5 min) to pellet the E.*coli* cells containing the DNA, and purified using the manufacturer's instructions. The constructs were eluted with 80 μL of molecular grade Tris-EDTA (TE) buffer (Sigma-Aldrich) and stored at -20ºC until required.

Transfection Grade Purification

To produce higher quality DNA for more sensitive applications, such as FRET analysis, the vector constructs containing the receptor and fluorescent protein DNA, were purified with either the HiSpeed Midi or Maxi Purification kit (Qiagen). A 50 mL or 150 mL, 16 hour bacterial culture seeded from the previous 8-12 hour bacterial culture of vector-receptor construct-containing E.*coli* cells was purified with a Midi or Maxi kit respectively, according to manufacturer's instructions. The purified DNA was eluted in 1 mL of molecular biology grade TE buffer (Qiagen), then divided into 200 μL aliquots and stored at -20°C until required for quantitation or cellular transfection.

The DNA concentration produced through purification was determined by 1% agarose gel electrophoresis. After linearization with the HindIII restriction enzyme, the purified DNA was serially diluted and its size and intensity compared to a DNA Mass Ruler (Quantum Scientific, Brisbane, Australia), thus determining concentration (±10%).

Cell Culture and Transfection

General Cell Culture

Baby Hamster Kidney cells (BHK-P21; American Type Culture Collection, Manassas, VA, USA) were cultured in a standard 75cm^2 cell culture flask, under sterile conditions in Dulbecco's Modified Eagles Medium (DMEM) (JRH Biosciences, Melbourne, Australia) supplemented with 10% Foetal Calf Serum (FCS) (Bio-Whittaker Inc., Walkersville, MD, USA), penicillin (10,000 U/mL) streptomycin (10 mg/mL) solution (Sigma-Aldrich) and L-glutamine (200 mM) (Sigma-Aldrich). The cells were incubated at 37^{o}C in a humidified CO_2 (5%) incubator until 80-90% confluent and required for FRET experiments.

Cell Culture for Fluorescence Resonance Energy Transfer (FRET)

To prepare for FRET analysis, 24 h prior to transfection, the standard 75cm^2 cell culture flask containing BHK-P21 cells was washed with 0.02% EDTA (Sigma-Aldrich) under sterile conditions, before being dissociated with 0.25% Trypsin-EDTA (Sigma-Aldrich) followed by a 5 minute incubation at 37^{o}C. The dissociated cells were pelleted via centrifugation at 500 rpm for 5 min and the Trypsin-EDTA-containing supernatant discarded. The cells were then resuspended in 4 mL of media with 100 µL (~1x10^5 cells) of this solution being seeded into a 24 well plate containing 500 µL of media in each well. This allowed 80-90% confluence at the time of transfection**.**

Transfection

The media was removed and replenished 1-2 h prior to transfection. Under sterile conditions, triplicates of 0.1-3.5 μg of vector DNA and 1-2 μL of Lipofectamine™ 2000 Reagent (LF2000) (Invitrogen) were separately combined with 50 μL of serum, antibiotic and glutamine free DMEM and incubated at room temperature for 5 min. The DNA and LF2000 plus media were then combined and incubated at room temperature for a further 20 min to produce DNA-LF2000 complexes. These complexes were added to the seeded BHK-P21 cells and incubated at 37^{o}C, 5% CO_2 for 24 h to produce a transiently transfected BHK-P21 cell line. Three wells were not transfected and served as blank controls.

Fluorescence Resonance Energy Transfer (FRET) Studies

In preparation for FRET experiments, media in the 24-well plate was replenished 4-6 h before analysis. Just prior to FRET analysis, this media was removed and 500 μL of non-enzymatic cell dissociation solution (Sigma-Aldrich) was added and incubated at 37^{o}C for 20 min with gentle shaking. The dissociated cells were then transferred to 1.5 mL microfuge tubes and centrifuged for 2 min at 1000 x g. The supernatant was removed and the pellet resuspended in 300 μL of Ca^{2+} and Mg^{2+} free phosphate buffered saline (PBS) and transferred to a 96-well cell culture plate.

The intensity of the fluorescent light emitted from cells transfected with the fluorescent protein-tagged receptor DNA was then monitored using a FLUOstar multifunctional microplate reader system (BMG Labtech, Melbourne, Australia). Fluorescence was measured using three protocols. Firstly, for cells transfected with CFP-tagged receptor vectors alone, the intensity of fluorescence from CFP was measured at a wavelength of 480 nm following excitation at a wavelength of 430 nm.

Secondly, for cells transfected with the YFP-tagged receptors alone, the fluorescence was measured at 530 nm following excitation at 500 nm. Lastly, for cells co-transfected with both CFP and YFP-tagged receptors, the intensity of the emitted fluorescent light was measured at both 480 nm and 530 nm following excitation of the donor fluorophore (CFP) at 430 nm.

FRET Ratio Calculations

The degree of receptor complexation was determined by calculating the FRET ratio. The FRET ratio is calculated by determining the difference between the emission ratio (530 nm/480 nm) for those cells co-transfected with the CFP and YFP proteins and the emission ratio for those cells transfected with CFP alone.

FRET ratio = [(E530/E480) co-expressed CFP and YFP] – [(E530/E480) CFP expressed alone]

Statistical Analysis

I used the non-parametric Wilcoxon Mann-Whitney test (one-tailed, 95% confidence interval), to determine if a significant increase in FRET ratio occurred. The Wilcoxon Mann-Whitney Test is one of the most powerful non-parametric tests for comparing two populations. It is used to test the *null hypothesis*, that two populations have identical distribution functions, against the *alternative hypothesis*, that the two distribution functions differ only with respect to location (median), if at all (Wilcoxon, 1945). This test does not require the assumption that the data in the two samples are normally distributed. In many applications, the Wilcoxon Mann-Whitney test is used in place of the two sample t-test when data are not normally distributed (Rosner & Glynn, 2008). The embedded statistical packages available in GraphPad Prism 4 software (GraphPad Software, La Jolla, CA, USA) were used in this analysis.

Results

Production of vector constructs

Transcription and amplification of both the human serotonergic $5HT_{2A}$ and cannabinoid CB_1 receptor cDNA, was achieved through a reverse transcription (RT) reaction. This reaction utilized random primers and a single round of Proofstart PCR. Thermocycling conditions are shown in *Table 2* and primers located in the 5' and 3' untranslated region (UTR) were specifically designed to flank the open reading frame (ORF) of each receptor. Receptor cDNA was then visualized on a 1% agarose gel, and corresponded to the respective size of each receptor ($5HT_{2A}$ receptor = 1332bp in length; CB_1 receptor cDNA = 1419bp in length; see *Figures 2.6, 2.7, 2.8* and *2.9*).

Table 2

		40 cycles			
Thermocycler Conditions	**Hot Start**	**Denaturing**	**Annealing**	**Extension**	**Polishing**
Temperature and Duration	5 min at 95°C	30 s at 95°C	30 s at 60°C	2 min 45 s at 72°C	8 min at 72°C

Table 2 - Thermocycling conditions used in amplification of the human serotonergic $5HT_{2A}$ and cannabinoid CB_1 receptor cDNAs by RT-PCR.

Construction of $CFP5HT_{2A}$ and $YFPHT_{2A}$ vectors

In an effort to determine which transmembrane regions of the dimeric complexes were involved in complexation, fluorophores were attached to the N-terminal end of the $5HT_{2A}$ receptor (and also the CB_1 receptor - discussed later). The amplified $5HT_{2A}$ receptor cDNA was subcloned into custom made mammalian expression vectors CFPzeo and YFPzeo (*Figure 2.10a*), which also contain the cDNA for CFP and YFP

fluorophores, respectively. The amplified ORF of the $5HT_{2A}$ receptor cDNA was prepared for ligation using BamH1 and XhoI restriction enzymes as described previously. The expression vectors CFPzeo and YFPzeo were also prepared for ligation using BamH1 and Xho I and treated with SAP. The ORF of the $5HT_{2A}$ receptor cDNA was then ligated into the CFPzeo or YFPzeo expression vectors. The $CFP5HT_{2A}$ and $YFP5HT_{2A}$ vector constructs (*Figure 2.10b*) were transformed into chemically competent E. *coli* cells as described previously. This process involves the genetic alteration of the cells via the uptake, genomic incorporation, and expression of foreign genetic material (DNA). Following purification of $CFP5HT_{2A}$ and $YFP5HT_{2A}$ from E. *coli*, restriction enzyme digestion of both vector constructs was undertaken in combination with agarose gel electrophoresis to determine if the $5HT_{2A}$ receptor cDNA was correctly inserted into the appropriate expression vector.

The molecular constituents of $CFP5HT_{2A}$ and $YFP5HT_{2A}$ are shown in *Figures 2.6* and *2.7*, respectively. Firstly, each vector was digested with Hind III producing a linear band 7052bp in length corresponding to the size of the expression vectors containing the ORF of the $5HT_{2A}$ receptor. Both constructs were also digested with BamH1 and XhoI to confirm that $5HT_{2A}$ receptor cDNA had been inserted into the vectors. *Figures 2.6 and 2.7* demonstrate a successful restriction enzyme digest showing fragments corresponding to the size of the $5HT_{2A}$ receptor, 1332bp, and another at 5720bp consistent with the size of the fluorescently tagged expression vectors seen in lane 3 of *Figures 2.6* and *2.7*. A final restriction enzyme digest to distinguish differentially tagged vectors utilized the enzymes PstI and XhoI. This digestion produced distinct results for the two vectors when visualised on an agarose gel. Because the CFP lacks a PstI recognition site, in contrast to the YFP and the serotonin $5HT_{2A}$ receptor cDNA,

digestion of the CFP5HT$_{2A}$ vector with the PstI enzyme in combination with XhoI produced only 2 bands (*Figure 2.6*, Lane 6). However, as a result of the extra PstI enzyme recognition site, when the YFP5HT$_{2A}$ vector was digested with PstI, an additional band was observed, as shown in *Figure 2.7*, lane 5.

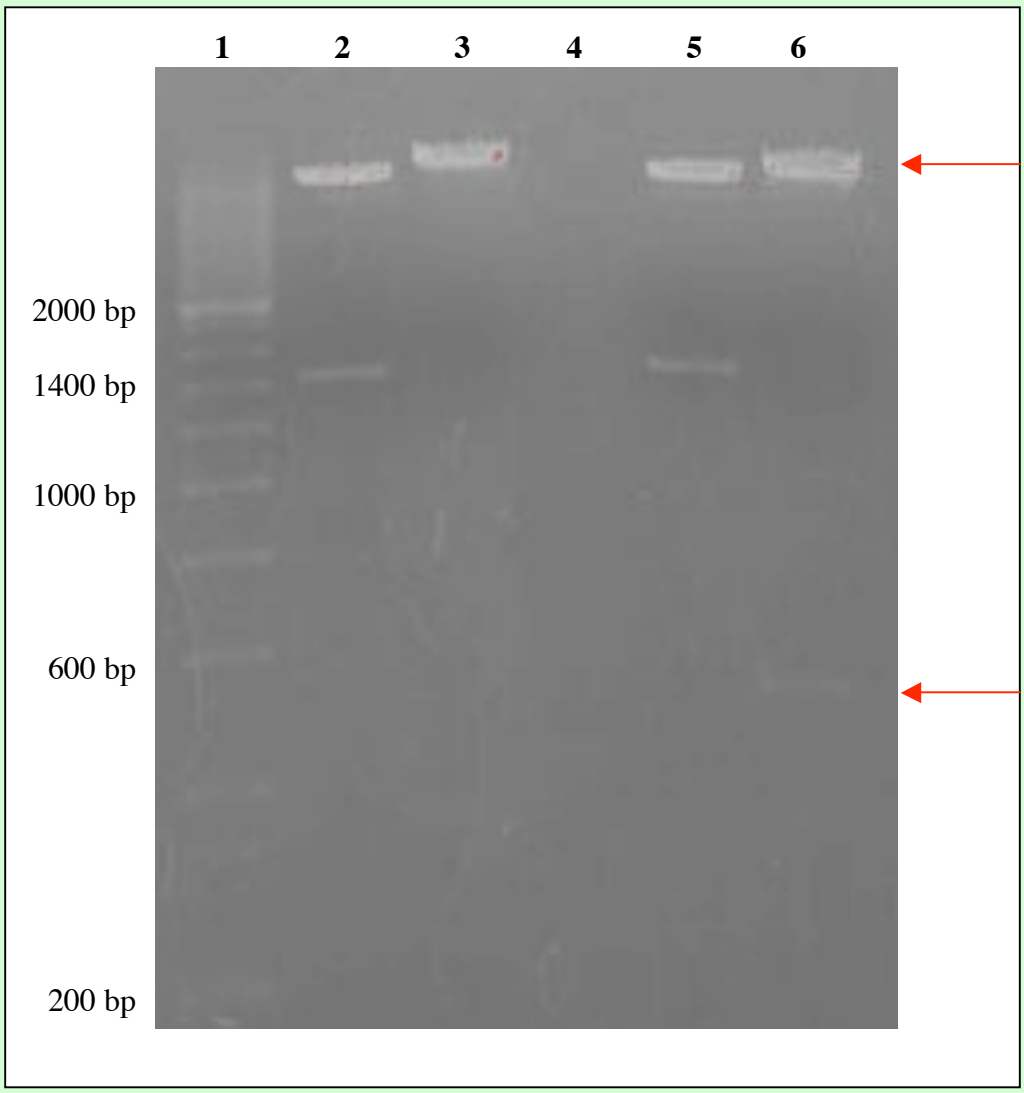

Figure 2.6 - Restriction Enzyme Analysis of the CFP5HT$_{2A}$ Vector Construct. *Prior to its use in FRET, the CFP5HT$_{2A}$ vector construct was digested with various restriction enzymes to ensure that the correct receptor cDNA was successfully ligated to the correct expression vector. Lane 1: 200bp ladder. Lane 2: CFP5HT$_{2A}$ digested with BamH1 and XhoI to produce the two bands corresponding to the length of the 5HT$_{2A}$ receptor cDNA (1332bp) and to the expression vector (5720bp). Lane 3: CFP5HT$_{2A}$ linearized with HindIII (7052bp). Lane 4: Blank. Lane 5: CFP5HT$_{2A}$ digested with BamH1 and XhoI to produce the two bands corresponding to the length of the 5HT$_{2A}$ receptor cDNA (1332bp) and to the expression vector (5720bp) (same as lane 2) Lane 6: CFP5HT$_{2A}$ digested with PstI and XhoI to indicate the presence of the CFP. The 5HT$_{2A}$ receptor cDNA possesses one PstI recognition site (~200bp in from the start codon), which is not present in the CFP. Consequently, digestion of CFP5HT$_{2A}$ with this combination of enzymes produces two bands as seen above (**red arrows**).*

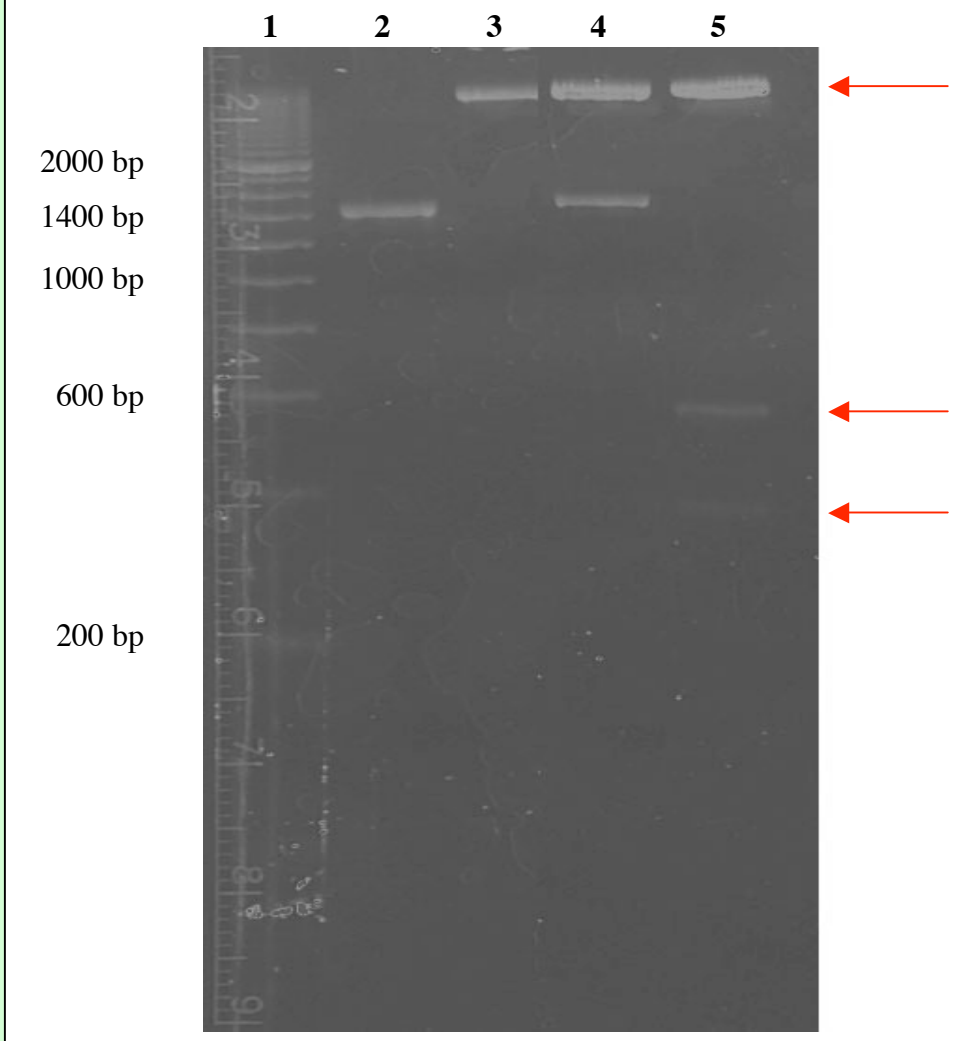

Figure 2.7 - Restriction Enzyme Analysis of the YFP5HT$_{2A}$ Vector Construct. *YFP5HT$_{2A}$ vector digested with various restriction enzymes prior to FRET analysis to determine the presence of the receptor cDNA and identify the desired fluorescently tagged vector. Lane 1: 200bp ladder. Lane 2: 5HT$_{2A}$ receptor cDNA amplified by PCR (1332bp). Lane 3: YFPzeo expression vector (5720bp). Lane 4: YFP5HT$_{2A}$ digested with BamH1 and XhoI to produce the two bands corresponding to the length of the 5HT$_{2A}$ receptor cDNA (1332bp) and to the expression vector (5720bp). Lane 5: YFP5HT$_{2A}$ digested with PstI and XhoI to distinguish YFP from CFP. Both the 5HT$_{2A}$ receptor cDNA and the YFP possess a PstI recognition site, therefore digestion of YFP5HT$_{2A}$ with this combination of enzymes produces three fragments as seen above (**red arrows**).*

Construction of the $CFPCB_1$ and $YFPCB_1$ vectors

The amplified CB_1 receptor cDNA was subcloned into the custom made CFPzeo and YFPzeo expression vectors respectively, containing cDNA for CFP and YFP fluorescent proteins (*Figure 2.10b*). The amplified ORF for the CB_1 receptor cDNA was prepared for ligation using the restriction enzymes HindIII and BamHI and treated with shrimp alkaline phosphatase (SAP). The PCR product and vectors were then ligated. Following ligation, the two fluorescently tagged CB_1 vector constructs were transformed into chemically competent E. *coli* cells and purified. Restriction enzyme digestions of the $CFPCB_1$ and $YFPCB_1$ vectors were carried out and the resulting fragments were visualized on a 1% agarose gel to identify the presence of the CB_1 receptor cDNA within the expression vectors.

Figures 2.8 and *2.9* represent the molecular constituents of the $CFPCB_1$ and $YFPCB_1$ vectors respectively. Both CB_1 vector constructs were linearized with HindIII to produce a band at 7139bp, corresponding to the predicted size of the fluorescently tagged expression vectors with the CB_1 cDNA insert (Lane 4, *Figure 2.8* for $CFPCB_1$ and *Figure 2.9* for $YFPCB_1$). The actual presence of the CB_1 cDNA insert was determined for both constructs through restriction enzyme digestion with HindIII and BamHI to produce two fragments corresponding to the size of the individual expression vectors, 5720bp, and the insert 1419bp (Lane 5, *Figure 2.8* for $CFPCB_1$, *Figure 2.9* for $YFPCB_1$). Finally, both vectors with the CB_1 receptor cDNA underwent a restriction enzyme digestion to distinguish between the CFP and YFP variants. The two enzymes HindIII and PstI were used in combination to digest $CFPCB_1$ into four distinct fragments due to the presence of two PstI sites in the CB_1 receptor DNA (*Figure 2.8*, Lane 6). In contrast, digestion of $YFPCB_1$ with HindIII and PstI produced five distinct

fragments (*Figure 2.9*, Lane 6) due to the presence of an extra Pst I restriction enzyme recognition site in YFP, which is absent in CFP.

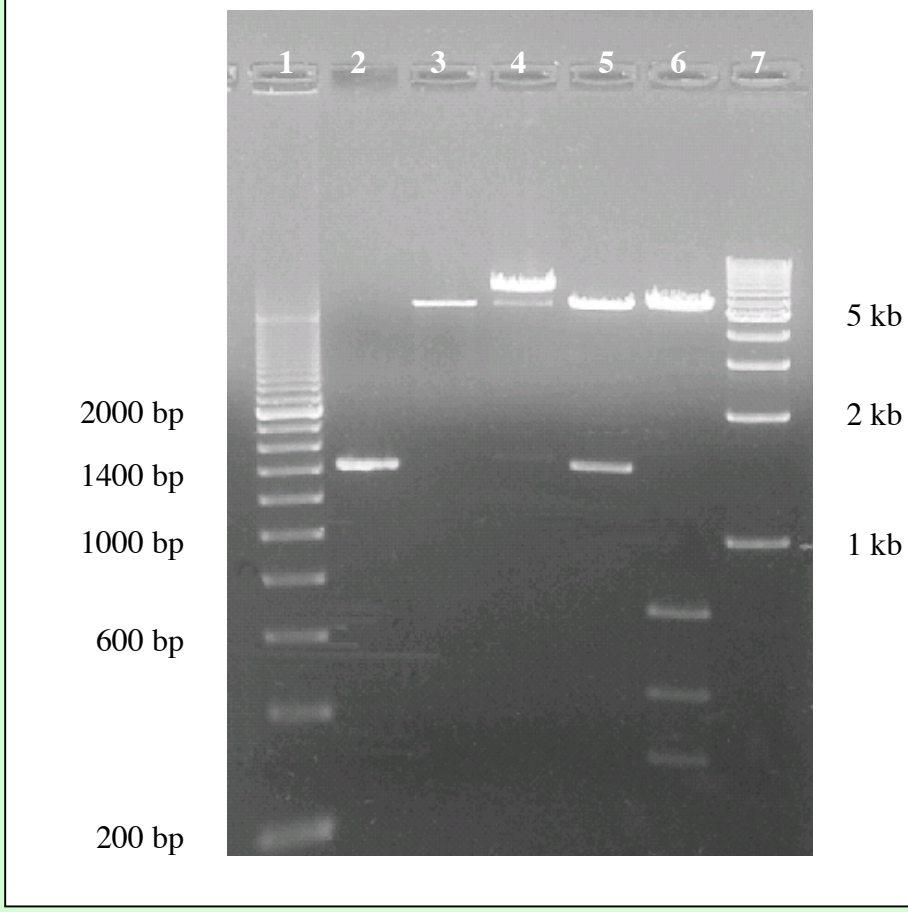

Figure 2.8 - Restriction enzyme analysis of the CFPCB$_1$ vector construct. *CFPCB$_1$ was digested with restriction enzymes to identify the presence of the CB$_1$ receptor cDNA in the CFPzeo expression vector. Lane 1: 200bp ladder. Lane 2: CB$_1$ receptor cDNA amplified by PCR (1419bp). Lane 3: CFPzeo expression vector (5720bp). Lane 4: CFPCB$_1$ linearized with HindIII (7139bp). Lane 5: CFPCB$_1$ digested with HindIII and BamHI to produce the two bands corresponding to the length of the CB$_1$ receptor cDNA (1419bp) and to the expression vector (5720bp). Lane 6: CFPCB$_1$ digested with HindIII and PstI to identify the presence of the CFP. The CB$_1$ receptor cDNA possesses PstI recognition sites (449bp and 1148bp in from the start codon), therefore digestion of CFPCB$_1$ with this combination of enzymes produces four bands as seen above. Lane 7: 1Kb ladder*

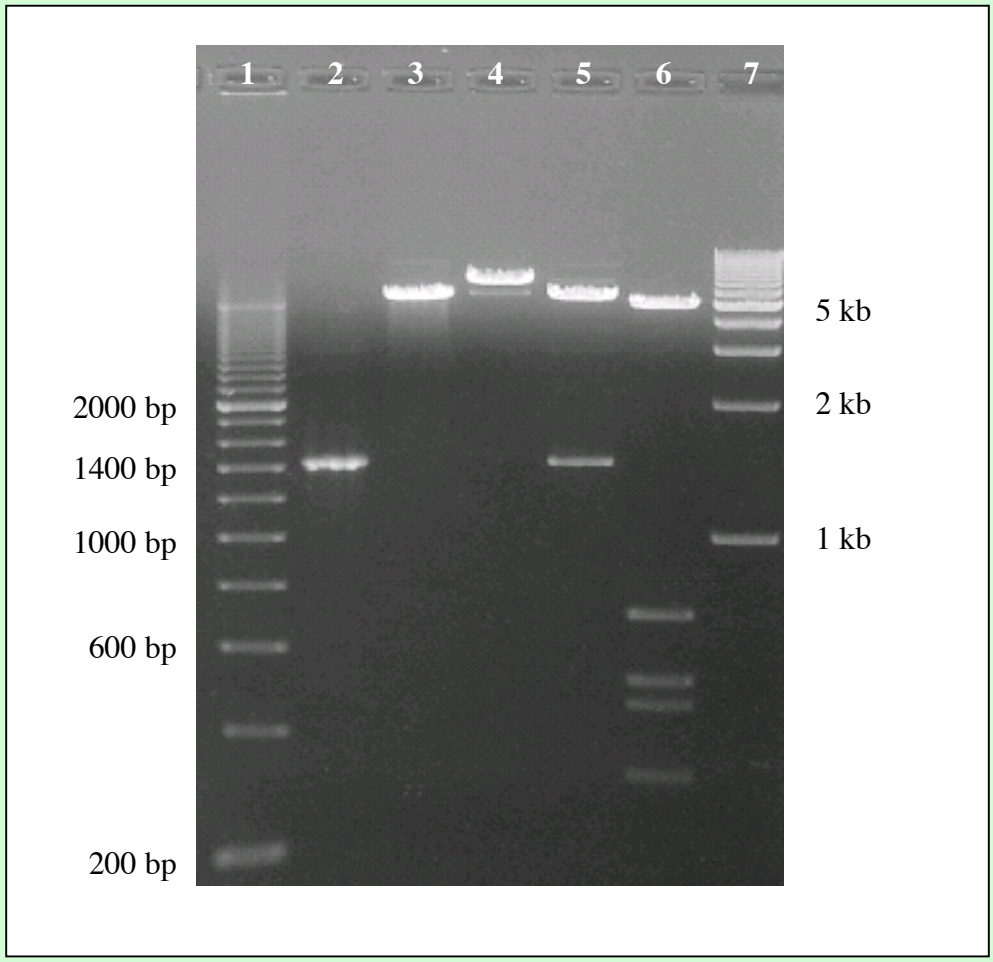

Figure 2.9 - Restriction enzyme analysis of the YFPCB$_1$ vector construct. *YFPCB$_1$ was digested with restriction enzymes to test for presence of the CB$_1$ receptor cDNA in the YFPzeo expression vector. Lane 1: 200bp ladder. Lane 2: CB$_1$ receptor cDNA amplified by PCR (1419bp). Lane 3: YFPzeo expression vector (5720bp). Lane 4: YFPCB$_1$ linearized with HindIII (7139bp). Lane 5: YFPCB$_1$ digested with HindIII and BamHI produces two bands corresponding to the length of the CB$_1$ receptor cDNA (1419bp) and to the expression vector (5720bp). Lane 6: YFPCB$_1$ digested with HindIII and PstI to identify the presence of the YFP. Three PstI recognition sites are located in the YFPCB$_1$ vector construct, two within the CB$_1$ receptor cDNA and one in the YFP cDNA. Therefore digestion of YFPCB$_1$ with this combination of enzymes produces five bands as seen above. Lane 7: 1Kb ladder*

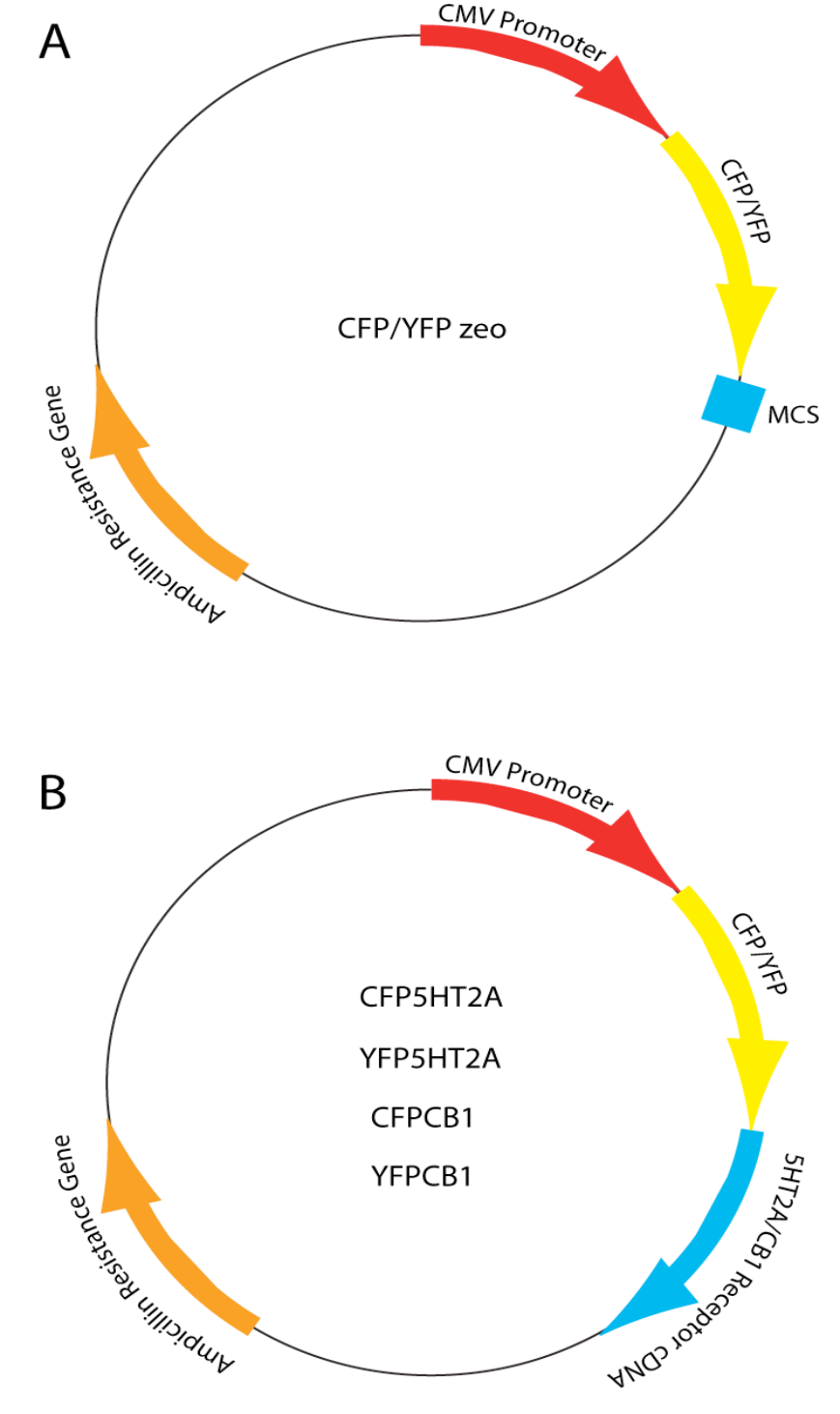

Figure 2.10 - Schematic Representation of Vector Constructs. *(A) Mammalian expression vectors were custom made through the ligation of the CFP or YFP cDNA into the pcDNA3.1zeo vector between the NheI/HindIII restriction enzyme sites to produce the N-terminal CFPzeo and YFPzeo vectors respectively. (B) N-terminally tagged $CFP5HT_{2A}$, $YFP5HT_{2A}$, $CFPCB_1$ and $YFPCB_1$ vector constructs shown above where prepared by the ligation of the respective receptor cDNA into the appropriate sites of the multiple cloning sequence (MCS) of CFPzeo or YFPzeo.*

After completion of the steps above, viable vector constructs were produced and FRET studies could be carried out (see below). The final list of vectors produced was: CFPzeo, YFPzeo, CFP-YFPzeo fusion protein, $CFPCB_1$, $YFPCB_1$, $CFP5HT_{2A}$, $YFP5HT_{2A}$.

FRET Studies

To determine whether the serotonin $5HT_{2A}$ and the cannabinoid CB_1 receptor complexed to form homodimers or heterodimers, BHK-P21 cells were transiently transfected with fluorescently tagged expression vectors containing the respective receptor cDNA. This was followed by analysis, using the FRET equation, of the resulting fluorescence at 480 and 530 nm after excitation at 430 nm. All experiments were performed in triplicate on twenty seven separate occasions (n=81).

Control Experiments

Control experiments were run to validate the use of the CFP and YFP in these FRET studies. A negative control for FRET analysis was run to determine the minimum FRET ratio that would indicate no protein-protein interaction. This was achieved by co-transfection of 0.1 µg of the donor fluorophore vector, CFPzeo, 0.1 µg of the acceptor fluorophore vector, YFPzeo using 2 µL of Lipofectamine 2000 (LF2000) in BHK-P21 cells to produce protein expression levels that would equate to those transfected for the positive controls. This negative control produced a FRET ratio of 0.005 ± 0.004 (Avg ± SEM; *Figure 2.11* column 1; *Table 6*).

The FRET ratio for the negative control was compared to values obtained for a CFP-YFP fusion protein, where the acceptor and donor fluorophores are close enough to ensure that transfer of resonance energy occurred. The positive control experiment

involved the transfection of 0.8 μg of the CFP-YFP fusion protein DNA with 2 μL of LF2000 into each well of BHK-P21 cells. Due to the close proximity of the fluorophores, where separation is via a 23 amino acid bridge, a significantly higher FRET ratio of 0.42 ± 0.02 (Avg ± SEM; *Figure 2.11*, column 2) was observed. This ratio represents 100% transfer of energy between donor and acceptor fluorophores. However, in homodimeric studies, the transfer of energy is only capable in 50% of cases, where a combination of acceptor and donor fluorophore exist (CFP + YFP, and YFP + CFP). The other 50% of interactions are due to formation of complexes between receptors tagged with CFP (CFP + CFP) or receptors tagged with YFP (YFP + YFP). Therefore, to correct this positive FRET ratio and allow it to be compared to the ratios obtained for homodimeric studies, the value obtained was halved to produce a ratio of 0.21 ± 0.01 (Avg ± SEM; *Figure 2.11*, column 3; *Table 6*). Additional negative controls were carried out for the serotonin $5HT_{2A}$ and cannabinoid CB_1 studies, which will be discussed in the appropriate sections.

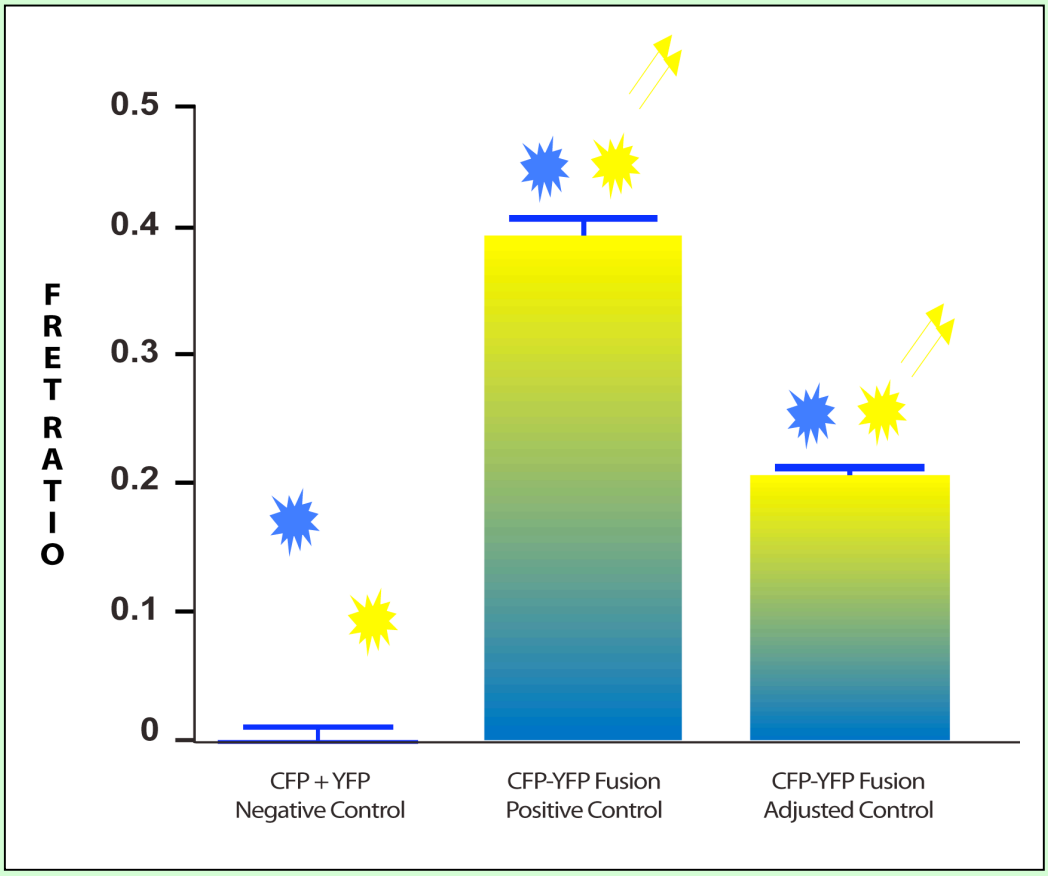

Figure 2.11 - Positive and Negative Controls Determined by FRET Analysis. *To validate the use of the CFP and YFP in these studies, positive and negative control experiments were performed. Column 1 depicts the FRET ratio, determined for the negative control following the co-transfection of equal amounts of the donor (CFP) and acceptor (YFP) fluorophores. Column 2 demonstrates the FRET ratio observed for the positive control, following the transfection of the CFP-YFP fusion protein. Column 3 depicts the adjusted positive control, which is 50% of the positive control and is adjusted to more closely represent the interaction of receptors in homodimeric receptor complexes. The minimal FRET ratio of 0.005 ± 0.004 (Avg ± SEM) indicates that no protein-protein interaction has occurred in the negative control and the close proximity of the two fluorophores in the positive control shows a FRET ratio of significant magnitude. (Blue and yellow "star" shapes indicate CFP and YFP fluorophores).*

Homodimerization Studies of the Serotonin $5HT_{2A}$ Receptor using FRET

Additional negative control experiments were carried out to determine if there was an increase in the FRET ratio when YFP tagged $5HT_{2A}$ receptors were co-expressed with the wild-type CFP fluorophore. If a significant increase in the FRET ratio was observed, it indicates that the CFP fluorophore was interacting with the $5HT_{2A}$ receptor protein. In these experiments zeoCFP (2 μg) was co-expressed with the $YFP5HT_{2A}$ (3.5 μg) using 2 mL of LF2000 in BHK-P21 cells. This produced a FRET ratio of 0.003 ± 0.002 (Avg ± SEM; *Figure 2.12*, column 2; *Table 6*) suggesting no interaction between the CFP protein and the $5HT_{2A}$ receptor.

Homodimerization experiments were performed for the $5HT_{2A}$ receptor with fluorophores attached to the N-terminal end of the receptor. The transfection protocol for these studies included the addition of 3.5 μg of each vector construct containing the receptor DNA and 2 μL of LF2000 into each well for all transfection experiments involving receptor cDNA. When the N-terminal $CFP5HT_{2A}$ and $YFP5HT_{2A}$ were co-expressed the resulting FRET ratio was 0.10 ± 0.02 (Avg ± SEM; *Figure 2.12*, column 3; *Table 6*). This represents a statistically significant increase in FRET ratio compared to negative controls (as determined by the Mann-Whitney test, where $p < 0.05$) indicating that homodimerization of the $5HT_{2A}$ receptor had occurred.

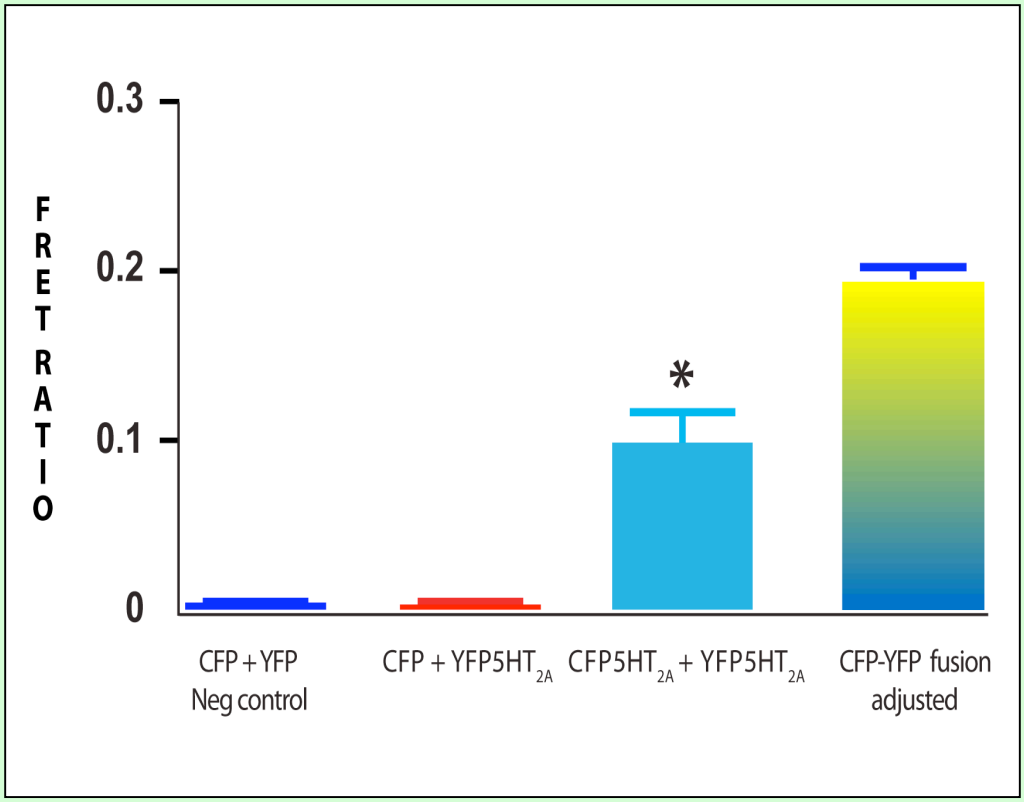

Figure 2.12 - Serotonin $5HT_{2A}$ Homodimerization Studies using FRET Analysis. *Column 1 depicts the negative control (co-transfection of equal amounts of the CFP and YFP vectors). Column 2 is an additional negative control where the CFP vector was co-transfected with the $YFP5HT_{2A}$ vector. Column 3 shows the FRET ratio after the co-transfection of the $5HT_{2A}$ receptor tagged at the N-terminus with CFP or YFP. Column 4 represents the adjusted positive control from co-transfection of the CFP-YFP fusion protein. The results show a significant increase in FRET ratio after $5HT_{2A}$ receptor constructs are co-transfected (n = 12 for each data point).*

** $p < 0.05$ (non-parametric Mann-Whitney test; 95% confidence interval).*

The Serotonin $5HT_{2A}$ Homodimer Saturation Curve

Quantitative analysis of the degree of complexation of the serotonin $5HT_{2A}$ receptor homodimer was performed by constructing a FRET saturation curve for the N-terminal homodimeric complex. This was achieved in a series of experiments where a constant amount of the donor fluorescent protein construct DNA, $CFP5HT_{2A,}$ (3.5 μg) was co-transfected with increasing quantities of the acceptor fluorescent protein construct DNA, $YFP5HT_{2A}$ (7, 14, μg) (*Table 3*). Experiments were performed twelve times in triplicate. The amount of the acceptor fluorescent protein construct DNA was increased until the FRET ratio (y-axis) of the saturation curve began to plateau. This point indicated that all of the donor fluorophores were interacting with an acceptor fluorophore, and the percentage of receptors forming complexes could then be determined.

Table 3

x$YFP5HT_{2A}$ (3.5 μg)	**FRET ratio ± SEM**	**n**
1	0.10 ± 0.02	12
2	0.18 ± 0.02	12
4	0.27 ± 0.05	12
8	0.33 ± 0.07	12
12	0.30 ± 0.07	12

Table 3 - FRET ratios obtained for the $5HT_{2A}$ saturation curve, after transfection of increasing levels of $YFP5HT_{2A}$ DNA.

The proportion of receptors participating in a homodimeric receptor complex can be determined by halving the saturated FRET ratio. This provides a predicted FRET ratio for 100% complexation of the receptors. The comparison of the predicted and observed FRET ratios provides a value for the degree of receptor complexation. *Figure 2.13* demonstrates that the FRET ratio obtained for the saturation level is 0.31 ± 0.04 (Avg ± SEM) with a predicted FRET ratio of 0.15 ± 0.02 (Avg ± SEM). Therefore, as the experimental FRET ratio observed was 0.10 ± 0.02, when the acceptor and donor tagged receptors are expressed in equal amounts, the percentage of receptors involved in heterodimeric complexes was calculated to be 64 ± 11%.

Homodimerization Studies of the Cannabinoid CB_1 Receptor using FRET

Homodimerization studies were also carried out for the CB_1 receptor with fluorophores attached on the receptor's N-terminus. The transfection protocol used here was the same as described for the $5HT_{2A}$ homodimer studies, whereby 3.5 μg of each vector construct containing the receptor DNA and 2 μL of LF2000 was added to each well. Further negative controls were performed to examine the interaction of the wild type CFP and $YFPCB_1$ proteins, as described for the $5HT_{2A}$ receptor homodimers. These experiments resulted in a FRET ratio of 0.001 ± 0.002 (Avg ± SEM; *Table 6*; *Figure 2.14***,** column 2) indicating that there is no interaction between the CFP fluorophore and the CB_1 receptor. Co-expression of the N-terminal $CFPCB_1$ and $YFPCB_1$ vectors resulted in a FRET ratio of 0.18 ± 0.10 (Avg ± SEM; *Figure 2.14*, column 3; *Table 6*). This represents a statistically significant increase in FRET ratio (as determined by the Mann-Whittney test, $P < 0.05$)**,** compared to negative controls (*Figure 2.14*, columns 1 and 2, *Table 6*). These results, obtained using FRET, show that interaction between two CB_1 receptors can occur, suggesting homodimerization of the CB_1 receptor.

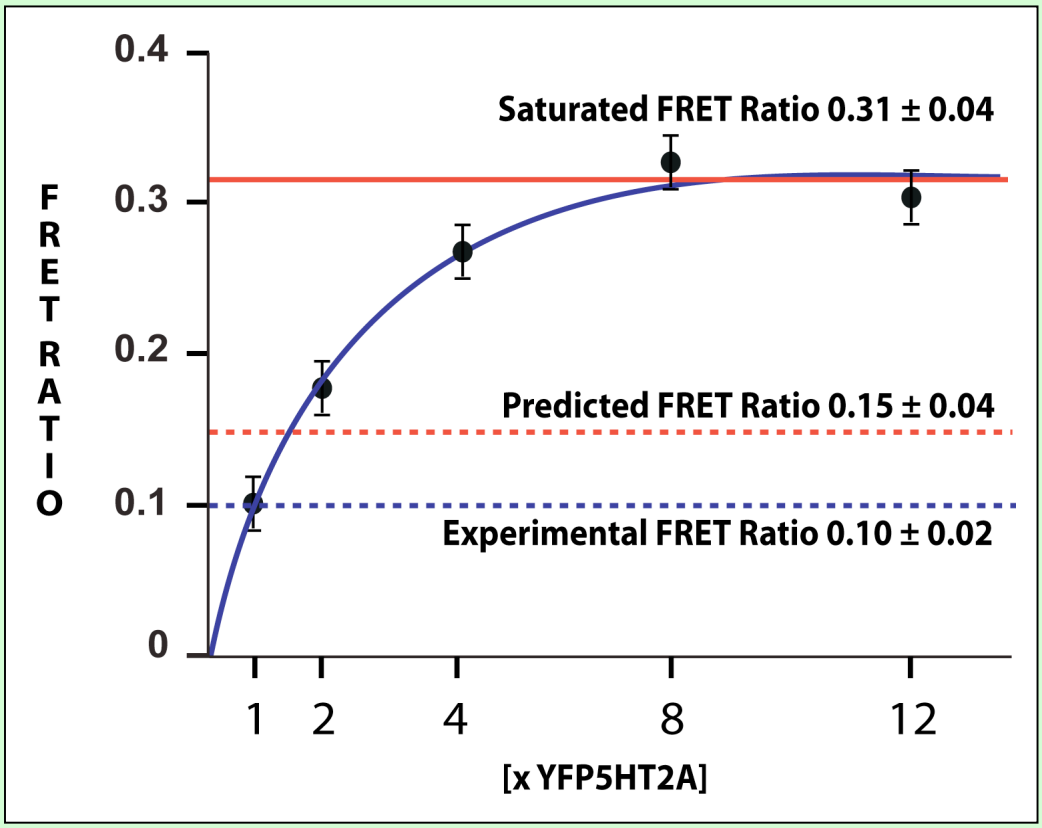

Figure 2.13 - Homodimer Saturation Curve for the $5HT_{2A}$ serotonin receptor. *A FRET saturation curve was constructed by co-transfecting increasing amounts of $YFP5HT_{2A}$ (x-axis) with constant amounts of $CFP5HT_{2A}$ until the FRET ratio (y-axis) plateaued. This indicates the point at which all donor fluorophores are interacting with acceptor fluorophores. The saturated FRET ratio of 0.31 ± 0.04 (Avg ± SEM), was divided by two to produce a predicted FRET ratio (0.15 ± 0.04; Avg + SEM) for 100% receptor complexation. The experimental FRET ratio of 0.10 ± 0.02 (Avg ± SEM) was then calculated as a percentage of the predicted FRET ratio to identify that approximately 64 ± 11% of $5HT_{2A}$ receptors in this system were involved in the formation of the $5HT_{2A}$ homodimer. (n = 12 for each data point).*

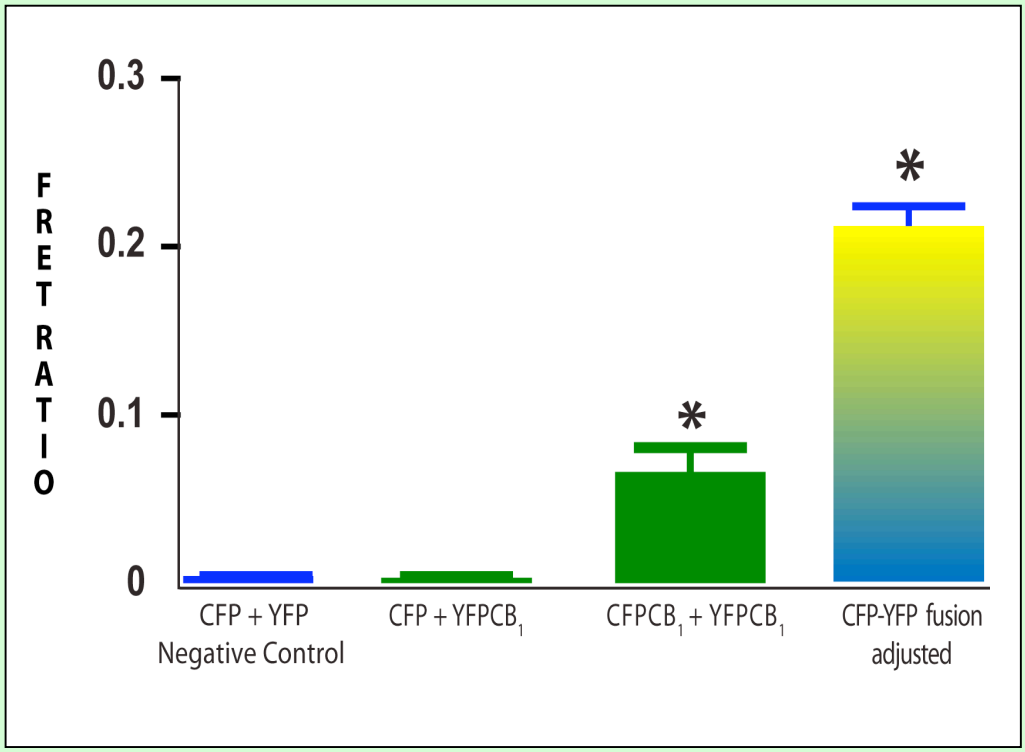

Figure 2.14 - Cannabinoid CB_1 Receptor Homodimerization Studies. *Homodimerization experiments were carried out in BHK-P21 cells for the cannabinoid CB_1 receptor tagged with fluorophores at the N-terminus. From left to right, Column 1 depicts the negative control, resulting from the co-transfection of equal amounts of the CFP and YFP vectors; Column 2 is an additional negative control where the CFP vector was co-transfected with the $YFPCB_1$ vector. Column 3, shows the FRET ratio resulting from co-transfection of the CB_1 receptor tagged at the N-terminus with CFP or YFP; Column 4 represents the adjusted positive control from co-transfection of the CFP-YFP fusion protein. The results show that a significant increase in FRET ratio was observed with co-transfection of the CB_1 receptor constructs. (n = 12 for each data point).*

** $p < 0.05$ (non-parametric Mann-Whitney test; 95% confidence interval).*

The Cannabinoid CB_1 Homodimer Saturation Curve

A saturation curve for the N-terminal labeled CB_1 receptor homodimeric complex was generated, as described for the serotonin $5HT_{2A}$ receptor. Increasing amounts of $YFPCB_1$ DNA (*Table 4*) were transfected in combination with a constant amount of $CFPCB_1$ DNA (3.5 μg) to produce the saturation curve shown in *Figure 2.15*. The percentage of CB_1 receptors involved in the formation of the CB_1 homodimeric complex was calculated as for the $5HT_{2A}$ homodimer above. *Figure 2.15* demonstrates that the saturated level was 0.165 ± 0.009 (Avg ± SEM), and produced a predicted FRET ratio of 0.083 ± 0.009 (Avg ± SEM). The experimental FRET ratio of 0.067 ± 0.010 was calculated as a percentage of the predicted FRET ratio and determined that approximately 81 ± 12% of CB_1 receptors within this system are forming homodimers, indicating a high degree of receptor complexation.

Table 4

x $YFPCB_1$ (3.5 μg)	FRET Ratio ± SEM	n†
1 (3.5 μg)	0.067 ± 0.01	12
2.5 (8.75 μg)	0.09 ± 0.01	12
5 (17.5 μg)	0.12 ± 0.01	12
7.5 (26.25 μg)	0.14 ± 0.01	12
10 (35.0 μg)	0.17 ± 0.01	12
12 (42.0 μg)	0.15 ± 0.01	12

Table 4 - FRET ratios obtained for the CB_1 saturation curve, after transfection with increasing levels of $YFPCB_1$ DNA .

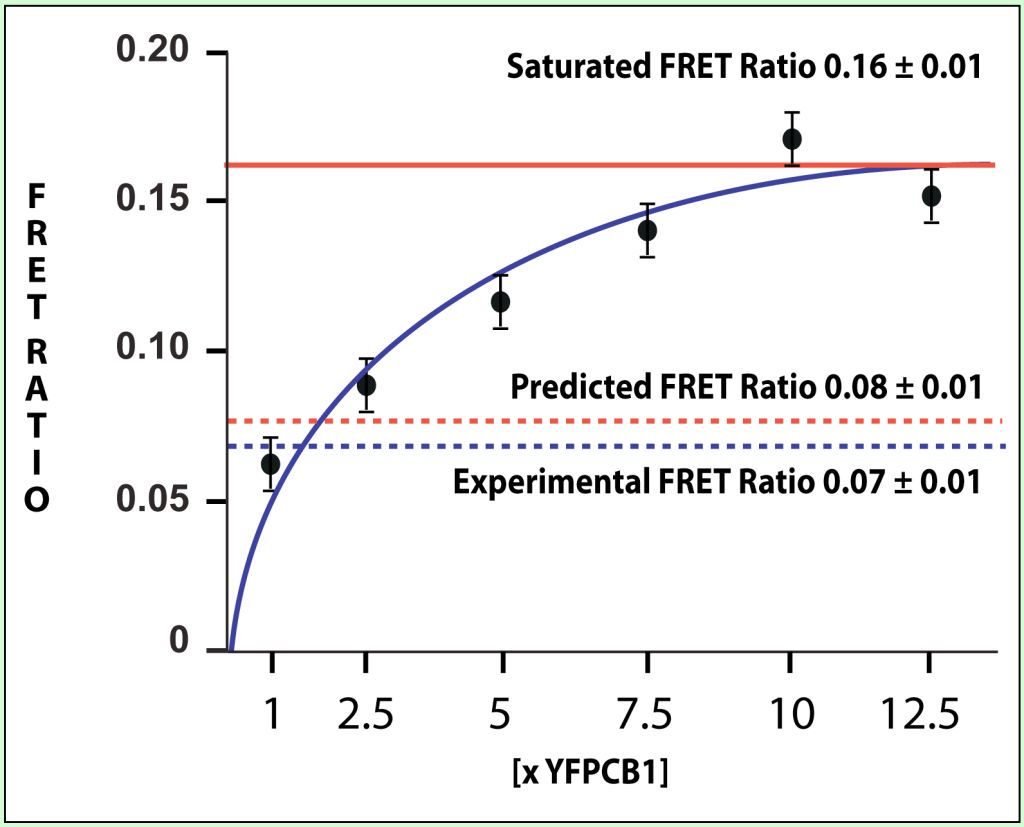

Figure 2.15 - Homodimer Saturation Curve for the cannabinoid CB_1 receptor. *This saturation curve was constructed in order to quantitate the degree of complexation of the cannabinoid CB_1 homodimer. To obtain saturation levels co-transfection of increasing amounts of $YFPCB_1$ (x-axis) and constant amounts of $CFPCB_1$ until the FRET ratio (y-axis) began to plateau. This indicates the point at which all donor fluorophores are interacting with acceptor fluorophores. To produce a predicted FRET ratio of 0.08 ± 0.01 (Avg ± SEM), the saturated FRET ratio (0.16 ± 0.01; Avg ± SEM) was halved. The experimental FRET ratio of 0.07 ± 0.01 (Avg ± SEM) was then calculated as a percentage of the predicted FRET ratio identifying that approximately 81 ± 12% of the CB_1 receptors in this system were involved in the formation of the homodimers. (n = 12 for each data point).*

N-terminal Heterodimerization Studies of the Serotonin $5HT_{2A}$ and Cannabinoid CB_1 Receptors using FRET

Heterodimerization studies were carried out between the serotonin $5HT_{2A}$ and cannabinoid CB_1 receptors contained within the N-terminal expression vectors. All experiments involved the transfection of 3.5 μg of each fluorescently tagged vector containing the receptor DNA and 2 μL of LF2000, into each well of BHK-P21 cells. For the N-terminal heterodimer the FRET ratio was determined for the two combinations of FRET pairs; $CFP5HT_{2A}$ + $YFPCB_1$, and $CFPCB_1$ + $YFP5HT_{2A}$. Co-expression of $CFP5HT_{2A}$ and $YFPCB_1$ resulted in a significantly increased FRET ratio of 0.16 ± 0.03 (Avg ± SEM; *Figure 2.16*, column 2) compared to negative controls, as determined by the Mann-Whitney test ($p < 0.05$). Similarly, the co-expression of the complementary set of receptors, $CFPCB_1$ and $YFP5HT_{2A,}$ resulted in a FRET ratio of 0.70 ± 0.2 (Avg ± SEM; *Figure 2.16*, column 3) which is significantly increased when compared to the negative control values ($p < 0.05$). These results suggest that heterodimerization occurs between these two receptor types.

The Heterodimer Saturation Curve:

To quantitate the percentage of receptor complexation occurring between the two different receptor types, the saturation curve for the serotonin $5HT_{2A}$ and cannabinoid CB_1 receptor heterodimer was generated in the same manner described for the serotonin $5HT_{2A}$ receptor. A constant amount of $CFPCB_1$ DNA (3.5 μg) was co-transfected with increasing amounts of $YFP5HT_{2A}$ (7, 14, 28, 42 μg) (*Table 5*) to produce the saturation curve shown in *Figure 2.17*. The percentage of receptors involved in the formation of the serotonin $5HT_{2A}$/cannabinoid CB_1 complex was calculated as described previously. The heterodimer saturation curve (*Figure 2.17*) demonstrates that the saturated level was 0.70 ± 0.04 (Avg ± SEM) from which the predicted FRET ratio was calculated as

0.35 + 0.02 (Avg ± SEM). The experimental FRET ratio of 0.09 ± 0.01 was calculated as a percentage of the predicted FRET ratio, which determined that 25 ± 3% of the expressed receptors were involved in the heterodimeric receptor complex.

Table 5

x $YFP5HT_{2A}$ (3.5 µg)	FRET ratio ± SEM	n
1 (3.5 µg)	0.09 ± 0.01	12
2 (7.0 µg)	0.30 ± 0.02	12
4 (14.0 µg)	0.46 ± 0.02	12
8 (28.0 µg)	0.63 ± 0.02	12
10 (35.0 µg)	0.73 ± 0.04	12
12 (42.0 µg)	0.71 ± 0.03	12

Table 5 - FRET ratios obtained for the $CB_1/5HT_{2A}$ heterodimer saturation curve, after transfection of increasing levels of $YFP5HT_{2A}$ DNA.

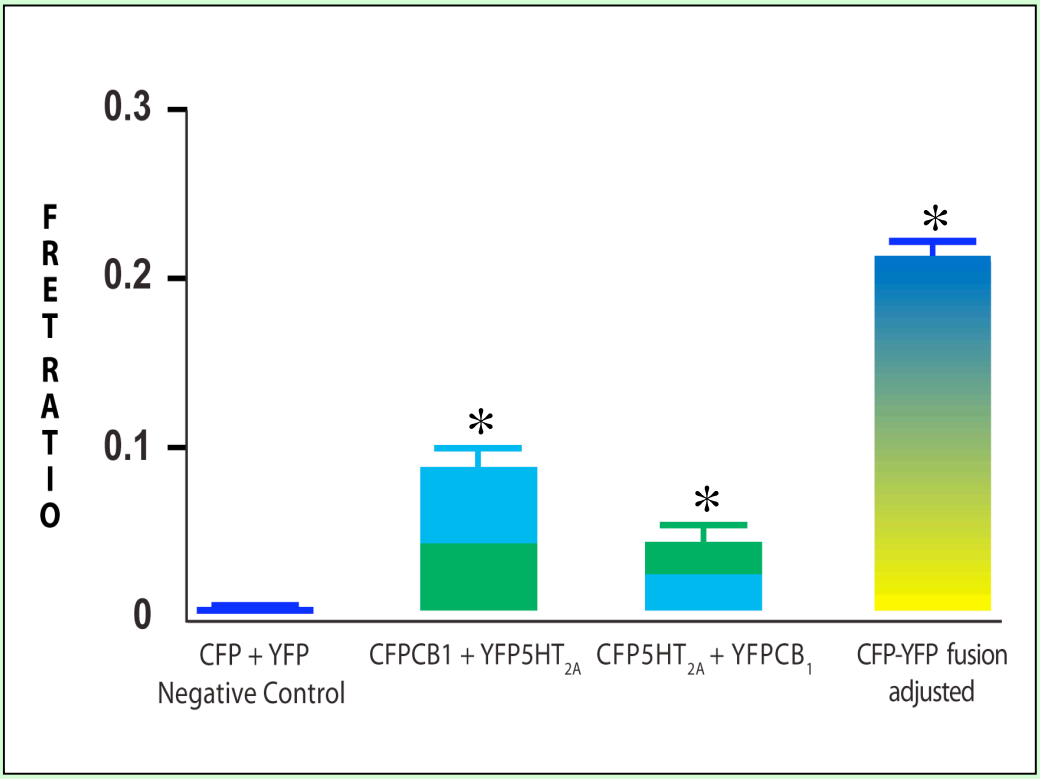

Figure 2.16 - N-terminal Heterodimerization Studies. *Heterodimerization experiments were carried out by determining the FRET ratios for the serotonin $5HT_{2A}$ receptors and cannabinoid CB_1 receptor tagged with fluorophores at the N-terminus when co-transfected into BHK-P21 cells. From left to right, Column 1 depicts the negative control, resulting from the co-transfection of the equal amounts of the CFP and YFP vectors; Column 2 depicts the FRET ratios for the N-terminally tagged $CFP5HT_{2A}$ and $YFPCB_1$; Column 3 represents the FRET ratios for the N-terminally tagged $CFPCB_1$ and $YFP5HT_{2A}$; Column 4 represents the adjusted positive control from co-transfection of the CFP-YFP fusion protein. The results show that the N-terminally tagged receptor/fluorophore combinations produced a significant increase in FRET ratio (Column 2 and 3; n = 12 for each data point).*

** $p < 0.05$ (non-parametric Mann-Whitney test; 95% confidence interval).*

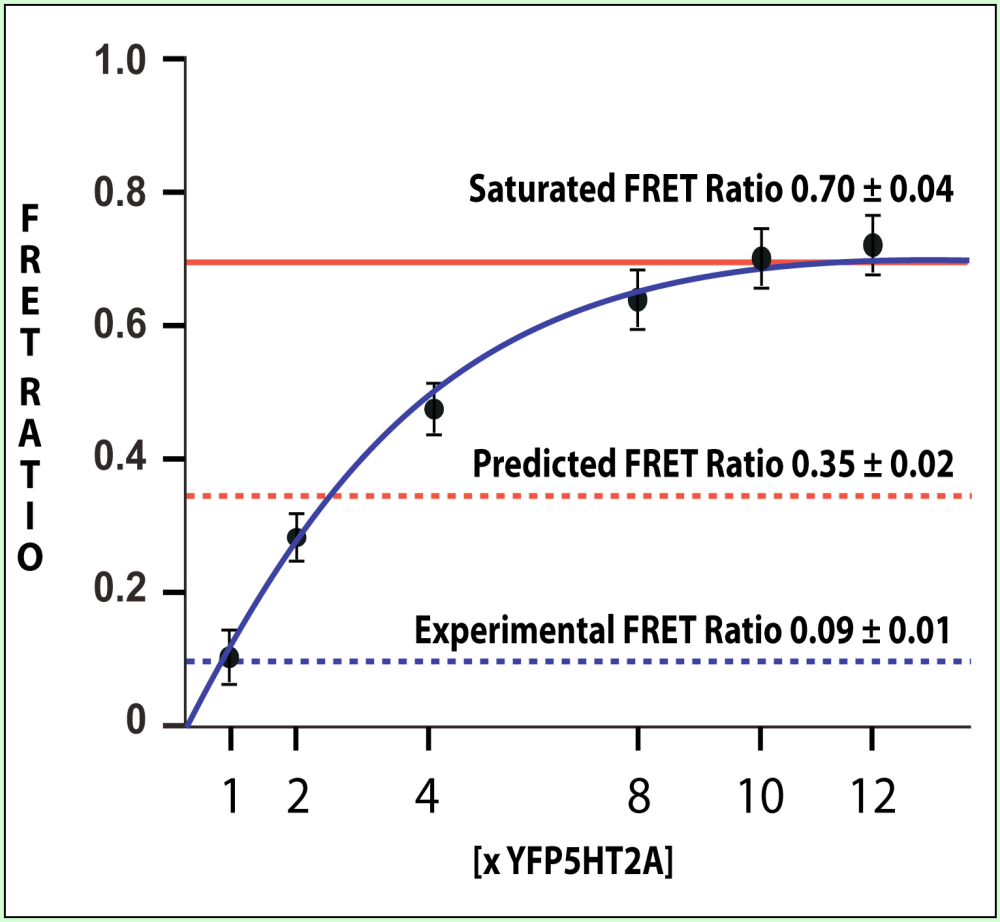

Figure 2.17 - Heterodimer Saturation Curve for the $5HT_{2A}$ and CB_1 receptors. *The percentage of receptor complexation occurring between the serotonin $5HT_{2A}$ and cannabinoid CB_1 receptors was determined following the construction of the FRET saturation curve above. Increasing amounts of $YFP5HT_{2A}$ (x-axis) and constant amounts of $CFPCB_1$ were co-transfected until the FRET ratio (y-axis) plateaued. This indicates the point at which all donor fluorophores are interacting with acceptor fluorophores. The saturated FRET ratio, determined as 0.70 ± 0.04 (Avg ± SEM), was divided by two to produce a predicted FRET ratio (0.35 ± 0.02; Avg + SEM) for 100% receptor complexation. The experimental FRET ratio of 0.09 ± 0.010 (Avg ± SEM) was then calculated as a percentage of the predicted FRET ratio. This suggested that approximately 25 ± 3% of $5HT_{2A}$ and CB_1 receptors in this system were involved in the formation of this complex. (n = 12 for each data point).*

At the completion of FRET studies, it was apparent that homo- and heterodimerization of various combinations of receptors had occurred. A summary table is provided below (*Table 6*), indicating the average FRET ratios for all control, homodimer and heterodimer experiments.

Table 6

Vector Constructs	**Average FRET ratio (± SEM)**	**Number of Experiments (n)**
Negative Control	0.005 ± 0.004	12
zeoCFP + $YFP5HT_{2A}$	0.003 ± 0.002	12
zeoCFP + $YFPCB_1$	0.001 ± 0.002	12
Positive Control Positive Control (corrected)	0.42 ± 0.02 0.21 ± 0.01#	12
$CFP5HT_{2A}$ + $YFP5HT_{2A}$ Homodimer	0.10 ± 0.02*	12
$CFPCB_1$ + $YFPCB_1$ Homodimer	0.07 ± 0.01*	12
$CFP5HT_{2A}$ + $YFPCB_1$ Heterodimer	0.05 ± 0.01*	12
$CFPCB_1$ + $YFP5HT_{2A}$ Heterodimer	0.09 ± 0.01*	12

Table 6 - Average FRET ratios for control, homodimer and heterodimer experiments.

** $p<0.05$ (non-parametric Mann-Whitney test; 95% confidence interval)*

 # Positive control value has been halved because only 50% of receptors are relevant for FRET

Discussion

The main findings of this chapter show that both serotonergic $5HT_{2A}$ and cannabinoid CB_1 receptors are capable of homodimerization when expressed in physiologically-relevant concentrations in cultured BHK cells. Additionally, it was shown that these receptors can form heterodimers, with each other, when co-expressed in the same cells.

Methodological Considerations

An important goal of this study was to determine the ability of the FRET expression system to detect constitutive homo- and heterodimeric serotonin and cannabinoid receptor complexes. To validate the FRET system, a series of control experiments were performed to obtain parameters from which GPCR receptor complexation could be measured. The minimum FRET ratio, which is due to the interaction of the donor and acceptor fluorophores following random collision, was identified by co-expression of the individual wild-type CFP and YFP in BHK-P21 cells. Additionally, the transfection of the CFP-YFP fusion protein was used as a positive control to determine the FRET signal for a fixed distance and orientation of the acceptor and donor fluorophores. For the CFP-YFP fusion protein, the two different fluorophores are fused together and are therefore fixed in a physical proximity. This allows the transfer of resonance energy between the two fluorophores in all of the expressed CFP-YFP protein, producing a significant increase in FRET ratio compared to the negative control (*Figure 2.11*). However, in homodimeric receptor studies where a 1:1 ratio of the donor and acceptor fluorophores are attached to the receptors, and assuming 100% complexation of the tagged receptors has occurred, it is assumed that the FRET signal obtained is due to only 50% of the interacting receptor population (i.e. CFP+YFP and YFP+CFP). The other 50% of tagged receptor interactions are occurring between receptors that are both

attached to CFP (25% of the population) or both attached to YFP (25% of the receptor population) (*Figure 2.19*). Since these last two possible combinations do not contain a mixture of donor and acceptor fluorescent proteins, transfer of resonance energy does not occur and are thus irrelevant for the purpose of FRET analysis. Therefore to provide a more suitable positive control for the receptor studies, the FRET ratio for this CFP-YFP fusion protein was taken as 50% of the observed value (*Table 6*, *Figure 2.11*).

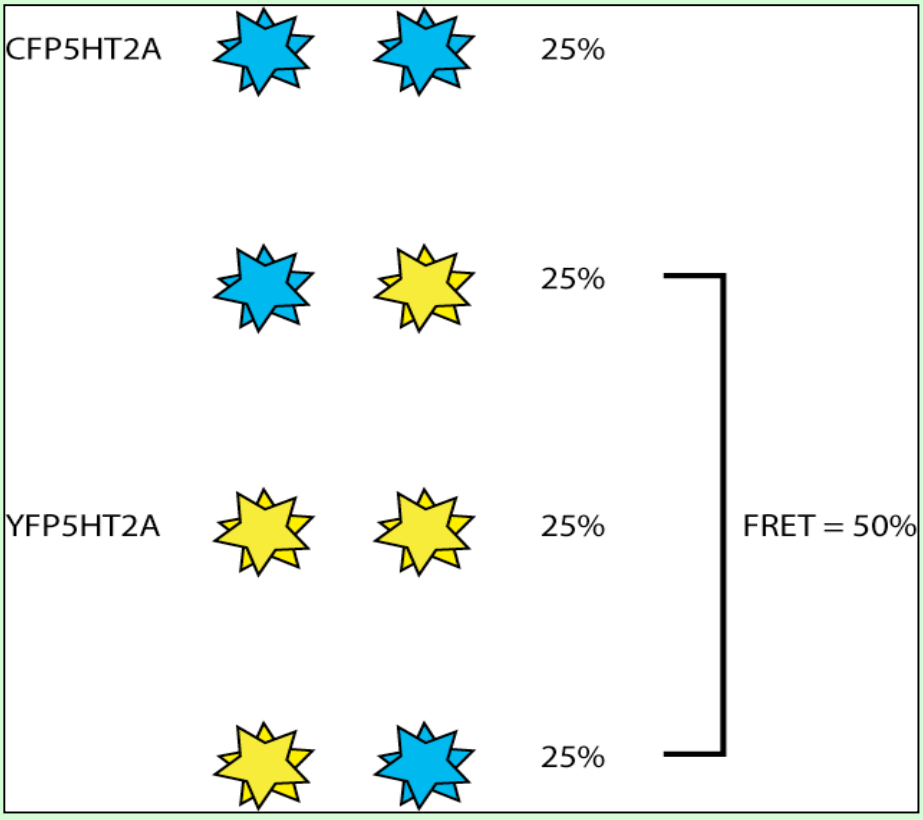

Figure 2.19 - *The distribution of possible combinations of fluorophores in a homodimeric receptor complex following co-expression of equal quantities of CFP and YFP-tagged receptors. Only 50% of combinations are relevant for FRET.*

Further negative controls involving the co-expression of the wild type CFP and either the serotonin $5HT_{2A}$ or cannabinoid CB_1 receptor tagged with YFP, were also carried out to ensure that an increase in the FRET signal was not due to the interaction of the fluorophores with the receptor protein (*Figure 2.12* and *2.14* respectively; *Table 6*). The FRET ratios yielded by these controls were extremely low, indicating that no interaction occurred between the wild type CFP and the $YFP5HT_{2A}$ or the $YFPCB_1$. Therefore, any increase in the FRET ratio observed following the co-expression of fluorescently tagged receptors was concluded to be the result of receptor complexation.

The serotonin and cannabinoid receptors have both been previously shown to exist as homodimers. However, rather than utilising sensitive techniques like BRET or FRET, these studies have generally employed biochemical techniques such as co-immunoprecipitation or radio-labeling (Ng *et al.*, 1993; Wager-Miller *et al.*, 2002). Although biochemical techniques are capable of detecting complexation, it is associated with several disadvantages. These include the use of non-living tissue where the invasive lysis of cells and solubilization of receptors are required. This can lead to artefacts associated with the aggregation of proteins, which can be mistaken for receptor complexes (Angers *et al.*, 2001).

My studies were able to use a validated FRET technique to provide supporting evidence for the existence of both the human serotonin $5HT_{2A}$ and human cannabinoid CB_1 receptor as homodimers. Furthermore, the percentage of complexation is greater in CB_1 than $5HT_{2A}$ receptor homodimers. This phenomenon may be due to the higher tendency for CB_1 receptors to form constitutive homodimers, or an equally plausible scenario whereby $5HT_{2A}$ receptors could be complexing with endogenous receptors in the

experimental kidney cells, as reported by Endlich *et al.* (1993), leading to a lower availability of receptors to participate in FRET.

Reports have shown that the transmembrane regions acting as interfaces for GPCR homodimeric complexes can differ. For example, the interface for the β_2-adrenergic receptor was shown to involve the TM6 regions (Hebert *et al.*, 1996), whilst the interaction between yeast α-factor GPCRs has been demonstrated to occur between TM1 regions (Overton *et al.*, 2003). This suggests that the TM domain involved in the complexation of receptors, is dependant upon the receptor type. Currently, the TM interface for both the CB_1 homodimer and $5HT_{2A}$-CB_1 heterodimer is unknown. The future identification of these receptor complex interfaces would be useful in determining the conformational structure of these receptor complexes.

This thesis, reports the first observation of a heterodimeric $5HT_{2A}$-CB_1 receptor complex. It was observed that when the $5HT_{2A}$ and CB_1 receptors were attached to N-terminal fluorophores to produce the two possible combinations of FRET pairs $CFP5HT_{2A}$ + $YFPCB_1$ and $CFPCB_1$ + $YFP5HT_{2A}$, a significant increase in FRET ratio was observed for both combinations compared to negative controls, indicating the formation of a novel heterodimeric complex (*Table 6*; *Figure 2.16*). However, after comparison of the two FRET ratios, it was recognized that the switching of the donor and acceptor fluorophores to the different receptors produced a FRET ratio of lesser magnitude for the $CFP5HT_{2A}$ + $YFPCB_1$ FRET pair with respect to the $CFPCB_1$ + $YFP5HT_{2A}$ combination (*Table 6*; *Figure 2.16*). Although this difference in the FRET ratio following the switching of the fluorophores has also been identified in a number of heterodimeric complexes (Mercier *et al.*, 2002; Kamiya *et al.*, 2003; Stanasila *et al.*,

2003; Terrillon *et al.*, 2003; Breit *et al.*, 2004), an explanation of this reproducible effect does not exist in the literature. I propose that the switching of the fluorophores in a heterodimeric receptor complex results in a change in relative orientations of the dipole of the acceptor and donor fluorophores. The influence of this change in orientation on the FRET ratio may cause the fluorophores to be fixed in a less favourable orientation, which would decrease the efficiency of resonance energy transfer. This demonstrates that in addition to the distance between the fluorophores, the relative orientation of the fluorescent proteins is also an important factor in determining FRET efficiency.

An increase in FRET ratio when the receptors are tagged to the donor and acceptor fluorophores and expressed in equal proportions (1:1 ratio), indicates that the distance between the fluorophores is small enough for the transfer of energy to occur and hence complexation has occurred. However, the magnitude of the FRET ratio does not correlate with the degree or percentage of the receptor complexation taking place.

To reliably determine the amount of receptor complexation occurring, a FRET signal when 100% of the donor fluorophores were participating in FRET interactions with acceptor fluorophores was required. This was achieved by a series of co-transfection experiments, whereby the quantity of the YFP-tagged receptor vector DNA was increased relative to the CFP-tagged receptor vector DNA until there was no significant increase in the observed FRET ratio. When the FRET ratio achieved a plateau with respect to increasing YFP fluorescence, this indicated that the CFP fluorophores were 100% involved in receptor complexation. This saturated FRET value could then be divided in half to give the predicted FRET ratio that represents the FRET signal for a theoretical 50% of the population of expressed receptors involved in receptor complexes. Comparison of the experimental or observed FRET ratio to this figure was a

measure of the percentage of the population of receptors participating in complexation (Mercier *et al.*, 2002).

The saturation curves for the $5HT_{2A}$ and CB_1 homodimeric receptor complexes indicated that a large percentage of the expressed receptors were involved in constitutive homodimerization, 64 ± 11% and 81 ± 12% respectively (*Figures 2.13* and *2.15*). This high degree of homodimerization is comparable to the 82 ± 10% homodimerization reported for the β_2-adrenergic receptor (Mercier *et al.*, 2002). Indeed, there is a wealth of radioligand binding and co-immunoprecipation studies that also support this high level of constitutive homodimerization of GPCRs in general. This data is exemplified by Atomic Force Microscopy of rhodopsin receptors in the retina that are pictured as highly organized rows of dimeric structures with very few individual receptors observed (Liang *et al.*, 2003). This study also showed that at the very least, a dimer would be required to provide an appropriate 'footprint' for the binding of a single heterotrimeric G protein, although this assumption has now been refuted (Goudet *et al.*, 2005; Hlavackova *et al.*, 2005).

In contrast, the saturation curve constructed for the $5HT_{2A}$-CB_1 heterodimeric receptor complex indicates that a lower level of heterodimerization occurred, 25 ± 3% (*Figure 2.17*) relative to the homodimerization of each of the receptors. Similar reports of the low ability of GPCRs, which possess a dissimilar sequence homology such as the δ opioid (DOP) and β_2-adrenergic receptors to form heterodimeric receptor complexes have been published (Ramsay *et al.*, 2002). In contrast, GPCRs with significant sequence homology such as that shared by the DOP and KOP opioid receptor, display a greater ability to form heterodimeric receptor complexes (Ramsay *et al.*, 2002).

The saturated FRET ratio for the CB_1-$5HT_{2A}$ receptor pairing I found (0.70) is clearly not only significantly greater in magnitude with respect to the experimental FRET ratio observed for the 1:1 ratio of expressed CFP and YFP tagged receptors, indicating the low percentage of the $5HT_{2A}$ and CB_1 receptors that are involved in heterodimerization, but also exceeds the magnitude of the saturated FRET ratio for both $5HT_{2A}$ and CB_1 homodimeric receptor complexes. There are a number of possible reasons to account for this large shift in the intensity of the FRET interaction in the heterodimeric receptor complex. It may indicate that there is a significant decrease in the distance between the fluorophores and/or a marked change in their relative orientations. A large decrease in the distance, or shift in the orientation of the fluorophores, suggests that the receptor interface for the heterodimeric receptor complex is likely to be different to the interface of homodimeric receptor complexes. The large increase in the saturated FRET ratio for the $5HT_{2A}$-CB_1 heterodimeric receptor complex suggests that the interface has shifted closer to the N-terminal tagged fluorophores indicating that the interface is more likely to be closer to the TM 1-2 regions rather than at the TM4 region that has been shown for the D_2 homodimer (Guo *et al.*, 2003) or the TM5-7 regions as reported for the β_2-adrenergic receptor (Hebert *et al.*, 1996).

In addition, the receptor-receptor interaction may be occurring with more than two receptors, allowing the formation of a hetero-oligomer. In this complex the donor CFP tagged to the CB_1 receptor could be transferring energy to two or more YFP-tagged $5HT_{2A}$ receptors, depending upon how many $5HT_{2A}$ receptors are associated in the receptor complex. This would result in an increase in yellow fluorescence emission, producing a higher FRET ratio. Further experimentation using the various combinations of fluorophore-tagged and untagged receptors will be required to determine whether the

formation of a hetero-oligomeric receptor complex occurs following the co-expression of $5HT_{2A}$ and CB_1 receptors.

Biological implications of GPCR dimerization

Since GPCR dimerization can result in functional changes in the activity of various receptors, this raises questions about the physiological relevance of the dimerization I observed for CB_1 and $5HT_{2A}$Rs. It has been suggested that GPCR heterodimerization provides yet another level of control at synapses, and that the co-release of neuromodulators could selectively activate postsynaptic heterodimers (Rios *et al.*, 2001). The fact that heterodimers form unique signaling entities, could mean that they are a target for particular orphan peptide ligands (i.e. ligands for which receptors have not yet been identified or *vice versa*). Furthermore, a neuron could regulate the level of expression and type of GPCR dimer pairings in response to certain ligands.

Hermann *et al.* (2002) reported that the CB_1 receptor is coexpressed in mouse forebrain with dopamine and serotonin receptors either in principal projecting neurons or in interneurons. These receptor systems are suggested to synergistically modulate both excitatory and inhibitory circuits. In the striatum, high coexpression of CB_1 with dopamine and serotonin receptors suggests putative crosstalk between the cannabinoid system and other neurotransmitter systems involved in regulating locomotor activity. Whilst in the cortex, high coexpression levels of cannabinoid, dopamine and serotonin receptors suggest a functional role of these systems in working memory and cognitive functions. Further, the dimerization of CB_1 and $5HT_{2A}$ receptors could have dramatic effects on the pronociceptive nature of the serotonergic system in the spinal cord. That is, if the CB_1 receptor can prevent the binding, trafficking or internalization of $5HT_{2A}$

receptors, then neuropathies that are known to occur via $5HT_{2A}$R-mediated mechanisms could be effectively treated.

Whatever the case, it is clear that further studies of the biological, biochemical, and biophysical properties of GPCR dimers are necessary to fully understand the physiological significance of this phenomenon. Improved techniques for the study of GPCR dimerization in the whole animal, and the development of reagents such as antibodies, specific for the dimeric forms of the receptors, will assist in the elucidation of this phenomenon. Indeed, it may turn out that targeting particular GPCR dimer pairings proves fruitful in rational drug design.

Summary

In summary, I have shown that CB_1 and $5HT_{2A}$ receptors can form both homo- and heterodimers. This interaction has implications for the involvement of cannabinoid CB_1 and serotonergic $5HT_2$ receptors in pain signaling. Thus, future studies aimed at understanding the role of either cannabinoid or serotonergic receptors must consider the potential interaction of these two receptor types.

CHAPTER 3

Cannabinoids and inhibitory mechanisms in the dorsal horn of the spinal cord

Introduction

A major theme discussed throughout this thesis is the interaction of cannabinoids with components of the pain system. The previous experiments dealt with issues that exist at the molecular level, specifically CB_1R and $5HT_{2A}$ receptor homo- and heterodimerization. In this chapter I used a number of techniques to examine the interactions between cannabinoids and various receptor and signaling molecules within the spinal cord dorsal horn, in an attempt to explain some of the mechanisms underlying cannabinoid analgesia.

When viewed in cross-section, the spinal cord can be subdivided into regions known as laminae (Rexed, 1952, 1954; *Figure 3.1*). The superficial dorsal horn (SDH) comprises laminae I and II, the intermediate dorsal horn lamina III (IDH) and the deep dorsal horn consists of laminae IV-VI (DDH). The ventral horn is made up of laminae VII-IX and lamina X surrounds the central canal. The SDH and DDH of the spinal cord dorsal horn are important sites for processing sensory information arising in skin, muscle, joints and viscera (Willis & Coggeshall, 2004a). This information arrives in the dorsal horn via primary afferents which have specific termination patterns in the SDH and DDH depending largely upon their peripheral origin, axon diameter and sensory modality (Light & Perl, 1979a, 1979b; Brown, 1982; *Figure 3.2*). The SDH receives inputs predominately from small diameter Aδ and C-fibres carrying nociceptive, thermal, itch, and innocuous tactile information (Christensen & Perl, 1970; Sugiura *et al.*, 1986; Tuckett & Wei, 1987a; Tuckett & Wei, 1987b; Vallbo *et al.*, 1999).

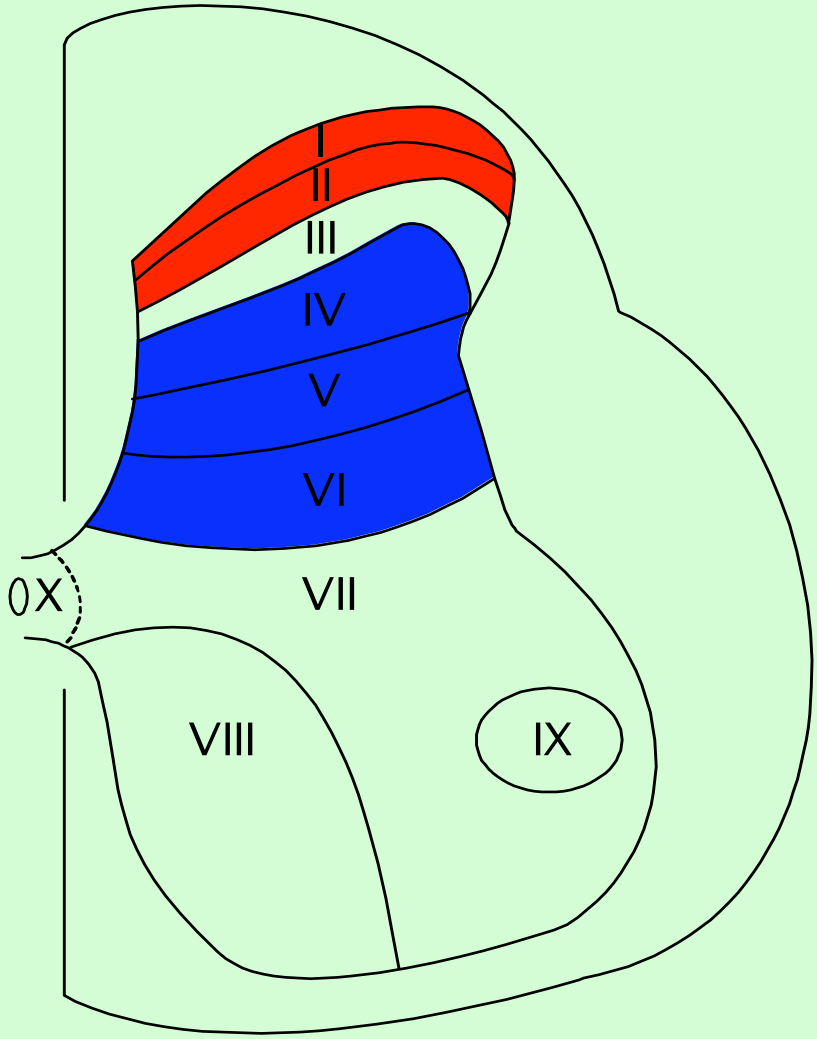

Figure 3.1 - Rexed Laminae of the Spinal Cord. *One classical system for describing the different regions of the spinal cord was devised by Bror Rexed (Rexed, 1952, 1954). He divided the spinal cord into 'laminae'. There are ten laminae and they are designated using Roman numerals I-X. The dorsal horn is considered to consist of laminae I-VI whilst the ventral horn contains laminae VII-IX and lamina X encircles the central canal. The dorsal horn can be further separated into the superficial dorsal horn (SDH; laminae I-II; shaded* ***RED****) the intermediate dorsal horn (IDH; laminae III; unshaded) and the deep dorsal horn (DDH; laminae IV-VI; shaded* ***BLUE****). Lamina II is also termed the substantia gelatinosa and has been subdivided further into an inner (II_i) and outer segment (II_o).*

The DDH, in contrast, receives predominately large Aβ myelinated fibres carrying tactile information, along with C-fibre input from viscera and some nociceptive information via Aδ and possibly Aβ fibres (Burgess & Perl, 1973; Schneider, 1992). Additional nociceptive information also arrives in the DDH via interneurons that connect the two regions (Burgess & Perl, 1973; Schneider, 1992; Willis & Coggeshall, 2004b). These connections possibly allow crosstalk between the SDH and DDH (Zeilhofer & Zeilhofer, 2008).

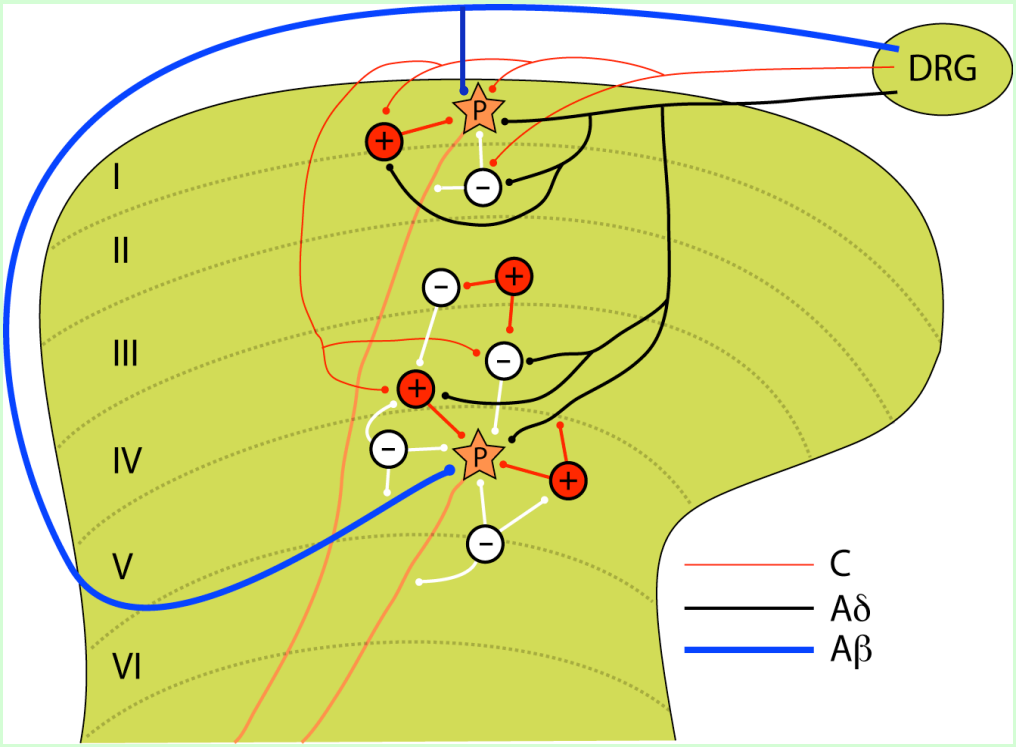

***Figure 3.2 - Spinal cord dorsal horn circuitry**. The spinal cord dorsal horn receives inputs from Aβ, Aδ, and C-fibre primary afferents, which terminate in different laminae throughout superficial and deep regions. A large proportion of neurons in the dorsal horn are interneurons. These can be either excitatory (**RED** circles) or inhibitory (**WHITE** circles) and modulate the actions of projection neurons in lamina I and V (**ORANGE** stars), to shape the output of the two regions and ultimately pain perception. Other inputs to dorsal horn neurons originate from the descending inhibitory system (Millan, 2002). Connections also exist between the SDH and DDH, meaning a certain level of crosstalk exists between the SDH and the DDH.*

Like the primary afferent termination patterns, outputs from the SDH and DDH via their projection neurons, also differ. Projections from the SDH terminate in various brainstem and midbrain structures, with recent work indicating the dominant projections are to brainstem sites like the parabrachial nuclei and periaqueductal grey (Klop *et al.*, 2005). In contrast, projections from the DDH terminate predominately in the thalamus (Kobayashi, 1998; Willis *et al.*, 2001). Importantly, more than 95% of neurons in the dorsal horn are local circuit interneurons whose axons are confined to the dorsal horn (Spike *et al.*, 2003; Polgar *et al.*, 2004; Willis & Coggeshall, 2004a). These interneurons can be excitatory or inhibitory in nature, and receive inputs from higher brain centres, the periphery, and other intra- and interlaminal interneurons (Light & Kavookjian, 1988; Willis & Coggeshall, 2004a; *Figure 3.2*).

Interneurons have a major impact on the output of the projection neurons (Melzack & Wall, 1962, 1965) (*Figure 3.2*). It is therefore understandable, that any process or agent that changes the excitability of these interneurons (such as cannabinoids) could have implications for spinal cord processing of nociceptive and tactile information. Recent evidence also suggests that synaptic processing differs in the SDH and DDH. Paired recordings from neurons in the SDH indicate that a modular pattern of synaptic linkages connects a “limited” number of specific neuronal types (Lu & Perl, 2003, 2005). Similar recordings in the DDH suggest more extensive synaptic connectivity between the various neuronal types (Schneider, 2008). Surprisingly, no study has simply compared synaptic transmission (either excitatory or inhibitory) in the SDH and DDH.

Inhibitory synaptic transmission in the dorsal horn

The importance of inhibitory synaptic transmission in processing nociceptive information in the spinal cord has been recognized since the publication of Melzack and Wall's "gate control theory of pain" (Melzack & Wall, 1965). Since that time, a critical role for glycine and GABA as the principal sources of fast synaptic inhibition has been established (Krnjevic & Schwartz, 1967; Werman *et al.*, 1967; Curtis *et al.*, 1968a, b; Curtis *et al.*, 1968c). Evidence is now accumulating to suggest inhibitory neurotransmission may differ in the SDH and DDH of the dorsal horn. For example, Cronin *et al.* (2004) showed that the relative contribution of glycine and GABA receptors (GlyR and $GABA_AR$ respectively) to tonic inhibition differs between the SDH and DDH in the rat. More recently, an unusual form of the GlyR, containing alpha3-subunits (α3/β), has been shown to be present in the SDH of mice, but not in the DDH (Harvey *et al.*, 2004). This exciting new finding means there is a specific type of GlyR in a region of the spinal cord that receives nociceptive signals. Previously, the α1/β form of the receptor was considered to be the only physiologically relevant GlyR in the adult nervous system.

$GABA_ARs$ are also widely distributed throughout the dorsal horn. There are 19 known GABA receptor subunit genes (α1-6, β1-3, γ1-3, δ, ε, θ, π, ρ1-3) (Collins *et al.*, 2006). Most $GABA_A$ receptors, however, that are expressed in the CNS, are composed of α1, β2/3 and γ2 subunits (Gao & Ziskind-Conhaim, 1995). Benzodiazepine sensitivity is conferred in $GABA_A$ receptors by the α1, α2, α3 or α5 subunits together with the γ2 subunit (Burt, 2005). In the spinal cord dorsal horn, most $GABA_A$ receptors are benzodiazepine-sensitive, however, their subunit composition differs between laminae. The superficial laminae have high levels of α2 and α3 subunits, with little expression of

α1 and α5, whilst expression of β2, β3 and γ2 appears evenly distributed throughout the grey matter of the spinal cord (Bohlhalter *et al.*, 1996). Other work suggests that α2 is dominant in dorsal root ganglion neurons, whilst α3 is most common in intrinsic dorsal horn neurons (Persohn *et al.*, 1991; Wisden *et al.*, 1991; Laurie *et al.*, 1992). In contrast to the SDH, in the deeper laminae the α1 subunit seems to predominate, particularly on projection neurons (Bohlhalter *et al.*, 1996).

The CB_1 receptor in the spinal cord

According to immunohistological evidence, the CB_1R is more highly expressed in the SDH versus DDH (Farquhar-Smith *et al.*, 2000). This concentration of CB_1Rs in the SDH is of physiological significance, as administration of cannabinoids to 'normal' animals produces antinociception mediated by spinal and supraspinal sites (Gilbert, 1981; Smith & Martin, 1992). The mechanisms underlying cannabinoid-induced analgesia have been shown to act in various ways at the level of the spinal cord. For example, CB_1 agonists can inhibit both capsaicin-sensitive fibres and wide dynamic range (WDR) neurons (Hohmann *et al.*, 1998; Richardson *et al.*, 1998a), and modulate the activity of the glutamatergic (Shen *et al.*, 1996; Richardson *et al.*, 1998b), noradrenergic (Lichtman & Martin, 1991) and opioidergic systems (Welch, 1993; Smith *et al.*, 1994; Pugh *et al.*, 1995; Pugh *et al.*, 1996; Reche *et al.*, 1996; Reche *et al.*, 1998).

Recently, reports have also suggested direct allosteric modulation of glycine receptors by cannabinoids (Lozovaya *et al.*, 2005; Hejazi *et al.*, 2006). Although both studies support allosterism, they disagree in the way cannabinoids effect the GlyR. The Lozovaya *et al.* study reports attenuation of glycinergic mIPSCs, whereas Hejazi *et al.* suggests cannabinoids potentiate signaling by the same receptor. No studies to date have

investigated this phenomenon at native synapses (i.e. those in a physiologically relevant setting) in an intact preparation, nor in the dorsal horn of the spinal cord where different GlyR types exist in superficial and deep regions.

As reported earlier, Herkenham *et al*. (1991) first studied the distribution of cannabinoid receptors in the spinal cord using binding assays. The ventral horn showed very sparse binding of the synthetic cannabinoid [^{3}H]CP-55,940, whilst denser binding was observed in lamina II and lamina X. Later, immunocytochemical studies using light microscopy, reported staining of individual axons in the rat spinal cord (Pettit *et al.*, 1998; Tsou *et al.*, 1998). These early studies suggested that CB_1 receptors were located in spinal cord regions known to be important for pain processing.

Ong & Mackie (1999b) carried out a detailed study of cannabinoid receptors in the spinal cord of primates using immunocytochemistry and electron microscopy. Their study showed that large numbers of neurons, labeled with an antibody generated against the first 77 amino acid residues of the rat CB_1 receptor, were present in all regions of the grey matter of the spinal cord with the dorsal horn containing many small diameter (9-16 μm) CB_1-positive neurons. Ong & Mackie also noted that neuropil in the dorsal horn was densely stained for CB_1 receptors. These findings were supported by Farquhar-Smith *et al.* (2000) in rat spinal cord, using immunohistochemistry, double-labeled immuno-fluorescence and Western blot analysis.

An important point to note from these anatomical studies is that the localization of CB_1-positive neurons in the spinal cord is concentrated in the 'nociceptive' laminae of the dorsal horn, lamina X and motor neurons of the ventral horn.

The CB_2 Receptor in the spinal cord

Evidence for the presence of the CB_2 receptor in the spinal cord is sparse. Recently, an immunohistochemical study showed the presence of CB_2 immunoreactivity in both cultured dorsal root ganglia (DRG) neurons and primary afferent fibres in the SDH of the spinal cord (Wotherspoon *et al.*, 2005). Others have shown that while CB_2 receptors are normally confined to peripheral immunological tissue, CB_2 receptor mRNA appears in the lumbar spinal cord of the rat following nerve injury (Zhang *et al.*, 2003). Indeed, Sagar *et al.* (2005) report that activation of spinal CB_2 receptors can modulate the spinal processing of innocuous and noxious mechanical stimuli in neuropathic rats following spinal nerve ligation. Further, they postulate that this spinal site of action may contribute to the inhibitory effects of systemically administered CB_2 receptor agonists on mechanical allodynia in neuropathic rats (Malan *et al.*, 2001; Ibrahim *et al.*, 2003; Scott *et al.*, 2004). Thus, CB_2 receptors may modulate pain responses via an action on glial cells in the spinal cord. The CB_2 type of cannabinoid receptor is not discussed in this thesis, although they may be important for pain research in the future.

In this chapter, I use the whole cell patch clamp technique to characterize inhibitory signaling events (sIPSCs and mIPSCs) in both the SDH and DDH of the mouse spinal cord. These experiments were aimed at clarifying the properties of glycinergic and $GABA_A$ergic signaling in the two discrete spinal cord regions. I also believe it is important to provide this comparison for the mouse as this species is increasingly used to explore the genetic aspects of pain, and the discovery of the α3-containing GlyR was made in the mouse. I then test whether the synthetic cannabinoid, methanadamide (methAEA), has direct effects on native synaptic glycine and $GABA_A$ receptors. Finally, I use real-time PCR (qPCR) to quantitate

and compare the subunit expression of glycine and $GABA_A$ receptors, and the CB_1 receptor in the SDH and DDH.

Materials and Methods

Tissue preparation

Mice (C57/BL6; both sexes, aged 17-37 days) were anaesthetized with Ketamine (100 mg kg^{-1} i.p.) and decapitated. The vertebral column (~T5-S1) was isolated and immersed in ice-cold oxygenated sucrose substituted artificial cerebro-spinal fluid (s-ACSF). This solution contained (in mM): 250 sucrose, 25 $NaHCO_2$, 10 glucose, 2.5 KCl, 1 NaH_2PO_4, 1 $MgCl_2$ and 2.5 $CaCl_2$ and was bubbled with Carbogen (95% O_2 and 5% CO_2) (Linde, Sydney, Australia). The lumbosacral enlargement (L1 - L6) of the spinal cord was removed, placed against a Styrofoam support block, and glued (rostral side down) to a cutting platform with cyanoacrylate glue (Loctite 454, Loctite, Sydney, Australia). The platform was then transferred to a cutting chamber, filled with ice-cold s-ACSF and transverse slices (300 μm-thick) were obtained from the L3-L5 segments using a vibratome (Leica Microsystems, Wetzlar, Germany). Slices were transferred to a storage chamber containing artificial cerebro-spinal fluid (ACSF; 118 mM NaCl substituted for sucrose in s-ACSF) and allowed to equilibrate for 1 h before electrophysiological recording.

Electrophysiology

Individual slices were transferred to a recording chamber (volume 0.4 ml) and held down using nylon netting fixed to a U-shaped platinum frame and continually perfused (exchange rate of 4-6 bath volumes/min) with oxygenated ACSF. Whole-cell voltage-clamp recordings were made at room temperature (22-24°C) from SDH and DDH neurons, visualized via infrared differential interference contrast optics and a Hamamatsu charge coupled device camera (Model C-2400-79H) linked to a video monitor. In animals older than postnatal day 6 (P6), lamina II appears as a translucent

band that clearly delineates the ventral extent of the SDH (Walsh *et al*., 2009; *Figure 3.3*). All SDH (laminae I-II) recordings were made between this boundary and the dorsal white matter. I defined the DDH (laminae IV-VI) as the spinal cord grey matter dorsal to the central canal and more than 100 μm ventral to the lamina II border. All DDH recordings were made within these boundaries. Patch pipettes (3-4 MΩ resistance), made from borosilicate glass (1.5 mm O.D; PG150T-15; Harvard Apparatus, UK) were filled with an internal solution containing (in mM): 130 CsCl, 10 HEPES, 10 EGTA, 1 $MgCl_2$, 2 ATP and 0.3 GTP (pH adjusted to 7.35 with 1 M CsOH). After obtaining the whole-cell recording configuration, series resistance and neuronal input resistance were assessed using the average response to a 5 mV hyperpolarizing step (20 repetitions, holding potential -70 mV). These values were monitored at the beginning and end of each recording session and data were rejected if values changed by more than 20%. Series resistance (< 20 MΩ) was uncompensated in all experiments. All synaptic currents were recorded at a holding potential of -70 mV, using an Axopatch 200B amplifier (Molecular Devices, Sunnyvale, CA, USA). Signals were filtered at 2 kHz and digitized on-line at 10 kHz via an Instrutech ITC-16i A/D board (Instrutech, Long Island, NY, USA). Data was stored on a Macintosh G4 computer and analysed offline using Axograph v4.6 software (Molecular Devices, Sunnyvale, CA, USA).

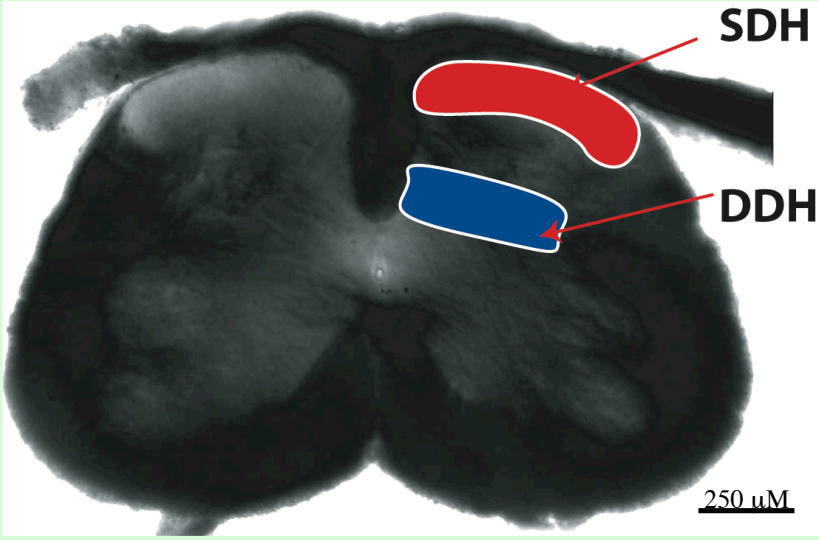

Figure 3.3 - Spinal cord slice from the lumbar region (L4 segment) of a P21 mouse. *Under IR-DIC optics the SDH (**RED**) appears as a translucent band that delineates the ventral extent of the SDH from the deeper regions of the dorsal horn. The DDH (**BLUE**), which comprises laminae IV-VI, was taken as the region dorsal to the central canal and greater than 100 µM ventral to lamina II.*

Experimental protocol

Characterizing inhibitory events in the SDH and DDH

Fast synaptic inhibition in the spinal cord, mediated by glycine and GABA, is critically important for the processing of peripheral nociceptive information. Indeed, a reduction in synaptic inhibition (disinhibition) has been associated with allodynia and hyperalgesia, in rodent models of inflammatory and neuropathic pain (Yaksh, 1989; Sivilotti & Woolf, 1994; Harvey *et al*., 2004). In order to understand the role of spinal inhibition in pain mechanisms, we must first understand or characterize what is happening in the 'normal' state. With that in mind, in this series of experiments I have characterized inhibitory events in both the SDH and DDH of the mouse spinal cord by recording both action potential-dependent spontaneous IPSCs (sIPSCs), and non-action potential-dependent miniature IPSCs (mIPSCs). Furthermore, due to the proposed spinally-mediated analgesic properties of cannabinoids (Hogestatt *et al*., 2005; Mallet *et al*., 2008) and the allosteric modulatory effects (Hejazi et al., 2006; Lozovaya et al., 2005), I also test the effect of a synthetic cannabinoid, methAEA, on these same inhibitory events.

Spontaneous inhibitory postsynaptic currents (sIPSCs)

Spontaneous IPSCs (sIPSCs) are generated by both action-potential dependent mechanisms and spontaneous quantal release from randomly firing neurons. Reports in the literature have shown that cannabinoids can presynaptically inhibit both sEPSCs and sIPSCs in the spinal cord and brainstem (Morisset & Urban, 2001; Jennings *et al.*, 2003). At the beginning of this series of experiments, I tested the ability of methanandamide to reduce the frequency of glycinergic and $GABA_A$ergic sIPSCs in the spinal cord. This ensured that the concentration of methanandamide (5 μM) added to the

bath was physiologically relevant, and could be confidently used for the remainder of my experiments.

Miniature inhibitory postsynaptic currents (mIPSCs)

Miniature inhibitory postsynaptic currents (mIPSCs), which are considered to be the postsynaptic response to the spontaneous release of single vesicles of neurotransmitter (Katz, 1969; Bekkers & Stevens, 1989), were recorded as follows. Glycinergic mIPSCs were pharmacologically isolated by bath application of the AMPA-kainate receptor antagonist 6-cyano-7-nitroquinoxaline-2,3-dione (CNQX; 10 μM), the $GABA_A$ receptor antagonist bicuculline (10 μM), and the sodium channel blocker tetrodotoxin (TTX; 1 μM). Data collection commenced 3 minutes after drug wash-on and proceeded for at least another 3 minutes. mIPSCs recorded under these conditions were completely abolished by the GlyR antagonist strychnine (1 μM; n = 10; Figure 3.4A). In experiments assessing $GABA_A$ergic mIPSCs the order of bicuculline (10 μM) and strychnine (1 μM) application was reversed. The $GABA_A$ergic nature of their events was confirmed by their bicuculline sensitivity (n = 10; Figure 3.4B).

Effects of cannabinoids on glycinergic and $GABA_A$ergic IPSCs

In another series of experiments, the effect of the cannabinoid (methAEA) on glycinergic and $GABA_A$ergic synaptic transmission was also tested. After collecting the initial glycinergic and $GABA_A$ergic IPSCs, a physiologically relevant concentration of methAEA (5 μM) was added to the bath (Fisyunov *et al*., 2006). The cannabinoid was allowed to wash-on for at least 10 min before IPSC data was recorded for analysis. In some experiments, drug vehicle was added to the bath to ensure that no effect was seen compared with control (data not shown).

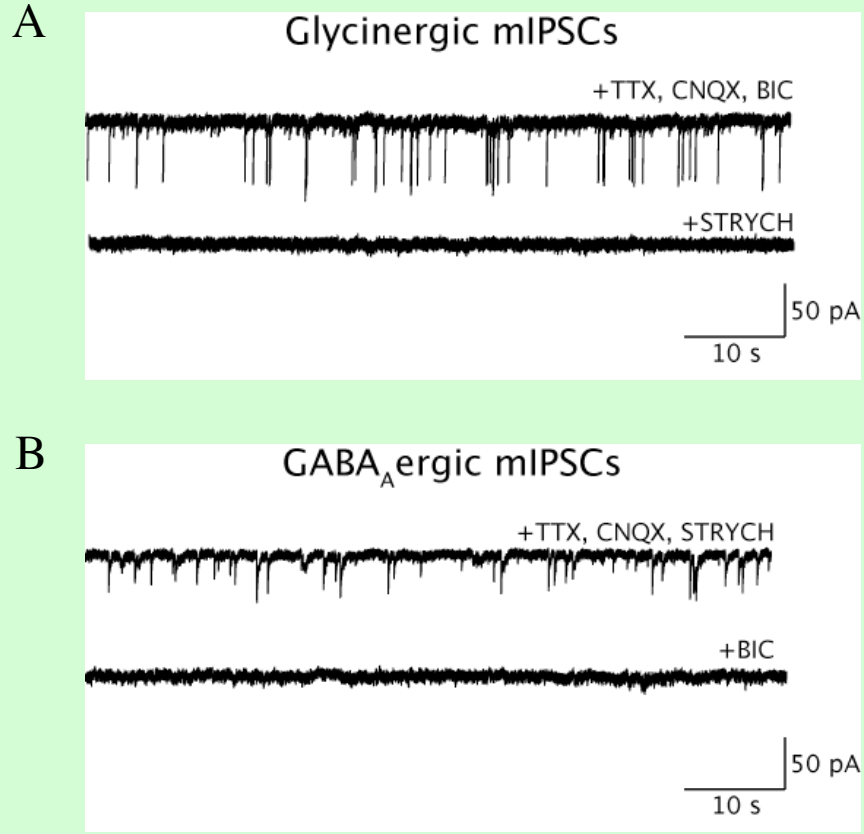

Figure 3.4 - Isolation of inhibitory synaptic events. *mIPSCs (at a holding potential of -70 mV) were pharmacologically isolated using CNQX (1 μM) and TTX (1 μM). These mIPSCs represented GlyR- and $GABA_A$R-mediated mIPSCs. Strychnine (1 μM) and/or bicuculline (10 μM) was subsequently applied to the bath to determine whether the mIPSCs were (A) GlyR- or (B) $GABA_A$R-mediated. Addition of CNQX, TTX, bicuculline and strychnine to the bath, abolished all synaptic activity. In other experiments, spontaneous IPSCs were recorded in the absence of TTX.*

At the completion of a recording session for each neuron, the entire dorsal horn was photographed using an Olympus DP50 digital camera and Viewfinder lite software (Olympus, Tokyo, Japan), while the patch pipette was still attached to the neuron in situ. Subsequently, three drawings of the dorsal horn in the transverse plane (segments L3, L4, L5 adapted from Franklin & Paxinos (1997), outlining the grey and white matter borders, were used as templates to plot each neurone's position. Dorsal horn images were matched to one of these templates according to: (1) the size of the dorsal columns in the mediolateral axis; (2) the size and shape of the dorsal grey matter; and (3) the distance from the central canal to the apex of the dorsal columns. The appropriate template for the photographed slice was superimposed and rescaled in the dorsoventral and mediolateral axes to optimize fits to the SDH and DDH regions. Patch pipette tip position was then plotted on the selected template. All templates were then rescaled back to their original dimensions. Finally, templates were grouped and overlayed, collapsing all recording locations in slices from each spinal segment (see Figure 3.5).

Analysis of IPSC properties

Pharmacologically isolated GlyR- and $GABA_A$R-mediated IPSCs were detected and captured using a sliding template method (semi-automated procedure within Axograph software package (Clements & Bekkers, 1997). Captured IPSCs were inspected individually and accepted for analysis when: (1) overlapping IPSCs were not present in the captured trace; (2) the baseline before the rise or after the decay phase of the IPSC was stable for > 5 ms; and (3) no time-dependent trend was evident in either IPSC amplitude or instantaneous frequency over the recording period (Callister & Walmsley,

1996). Analyses were performed on averaged IPSCs, obtained by aligning the rising phase of all accepted IPSCs for a given neuron. Peak amplitude, rise time (calculated over 10–90 % of peak amplitude), and decay time constant (calculated over 20-80% of the decay phase) were obtained using semi-automated procedures within Axograph software. Both GlyR- and $GABA_AR$-mediated IPSCs in the spinal cord of the mouse were best fit by a single decay time constant (Graham *et al*., 2003).

Single channel conductances

The single-channel conductance underlying GlyR- and $GABA_AR$-mediated mIPSCs, was determined via peak scaled nonstationary noise analysis (Robinson *et al*., 1991; Traynelis *et al*., 1993; Singer & Berger, 1999) using the Mini Analysis Program (v6; Synaptosoft, Fort Lee, NJ). This procedure calculates a weighted mean of the underlying multiple conductance states for synaptically located receptors, that is, those generating the recorded mIPSCs versus receptors located outside the synaptic cleft. For each neuron, mIPSCs were aligned at the midpoint of their rising phase and averaged. This "average" mIPSC was then scaled to the peak amplitude of all captured mIPSCs that contributed to the averaged mIPSC. The peak scaled average current was then subtracted from individual (scaled) mIPSCs to obtain a difference current, which represents random receptor fluctuations around the mean. Difference currents were binned over the decay phase of the mIPSC. The variance was then plotted against the mean current. A parabolic function (variance = I [current] - $[current^2]/N^P$ + baseline noise) was then fitted to the variance/mean plot, where I is single-channel current and N^P is the average number of channels open at mIPSC peak (Traynelis *et al*., 1993; Graham *et al*., 2006).

RNA extraction and relative real-time PCR

In a separate set of experiments aimed at quantifying the level of glycine, $GABA_A$ and CB_1 receptors and their subunits in the mouse spinal cord, slices were prepared as described above (Tissue preparation). Six spinal cord slices were used from an individual animal. Freshly cut slices were placed on filter paper (wet with ACSF) and a dissecting blade (made from a fragment of broken vibroslicer blade) was used to make 2 horizontal cuts through the slice. One cut was just ventral to the transluscent substantia gelatinosa, and the second cut at the level of the central canal. This procedure yielded 3 tissue regions per slice that corresponded to SDH, DDH, and ventral horn. These were pooled from each animal, by region, and prepared for relative real-time PCR (qPCR).

Total RNA was extracted from the tissue using TRIzol reagent (Invitrogen, USA) (Beveridge *et al*., 2008). Tissue was added to TRIzol reagent and total RNA was prepared according to the manufacturer's instructions. RNA integrity was assessed by A260/A280 ratios (> 1.8) or visualisation of 18s and 28s ribosomal bands by electrophoresis with formaldehyde denaturing 1% agarose gel. Total RNA was treated with DNAse1 (Invitrogen, USA) and reverse transcribed with SuperscriptII reverse transcriptase (Invitrogen, USA) as per manufacturer's instructions. Real-time PCR using SYBR green Mastermix (PE Applied Biosystems, UK) and an ABI prism 7500 sequence detection system (PE Applied Biosystems, UK) was performed to assess the expression of the GlyR subunit genes (α1-4 and β), $GABA_A$ subunit genes (α1-α3, α5, β2–3, γ2; the most common in the spinal cord) and CB_1 receptor levels. Primers (Table 1) were designed for each gene using Primer Premier 5.0 (Premier Biosoft International, USA). Reactions consisting of 2 × SYBR green mastermix, 40 nM of each primer, cDNA template and nuclease-free water were run in triplicate for each gene on the ABI

7500 sequence detection system under the following conditions: 50 °C for 2 min, 95 °C for 10 min then 45 cycles of 95 °C for 15 s and 60 °C for 90 s. Dissociation curves consisting of 95 °C for 15 s and 60 °C for 15 s followed by a 2% ramp to 95 °C were used to ensure a single product of the correct molecular size was present in each reaction. An average cycle threshold (Ct) value (ΔCt) was calculated from triplicate results for each gene. Expression levels were normalized to the housekeeping gene β-actin.

Statistical Analysis

SPSS v13 software package (SPSS Inc. Illinois, USA) was used for all statistical analyses. Student's unpaired t-tests were used to compare sIPSC and mIPSC properties (for glycine or $GABA_A$) recorded in the SDH and DDH. Student's paired t-tests were used to compare IPSC data (glycine or $GABA_A$) before, and after exposure to methAEA. One-way ANOVA's compared gene expression data for all GlyR subunits and $GABA_A$R subunits in the SDH and DDH. Student's unpaired t-tests compared gene expression for each subunit (GlyR, $GABA_A$R and CB_1) in the SDH versus DDH. All values are presented as means ± SEM. Statistical significance was set at $p < 0.05$.

Drugs

TTX was obtained from Alomone Laboratories (Jerusalem, Israel) and methanandamide from Tocris Bioscience (Bristol, UK). All other drugs were purchased from Sigma Chemicals (St Louis, MO, USA).

Table 1 – Real-time PCR (qPCR) Primers	
GlyRα1 Forward	5'CAACAGTTTCGGTTCCATC3'
GlyRα1 Reverse	5'CGCCTCTTCCTCCTAAATCGAAGCAGT3'
GlyRα2 Forward	5'GGGACAAACCACTTCAGGAGGC3'
GlyRα2 Reverse	5'TAGCATCTGCATCTTTGGGGGGT3'
GlyRα3 Forward	5'GATTTTACTTCTGGGAAGCCGC3'
GlyRα3 Reverse	5'GAACCACACCATCCTTTGCTTG3'
GlyRα4 Forward	5'GGTGTCCTACGTAAAGGCAATT3'
GlyRα4 Reverse	5'CTCCATACGCTGACGTCTCT3'
GlyRβ Forward	5'GGATCCATTCAAGAGACA3'
GlyRβ Reverse	5'AGCCACACATCCAGTGCCTT3'
$GABA_A$Rα1 Forward	5'TGCTGGACGGTTATGACAAT3'
$GABA_A$Rα1 Reverse	5'GAAACTGGTCCGAAACTGGT3'
$GABA_A$Rα2 Forward	5'ACAACCTTGAGCATCAGTGC3'
$GABA_A$Rα2 Reverse	5'AATTCACGGTTGCAAATTCA3'
$GABA_A$Rα3 Forward	5'GACAGTCCTGCTGAGACCAA3'
$GABA_A$Rα3 Reverse	5'ATAGCTGATTCCCGGTTCAC3'
$GABA_A$Rα5 Forward	5'TCCATTGCACACAACATGAC3'
$GABA_A$Rα5 Reverse	5'GCAGAGATTGTCAGACGCAT3'
$GABA_A$Rβ2 Forward	5'AGCTGCTAATGCCAACAATG3'
$GABA_A$Rβ2 Reverse	5'GTCCCATTACTGCTTCGGAT3'
$GABA_A$Rβ3 Forward	5'CAAAGCCATCGACATGTACC3'
$GABA_A$Rβ3 Reverse	5'CTTCTCCGCAAGCTTCTTCT3'
$GABA_A$Rγ2 Forward	5'TGGTCACCGAATGTGTTTCT3'
$GABA_A$Rγ2 Reverse	5'TACTTTGCCTTGCAGGTTTG3'
CB1 FWD	5'GCTTATCAAGACGGTGTTTGC3'
CB1 REV	5'GCATGTCTCAGGTCCTTGCT3'
β-actin FWD	5'TGAGACCTTCAACACCCCAG3'
β-actin REV	5'CATCTGCTGGAAGGTGGACA3'

Table 1 - Real-time PCR primers. *Quantitative real-time PCR was undertaken to determine the glycine and $GABA_A$ receptor subunit composition of different regions of the spinal cord dorsal horn. Subunits were selected according to published data (Bohlhalter et al., 1996).*

Results

Stable whole-cell patch clamp recordings were obtained from 92 neurons in 18 animals (male = 12; female = 6) in L3-L5 spinal cord segments. The location of the recorded neurons in spinal cord cross sections is shown in *Figure 3.5*. Recordings were restricted to either the SDH (n = 45) or DDH (n = 47). The age of animals yielding SDH and DDH recordings was similar (21.4 ± 0.3 days vs. 21.9 ± 0.3 days, respectively), and the series resistance of recordings in each region were identical (11.6 ± 0.7 MΩ vs. 11.6 ± 0.6 MΩ). These comparisons suggest that animal age, gender and recording conditions did not have a major influence on my results. The input resistance of neurons recorded in the SDH, however, was significantly higher than DDH neurons (640 ± 65 MΩ vs. 260 ± 30 MΩ). This suggests neurons in the SDH are smaller than neurons in the DDH, as input resistance is a crude measure of cell size (Henneman *et al*., 1965). This also agrees with histological data from Molander *et al*. (1984).

Glycinergic and $GABA_A$ergic transmission in the SDH and DDH

In recordings assessing glycinergic synaptic transmission in SDH neurons, ~25% did not exhibit mIPSCs (9/34), whereas almost all SDH neurons assessed for GABAergic synaptic transmission exhibited mIPSCs (14/15). In the DDH, all neurons assessed for glycinergic synaptic transmission exhibited glycinergic mIPSCs (25/25), and most neurons assessed for GABAergic synaptic transmission (18/19) exhibited $GABA_A$ergic mIPSCs. Thus, at the neuron level, GABA receptors play a more widespread role in fast inhibitory synaptic transmission in the SDH whereas the role for glycine appears more prominent in the DDH.

Glycine receptor-mediated synaptic transmission

In addition to the difference in the number of neurons receiving glycinergic mIPSCs in SDH versus DDH, mIPSC properties also differed in the two regions (*Figure 3.6*). The frequency of glycinergic mIPSCs in the SDH was markedly lower compared to the DDH (*Figure 3.6A* and *3.6D*; 0.15 ± 0.03 Hz vs. 0.72 ± 0.13 Hz, n= 25 and n = 25 respectively). Likewise, the peak amplitude of glycinergic mIPSCs in SDH neurons was approximately half that observed in DDH neurons (*Figure 3.6B-C*; 37.1 ± 3.9 pA vs. 64.7 ± 5.0 pA, n= 25 and n = 25 respectively).

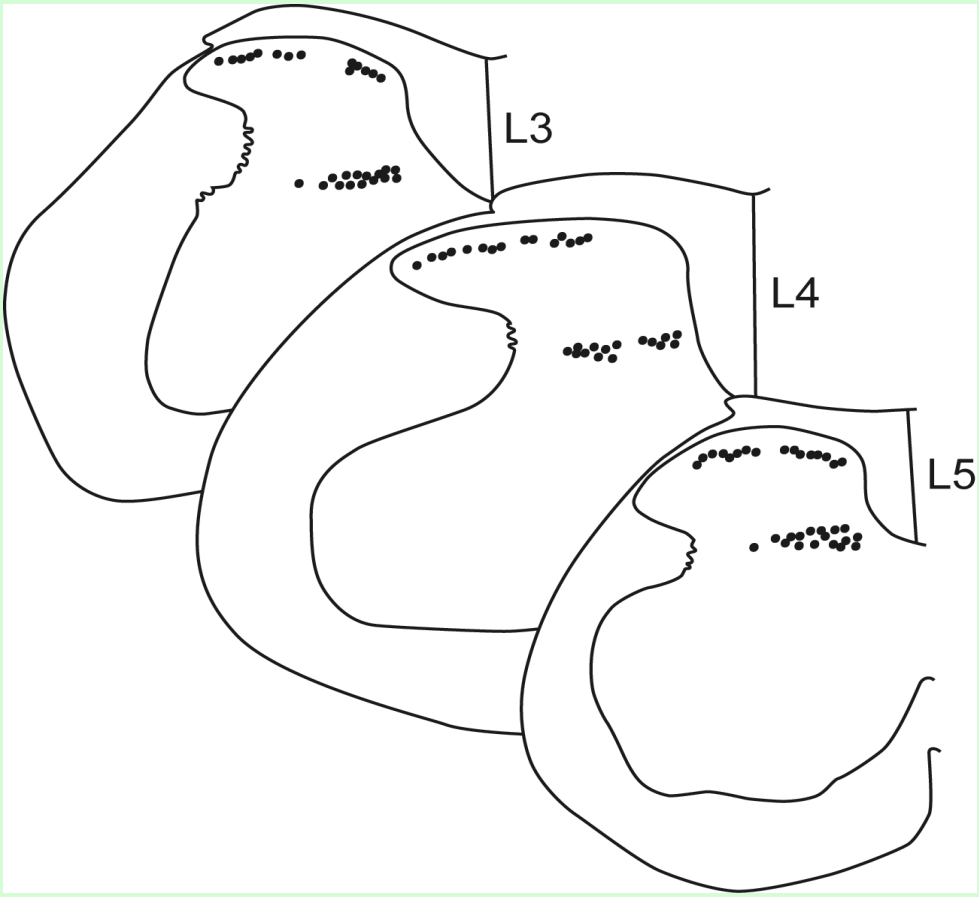

Figure 3.5 - Spinal cord mapping. Location of recorded dorsal horn neurons (SDH and DDH). Neurons in spinal cord slices were photographed and plotted on templates of L3, L4, and L5 segments. Approximately 30 neurons were recorded in each segment. For SDH neurons, recordings were obtained across the entire mediolateral extent of the dorsal horn. For the DDH, recordings were confined to the medial two-thirds of the dorsal horn, because dense myelination made it difficult to visualize neurons in the lateral DDH.

The decay time constant for glycinergic mIPSCs in the SDH was significantly slower than those in the DDH (*Figure 3.6B* and *3.6D*; 8.5 ± 0.8 ms vs. 5.5 ± 0.3 ms, n = 25 and n = 25 respectively), but mIPSC rise times were identical in the two regions (0.85 ± 0.07 ms vs. 0.85 ± 0.04 ms, n = 25 and n = 25, respectively). The combined effect of small slow decaying mIPSCs in the SDH and larger fast decaying mIPSCs in the DDH was to produce a similar charge transfer per mIPSC in the two regions (364.5 ± 57.7 pA.ms vs. 456.6 ± 39.9 pA.ms, n = 25 and n = 25, respectively). When reduced glycinergic mIPSC frequency was incorporated in calculations of total charge, however, glycinergic drive to SDH neurons was significantly reduced compared to neurons in the DDH (68.0 ± 26.8 pA.ms.Hz vs. 400.0 ± 107.9 pA.ms.Hz, n = 25 and n = 25, respectively).

The marked differences in glycinergic mIPSC amplitude between the SDH and DDH could be attributable to specific properties of the GlyR, including differences in single-channel conductance, number of open receptors in response to quantal release (N_o), or open probability of the individual channels (P_o) (Legendre, 2001). To distinguish between these possibilities, I performed peak-scaled nonstationary noise analysis on a subset of recordings from SDH and DDH neurons. The resultant variance-mean plots are shown in *Figures 3.7A & 3.7B.* This analysis showed that GlyR mIPSCs had an identical unitary conductance in the SDH and DDH (54.3 ± 1.6 pS vs 55.7 ± 1.8 pS, n = 8 and n = 11, respectively), similar P_o (0.97 ± 0.01 vs. 0.99 ± 0.01, n = 8 and n = 11, respectively), but only half the number of channels were involved in quantal transmission in the SDH (10.3 ± 0.5 vs. 19.0 ± 5.3). In summary, the noise analysis data suggest that the major difference in GlyRs found at synapses in the SDH versus DDH is the number of receptors located postsynaptically.

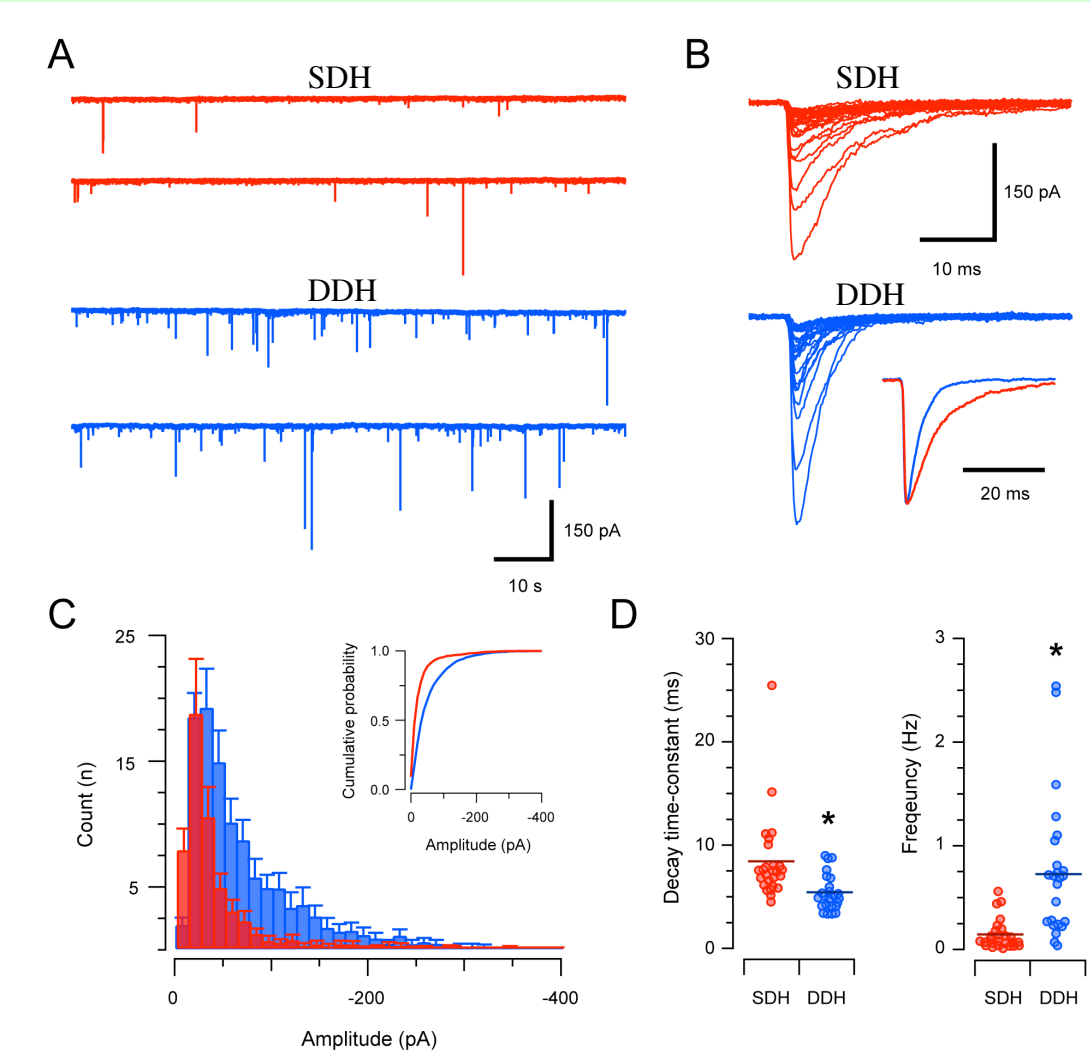

Figure 3.6 Glycinergic synaptic transmission differs in the SDH and DDH

A. *Continuous recordings of glycinergic mIPSCs in the presence of TTX (1μM), CNQX (10 μM), and bicuculline (10 μM) from an SDH neuron (upper, red) and a DDH neuron (lower, blue). Note the frequency of mIPSCs is considerably greater in DDH versus SDH neurons.* ***B.*** *Individual mIPSCs captured from traces in A, overlayed and aligned to rise time to compare the range of amplitudes and the time course of glycinergic mIPSCs recorded in the SDH (upper, red) and DDH (lower, blue). Inset shows averaged mIPSCs (15 records) from neurons recorded in A, normalised to the same amplitude. Note the significantly slower decay time of glycinergic mIPSCs in SDH neurons.* ***C.*** *Overlayed group data histograms compare amplitude distributions of glycinergic mIPSCs in SDH (red) and DDH (blue) neurons. In the SDH distribution, only 10% of mIPSCs have amplitudes greater than 50 pA, whereas 35% of the mIPSCs are greater than 50 pA in the DDH distribution. Inset shows data presented as a cumulative probability plot.* ***D.*** *Plots comparing group data for glycinergic mIPSC decay time-constant and frequency in SDH and DDH neurons. Decay time-constants were significantly slower in SDH neurons and glycinergic mIPSC frequency was significantly lower.*

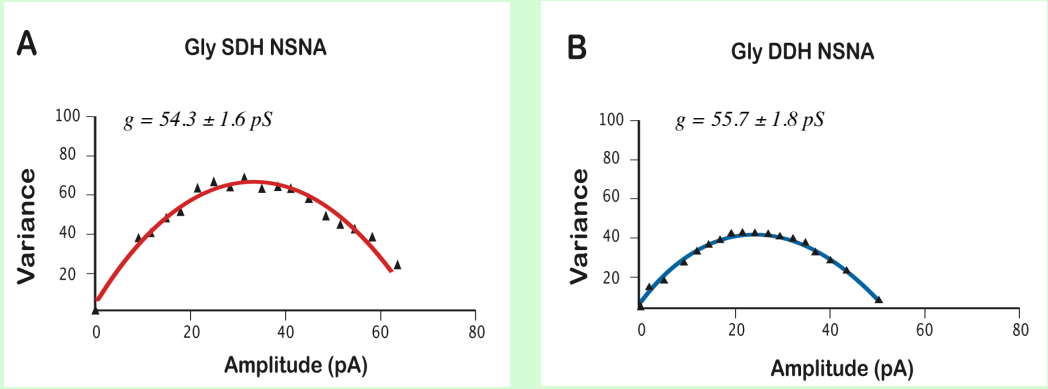

Figure 3.7 - Peak-scaled nonstationary noise analysis on glycinergic mIPSCs in the SDH and DDH. *Marked differences in mIPSC amplitude between the SDH and DDH could be attributable to disparities in either the single-channel conductance (γ), number of open channels underlying quantal release (N_o), or the open probability of the ion channels (P_o). To distinguish between these possibilities, peak-scaled nonstationary noise analysis was undertaken on a subset of glycinergic neurons in the SDH (A) and DDH (B). The variance-mean relationship plotted over a range of release probabilities is approximately parabolic. The initial slope of the parabola provides an estimate of the average amplitude of the postsynaptic response to a vesicle of transmitter (Q_{av}), and the degree of curvature of the parabola provides an estimate of the average probability of vesicle release from a release site (Pr) (Reid & Clements, 1999). The analysis showed there is no difference in the unitary conductance (g) of GlyRs in the SDH and DDH (54.3 ± 1.6 pS vs 55.7 ± 1.8 pS), and that the major difference in GlyRs found at synapses in the SDH versus DDH is the number of receptors located postsynaptically.*

$GABA_A$ receptor-mediated synaptic transmission

Figure 3.8 compares $GABA_A$ergic neurotransmission in the SDH and DDH. Unlike glycinergic mIPSCs, many of the properties of $GABA_A$R-mediated mIPSCs were similar in SDH and DDH neurons. Specifically, mIPSC frequency (*Figure 3.8A* and *3.8D*; 0.21 ± 0.08 Hz vs 0.18 ± 0.04 Hz, n = 14 and n = 18, respectively), and amplitude (*Figure 3.8B-C*; 25.6 ± 2.4 pA vs. 25.3 ± 2.0 pA, n = 14 and n = 18, respectively) were comparable in both regions. The rise time and decay time constant of $GABA_A$R-mediated mIPSCs, however, was significantly slower in the SDH compared to the DDH (*Figure 3.8B* and *3.8D*; 1.97 ± 0.18 ms vs. 1.49 ± 0.10 ms, and 23.0 ± 3.2 ms vs. 18.9 ± 1.6 ms, n = 14 and n = 18, respectively). These slower kinetic properties resulted in a significantly greater charge transfer per mIPSC in SDH neurons compared to DDH neurons (717.3 ± 75.5 pA.ms vs. 486.3 ± 52.4 pA.ms, n = 14 and n = 18, respectively). This difference, however, was not borne out in calculations of total charge (152.4 ± 61.9 pA.ms.Hz vs. 92.8 ± 21.1 pA.ms.Hz, n = 14 and n = 18, respectively)

Peak-scaled nonstationary noise analysis was also applied to GABAergic mIPSCs to compare the single channel conductance, number, and open probability of synaptically located $GABA_A$ receptors. The resultant variance-mean plots are shown in *Figures 3.9A & 3.9B.* This analysis showed that $GABA_A$R-mediated mIPSCs had an identical unitary conductance in the SDH and DDH (22.7 ± 1.7 pS vs. 22.4 ± 2.0 pS, n = 8 and n =11, respectively). Open probability was lower in SDH neurons compared to neurons in the DDH (0.76 ± 0.04 vs. 0.94 ± 0.02, n = 8 and n =11, respectively), whereas the number of channels involved in quantal transmission was greater in SDH compared to the DDH (18.5 ± 1.6 vs. 12.9 ± 1.0). These data suggest that even though more channels underlie quantal transmission in the SDH, this is offset by the lower P_o value. Thus, the net effect

is no significant difference in peak mIPSC current amplitude at GABAergic synapses in the SDH and DDH (as indicated in *Figure 3.8*).

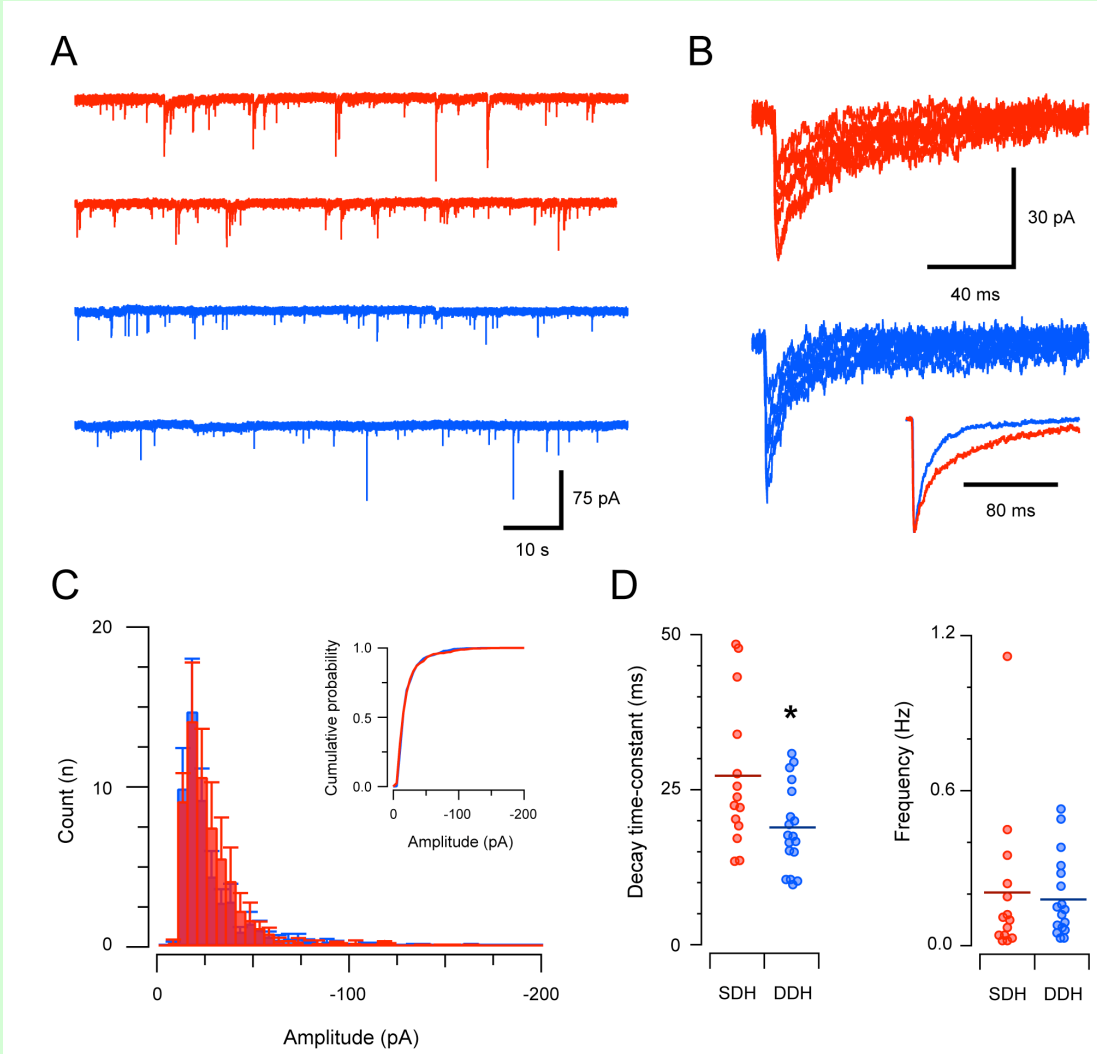

Figure 3.8 GABA$_A$ergic synaptic transmission differs in the SDH and DDH

A. *Continuous recordings of GABA$_A$ergic mIPSCs in the presence of TTX (1μM), CNQX (10 μM), and strychnine (1 μM) from an SDH neuron (upper, red) and a DDH neuron (lower, blue). Similar mIPSC frequencies were observed in both regions.* ***B.*** *Individual mIPSCs captured from traces in A, overlayed and aligned to rise time to compare the magnitudes and time course of GABA$_A$ergic mIPSCs recorded in the SDH (upper, red) and DDH (lower, blue). Inset shows averaged mIPSCs (15 records) from neurons recorded in A, normalised to the same amplitude. Note the significantly slower decay time of GABA$_A$ergic mIPSCs in SDH neurons.* ***C.*** *Overlayed group data histograms compare amplitude distributions of GABA$_A$ergic mIPSCs in SDH (red) and DDH (blue) neurons. The almost complete overlap of the histograms indicates that GABA$_A$ergic mIPSC amplitudes are indistinguishable in SDH and DDH neurons.* ***D.*** *Plots compare group data for GABA$_A$ergic mIPSC decay time-constant and frequency recorded in SDH and DDH neurons. Decay time-constants were significantly slower in SDH neurons but GABA$_A$ergic mIPSC frequency was similar in both regions*

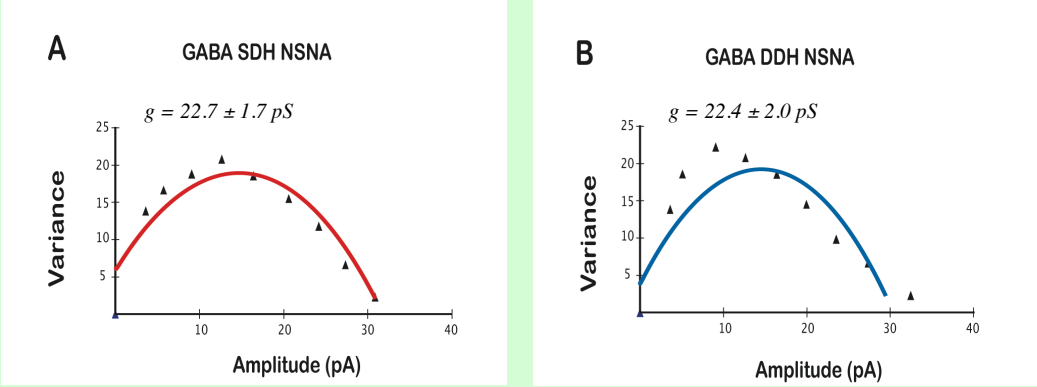

Figure 3.9 - Peak-scaled nonstationary noise analysis on $GABA_A$ergic mIPSCs in the SDH and DDH. *Analysis performed as in Figure 3.7. Single channel conductance values were compared for $GABA_A$Rs in both the SDH and DDH. As for GlyRs, it was shown that there was no difference between unitary conductance in the SDH versus DDH (22.7 ± 1.7 pS vs 22.4 ± 2.0 pS).*

Cannabinoid effects on glycinergic synaptic transmission

Cannabinoid's are known to have analgesic properties; and some of this analgesic action is thought to be spinally-mediated (Hogestatt *et al*., 2005; Mallet *et al*., 2008). Furthermore, a number of studies have proposed that, in addition to the well characterised actions that cannabinoids exert through the CB_1 receptor, they may also have direct effects on ligand gated ion channels, including the glycine receptor (Lozovaya *et al*., 2005; Hejazi *et al*., 2006). To examine direct cannabinoid effects on glycine receptors in the SDH or DDH, I compared the properties of glycinergic IPSCs, recorded in both regions, before and after bath application of the synthetic cannabinoid, methanandamide (methAEA - 5 μM).

The effect of methAEA on glycinergic mIPSCs in the SDH is summarized in *Figure 3.10A*. MethAEA significantly reduced mIPSC frequency (0.18 ± 0.03 vs 0.08 ± 0.02 events/s, p = 0.004, n = 7). In contrast, methAEA had no significant effect on mIPSC amplitude (35.9 ± 5.7 vs 31.7 ± 3.4 pA, p = 0.31), rise time (0.81 ± 0.16 vs 0.96 ± 0.08 ms, p = 0.37), or decay time constant (7.86 ± 1.10 vs 7.93 ± 1.03 ms, p = 0.88). *Figure 3.10B* summarizes the effect of methAEA on glycinergic mIPSCs in the DDH. Similar to its effects in the SDH, methAEA significantly reduced $GABA_A$ergic mIPSC frequency (0.37 ± 0.09 vs 0.15 ± 0.03 events/s, p = 0.01, n = 8) in DDH neurons. MethAEA did not significantly effect mIPSC amplitude (62.4 ± 6.0 vs 52.2 ± 6.8 pA, p = 0.08), rise time (0.63 ± 0.03 vs 0.60 ± 0.09 ms, p = 0.73), or decay time constant (5.04 ± 0.68 vs 5.02 ± 0.57 ms, p = 0.90), though a consistent modest reduction in mIPSC amplitude approached significance (p = 0.08). In summary, I find little evidence for a direct effect of methAEA on glycine receptors in either SDH or DDH neurons.

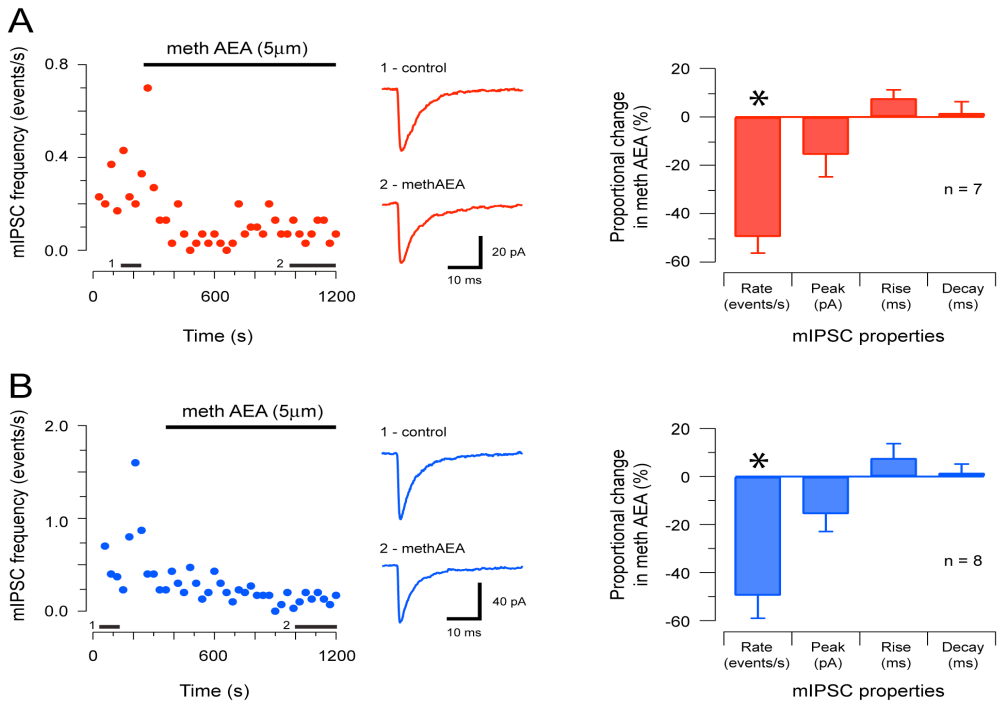

Figure 3.10. Effects of methanandamide on glycinergic synaptic transmission in the SDH and DDH

A. *Time plot (left) showing glycinergic mIPSC frequency recorded in an SDH neuron during bath application of methAEA (5 µM, upper bar). Glycinergic mIPSC frequency declines significantly in the presence of methAEA. Middle traces are averaged mIPSCs (15 records) in control conditions and after 10 minutes of methAEA exposure. Lower bars in time plot indicate epoch for averaged mIPSCs. Despite significantly reduced mIPSC frequency, remaining mIPSCs properties are relatively unaltered in methAEA. Right plots summarise proportional change to glycinergic mIPSCs properties for group data in methAEA. MethAEA produced a significant reduction in mIPSC frequency, without altering mIPSC peak amplitude, rise time or decay time-constant.* ***B.*** *Summary of methAEA induced effects on glycinergic mIPSC in DDH neurons (data presented in identical format to A). As in the SDH, methAEA significantly reduced glycinergic mIPSC frequency in DDH neurons without significantly altering mIPSC peak amplitude, rise time or decay time-constant.*

Cannabinoid effects on $GABA_A$ergic synaptic transmission

To examine cannabinoid effects on $GABA_A$ergic mIPSCs in the SDH or DDH, I compared the mIPSC properties recorded in both regions, before and after bath application of methAEA (5 μM). *Figure 3.11A* summarises the effect of methAEA on $GABA_A$ergic synaptic transmission in SDH neurons. MethAEA produced a significant reduction in mIPSC frequency (0.27 ± 0.05 vs 0.18 ± 0.03 events/s, p = 0.04, n = 6), without altering mIPSC amplitude (-30.1 ± 1.7 vs -28.1 ± 0.9 pA, p = 0.28), or decay time constant (29.51 ± 7.39 vs 37.52 ± 12.57 ms, p = 0.20). The rise time of $GABA_A$ergic mIPSCs, however, was significantly slower (1.89 ± 0.52 vs 2.51 ± 0.69 ms) in the presence of methAEA. *Figure 3.11B* summarises the effect of methAEA on $GABA_A$ergic synaptic transmission in DDH neurons. Bath application of methAEA significantly reduced mIPSC frequency (0.20 ± 0.04 vs 0.05 ± 0.02 events/s, n = 7). MethAEA did not significantly affect mIPSC amplitude (-19.6 ± 1.3 vs -17.0 ± 1.1 pA, p = 0.08), rise time (1.58 ± 0.17 vs 2.10 ± 0.51 ms, p = 0.02), or decay time constant (19.70 ± 3.52 vs 23.10 ± 4.64 ms, p = 0.22), although, as for glycinergic mIPSCs in the DDH, a modest reduction in mIPSC amplitude approached significance (p = 0.08). These results suggest the predominant effect of methAEA is to reduce $GABA_A$ergic mIPSC frequency, though evidence of a slowed time course may suggest some direct effect of methAEA on $GABA_A$ receptors.

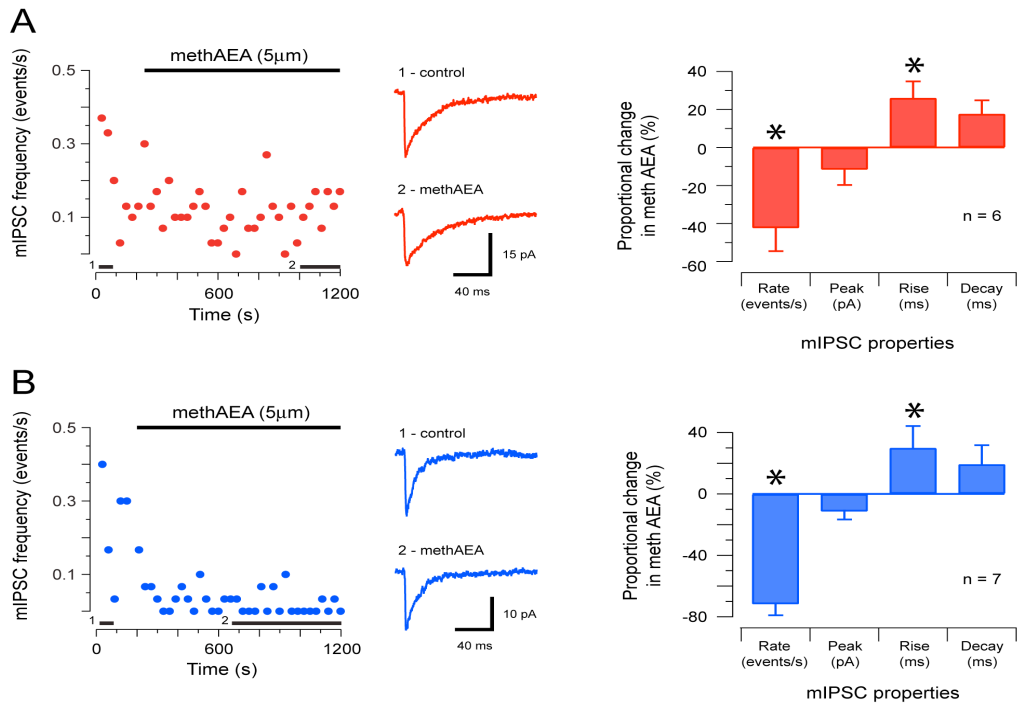

Figure 3.11 Effects of methanandamide on $GABA_A$ergic synaptic transmission in the SDH and DDH

A. *Time plot (left) showing $GABA_A$ergic mIPSC frequency recorded in an SDH neuron during bath application of methAEA (5 µM, upper bar). $GABA_A$ergic mIPSC frequency declines significantly in the presence of methAEA. Middle traces are averaged mIPSCs (15 records) in control conditions and after 10 minutes of methAEA exposure. Lower bars in time plot indicate epoch for averaged mIPSCs. mIPSC peak amplitude is unaltered in methAEA, however, mIPSC time course is slower. Right plots summarise proportional change to $GABA_A$ergic mIPSCs properties for group data in methAEA. methAEA produced a significant reduction in mIPSC frequency, showed no signifcant change in mIPSC peak amplitude or decay time constant, but significantly slowed rise time.* ***B.*** *Summary of methAEA induced effects on $GABA_A$ergic mIPSC in DDH neurons (data presented in identical format to A). methAEA significantly reduced $GABA_A$ergic mIPSC frequency in DDH neurons but did not significantly alter mIPSC peak amplitude, rise time or decay time-constant.*

Spontaneous glycinergic currents (sIPSCs)

The effects of methAEA on spontaneous glycinergic currents (sIPSCs) in both the SDH and DDH was assessed. Experiments in the SDH showed that methAEA had no effect on sIPSC amplitude (87.1 ± 12.7 vs 73.1 ± 11.6; n = 7) or decay time (8.2 ± 1.1 vs 9.2 ± 1.3), but it did have a significant effect on sIPSC frequency (1.11 ± 0.36 vs 0.62 ± 0.28 Hz; *Figures 3.12A-C*). Similarly, in the DDH, methAEA had no effect on amplitude (132 ± 16 vs 137 ± 25; n = 5) or decay time (6.6 ± 1.2 vs 6.6 ± 0.6) but frequency was significantly reduced (3.40 ± 1.20 vs 1.30 ± 0.63 Hz; *Figures 3.12D-F*).

Spontaneous $GABA_A$ergic currents (sIPSCs)

Further experiments also studied the effects of methAEA on spontaneous $GABA_A$ergic currents in both the SDH and DDH (sIPSCs). In the SDH, methAEA significantly decreased amplitude (51.4 ± 4.7 vs 35.3 ± 4.6 pA; n = 5) and frequency (0.34 ± 0.13 vs 0.10 ± 0.03 Hz; *Figures 3.13A-C*), but had no effect on decay time (31.6 ± 1.2 vs 30.5 ± 1.2). Interestingly, methAEA had no effect on amplitude (75.5 ± 15.5 vs 55.8 ± 12.5; n = 5), decay time (14.0 ± 2.5 vs 17.1 ± 4.2) or frequency (2.2 ± 1.2 vs 1.5 ± 1.0) in the DDH (*Figures 3.13D-F*). However, there did appear to be a trend towards a reduction in mIPSC amplitude, which may become significant with greater numbers of cells.

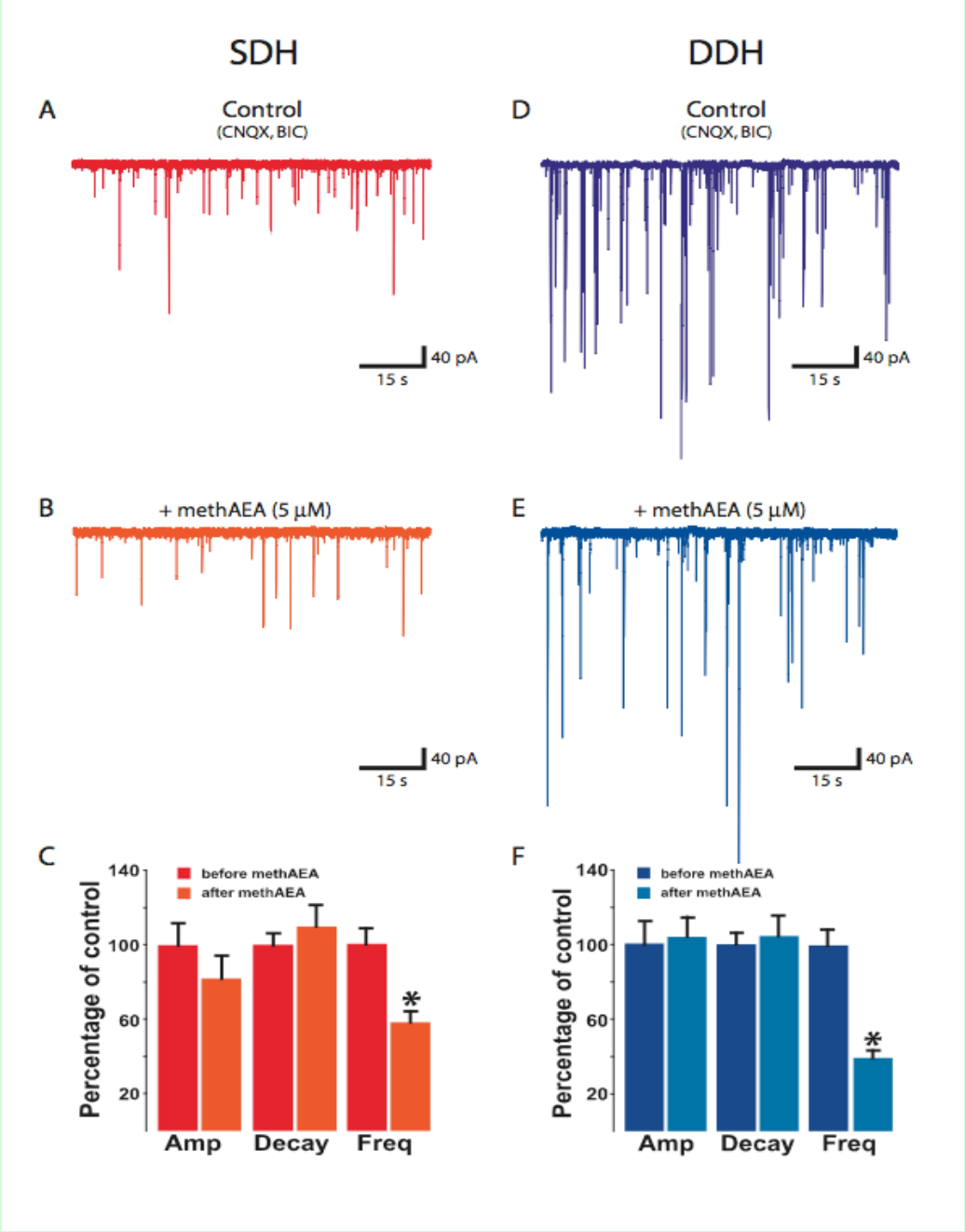

Figure 3.12 – Effect of methanandamide (methAEA) on glycinergic sIPSCs in the SDH and DDH of the mouse spinal cord. *sIPSC frequency was significantly decreased after the addition of methAEA (A-C); Similarly, glycinergic sIPSC frequency was significantly reduced by methAEA in the DDH (D-F).*

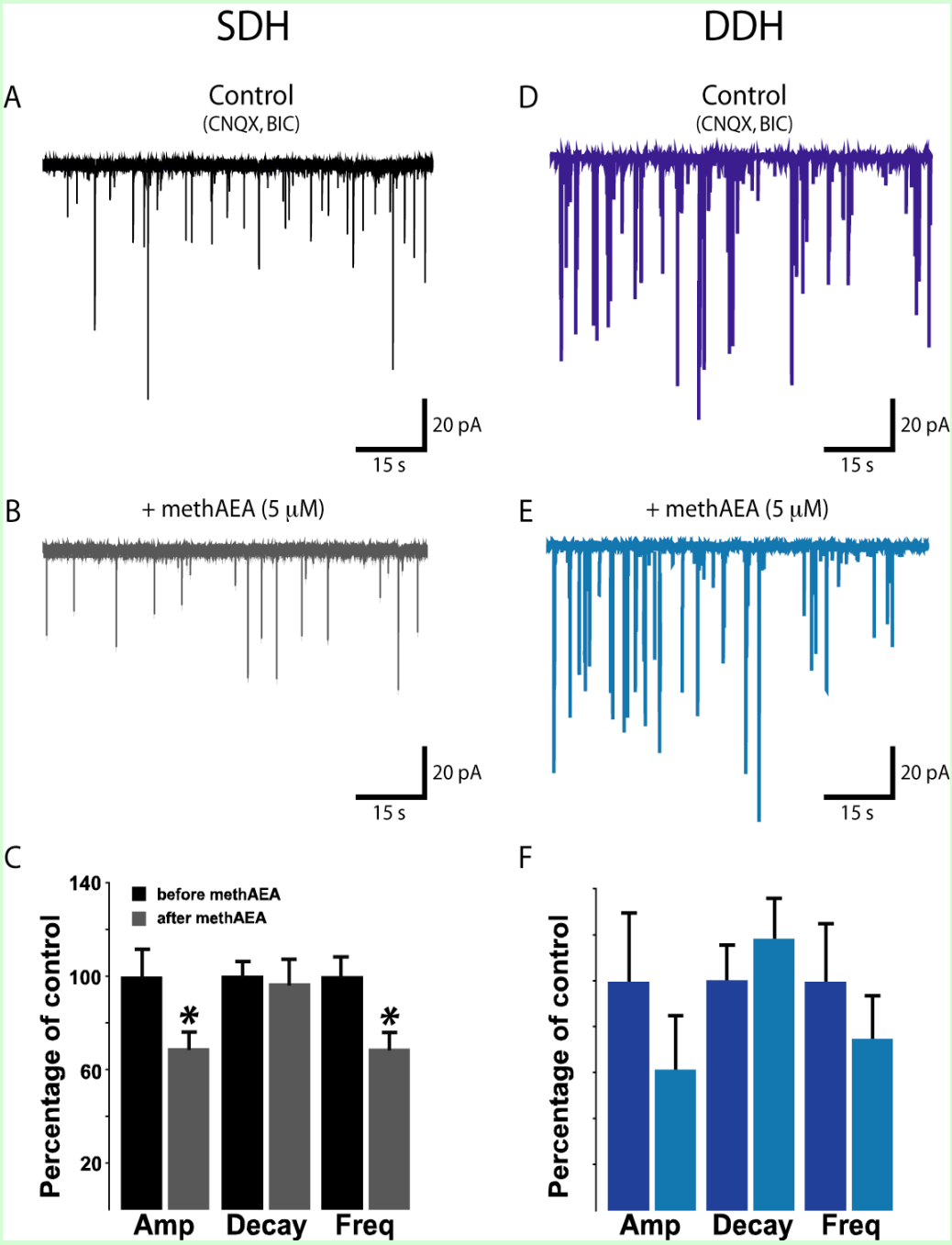

Figure 3.13 – Effect of methanandamide (methAEA) on $GABA_A$ergic sIPSCs in the SDH and DDH of the mouse spinal cord. *In the SDH, sIPSC amplitude and frequency was significantly decreased after the addition of methAEA (A-C); MethAEA had no effect on amplitude, decay time or frequency in the DDH (D-F)*

Expression of Glycine, $GABA_A$, and CB_1 receptor subunits in SDH and DDH

In light of the electrophysiological data showing that glycinergic and $GABA_A$ergic mIPSC properties differ between the SDH versus DDH neurons, I undertook an analysis of the subunit expression for both receptors (glycine and $GABA_A$) and the CB_1 receptor using real-time RT-PCR (qPCR). *Figure 3.14A-B* summarises qPCR results for the expression of GlyR subunits (α1-4, and β), $GABA_A$R subunits (α1-3, α5, β2-3, and γ2), and the CB_1 receptor in the SDH and DDH. Data are presented as ΔCT values, where ΔCT represents the difference in the mean cycle threshold (CT) of β-actin and the mean CT of each gene of interest. Thus, **lower** ΔCT values indicate **higher** relative gene expression and conversely higher ΔCT values indicate lower relative gene expression.

The results of GlyR subunit expression in the SDH (*Figure 3.14A*, left) indicate that Glyα1 is highest, followed by Glyβ, Glyα2 and Glyα3, with negligible expression of Glyα4. In the DDH (*Figure 3.14B*, left), Glyα1 and Glyβ are highly expressed at similar levels, then Glyα2, Glyα3, and Glyα4. Comparison of each GlyR subunit in SDH versus DDH shows that only expression levels of Glyα1 and Glyα2 differed in the two regions, with higher expression of both genes in the DDH. The results of $GABA_A$R subunit expression in the SDH (*Figure 3.14A*, middle) indicate that GABAβ3 is expressed at a significantly higher level than GABAα5 and GABAβ2. No significant differences were detected in the expression of the remaining subunits. In the DDH (*Figure 3.14B*, right) GABAα1, GABAα5, and GABAβ2 were all expressed at similar levels; GABAα2, GABAα3, GABAβ3, and GABAγ2 were also expressed at similar levels, however the expression of these two groups of subunits differed, with significantly greater expression of the latter. Comparison of each $GABA_A$R subunit in SDH versus DDH shows that only expression levels of GABAα1 and GABAβ2 differed

in the two regions, again with higher expression detected in the DDH. Finally, comparison of CB_1 receptor expression in the SDH versus DDH detected significantly higher expression in the DDH.

SDH

DDH

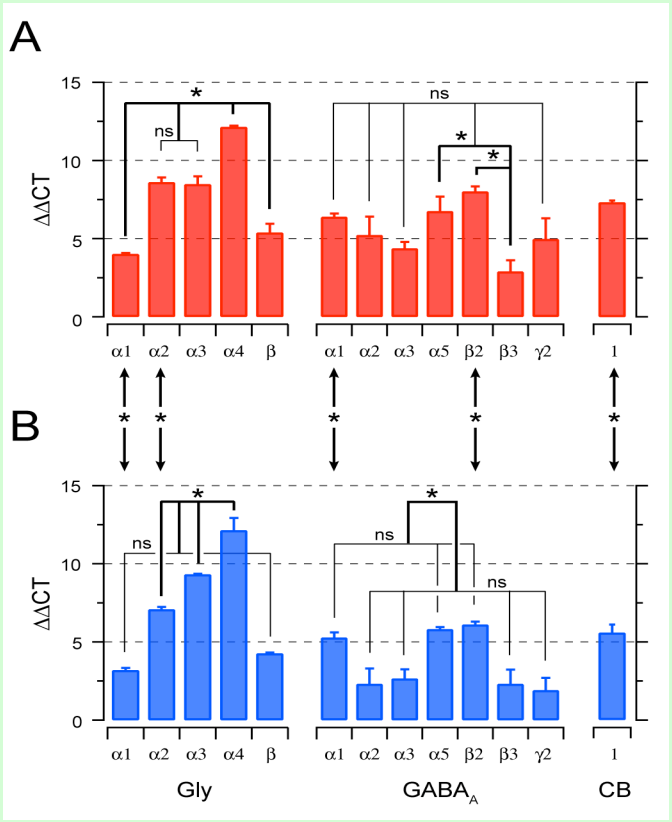

Figure 3.14 Comparison of GlyR, GABA$_A$R, and CB$_1$ receptor expression in the SDH and DDH.

A. *Plots summarising results from qPCR analysis of glycine receptor subunit, GABA$_A$ receptor subunit, and cannabinoid receptor expression in the SDH. Data are presented as ΔCT values, where ΔCT represents the difference in the mean cycle threshold (CT) of β-actin and the mean CT of each gene of interest. Thus,* ***lower*** *ΔCT values indicate higher relative gene expression and conversely higher ΔCT values indicate lower relative gene expression. All glycine receptor subunits (left bars) were expressed at significantly different levels (heavy line, *), except Glyα2 and Glyα3, which were similarly expressed (thin line, ns). Glyα1 and Glyβ were highly expressed while Glya4 expression was negligible. Across GABA$_A$ receptor subunits (middle bars), most were not expressed at significantly different levels, with the exception of GABAα5 and GABAβ2, which were expressed at significantly lower levels than GABAβ3 (the most highly expressed mRNA in SDH).* ***B.*** *Plots summarise results from qPCR analysis of mRNAs presented in identical format to A. All glycine receptor subunits (left bars) were expressed at significantly different levels (heavy line, *), except Glyα1 and Glyβ, which were similarly expressed (thin line, ns). Similar to SDH results, Glyα1 and Glyβ were highly expressed while Glyα4 expression was negligible. GABA$_A$ receptor subunit expression levels (middle bars) could be divided into two significantly different groups; GABAα1, GABAα5, and GABAβ2, which were expressed at similarly low levels; and GABAα2, GABAa3, GABAβ3, and GABAγ2 which were expressed at similarly high levels. Arrows between A and B denote subunits expressed at significantly different levels in SDH versus DDH (Glyα1, Glyα2, GABAα1, GABAβ2, and CB$_1$).*

Discussion

The experiments undertaken in Chapter 3 compared the features of fast inhibitory synaptic transmission in the mouse SDH and DDH, two spinal cord regions critical for the receipt, processing, and transmission of pain related information. Clear differences were found in the properties of glycinergic and $GABA_A$ergic mIPSCs in the two regions, and provide evidence of a role for inhibition mediated by $GABA_A$ergic sources in both the SDH and DDH, whereas inhibition from glycinergic sources certainly dominates in the DDH. The effect of the cannabinoid, methAEA, on glycinergic and $GABA_A$ergic inhibition in both SDH and DDH was assessed to investigate potential interactions cannabinoids may have with fast inhibitory neurotransmitter systems in the spinal cord. I found no evidence for 'direct effects' of the tested cannabinoid on glycine receptor function in either the SDH or DDH, though I did detect evidence for a subtle 'direct effect' on $GABA_A$ergic synaptic transmission in both regions. Specifically, methAEA slowed mIPSC rise time in both the SDH and DDH. Finally, I used real-time PCR to assess the relative expression of glycine receptor subunits, $GABA_A$ receptor subunits, and the CB_1 cannabinoid receptor in the SDH and DDH. These experiments show that the balance of glycinergic and $GABA_A$ergic subunit expression differs in the two regions and CB_1 receptor expression is greater in the DDH.

Inhibitory signaling in the SDH and DDH

Miniature inhibitory postsynaptic currents (mIPSCs)

My results show that glycinergic and $GABA_A$ergic receptors with differing physiological properties contribute to fast synaptic inhibition in the mouse SDH and DDH (*Figures 3.6 & 3.8*). The contribution of GlyRs to synaptic inhibition appears to be greatest in the DDH, whereas inhibition from GABAergic origins is important in

both regions.

Indeed, my study shows that glycinergic mIPSCs are larger, faster and more frequent in the DDH versus SDH. It is possible that this situation exists because the DDH receives the fastest inputs (based on axon conduction velocity) from large myelinated Aβ fibres that are not present in the SDH. This would allow much finer on/off modulation of inhibitory control needed for the processing of temporal information important for tactile responses. Furthermore, the DDH is involved in ***reflex*** motor pathways, via the spinothalamic tract and the motor cortex, where the timing of information transfer may be critical for the escape and survival of the species. Therefore, one would assume that signaling mechanisms in this region would have much faster kinetics due to their ***feed forward*** nature. In contrast, the slower kinetics of glycinergic mIPSCs in the SDH allows the sustained inhibitory action required by nociceptive inputs. Information from the SDH is more involved in ***processing*** of nociceptive signals and the descending inhibitory circuit, which involves ***feedback*** mechanisms via the parabrachial nucleus, the PAG, the RVM, and also emotional centres such as the amygdala. It can be imagined that temporal factors are not so important in this system, as events are not particularly time critical, but are rather more concerned with whether an event is present or not. When comparing the kinetics of the two inhibitory systems, the faster decay time and frequency of glycinergic mIPSCs would allow inhibition on a faster timescale, whereas the $GABA_A$ergic component would be involved in sustained inhibition.

My results bare some similarities and some differences to a study comparing GABAergic and glycinergic inhibitory synaptic transmission in lamina II and laminae III-IV of the young rat spinal cord (Inquimbert *et al*., 2007). These authors used mIPSC

properties to show that glycinergic inhibition dominated in the deep laminae. In contrast to my study, they reported that the kinetics of GlyR-mediated mIPSCs were similar in the two regions they studied. mIPSC frequency however, was significantly greater in the DDH in agreement with my findings. Further, it was shown that $GABA_A$ergic mIPSCs had similar amplitude, rise time and frequency in the SDH versus DDH, but that the decay time was significantly slower in the SDH, as it is with my results. The differences between the Inquimbert study and mine could be attributable to several possibilities. Firstly, there may be species differences in the anatomy and circuitry between the mouse and rat spinal cord. Secondly, these authors used young rats (P10-15) compared to the older mice in my studies, which were aged between 17-37 days. The age differences have implications for the kinetics of both glycinergic and $GABA_A$ergic receptors. For example, it is known that the adult form of the glycine receptor is not completely established until P21 (Becker *et al*., 1988; Kuhse *et al*., 1990; Akagi *et al*., 1991). Similar developmental profiles have been established for $GABA_A$Rs in the SDH of rats (Baccei & Fitzgerald, 2004). Finally, differences between their study and mine may be attributable to the fact that the precise definition of the SDH and DDH differs. I defined the SDH as laminae I-II, and the deeper dorsal horn as laminae IV-VI. In contrast, Inquimbert *et al*. only studied lamina II neurons and defined the deeper dorsal horn as laminae III-IV.

Further to the above, Cronin *et al*. (2004) used a systems level analysis to show that GABAergic mechanisms are more important than glycinergic mechanisms in setting inhibitory tone in the SDH, and that glycinergic mechanisms are more important than GABAergic mechanisms in the DDH. In support of this concept, it has been shown previously that the cell bodies of glycinergic neurons are located in lamina III and

deeper laminae (Ribeiro-Da-Silva & Coimbra, 1980; Todd & Sullivan, 1990; Zeilhofer *et al*., 2005) and indeed that the density of glycinergic fibres is much greater in the DDH (Zeilhofer *et al*., 2005). In contrast, GABAergic neurons are more abundant in the SDH (Todd & Sullivan, 1990; Todd & Spike, 1993; Mackie *et al*., 2003). This literature supports a clear regional variation for glycinergic and GABAergic inhibitory mechanisms in the dorsal horn of the spinal cord. My data shows this situation also pertains to the mouse.

One potential explanation for the large difference in peak amplitude and decay times of GlyR-mediated mIPSCs in the SDH and DDH reported here is recent work showing that a distinctly expressed GlyR containing the α3 subunit exists in the SDH, but is absent from the DDH of the spinal cord (Harvey *et al*., 2004). This study also went on to show that the GlyRα3 variant is selectively involved in spinal nociceptive processing, especially inflammatory pain (Harvey *et al*., 2004).

In spite of this electrophysiological and immunological evidence, my qPCR data do not agree with these findings. Indeed, I found no difference in GlyR α3 expression levels in the SDH versus DDH (*Figure 3.14*). It may be that the mRNA levels found in my studies using qPCR do not directly correlate to the amount of translated receptor protein found using immunohistochemistry, or that which is actually located at synapses. That is, just because mRNA is present, does not automatically mean that it will be translated into receptor protein in all areas of the spinal cord dorsal horn. Furthermore, the qPCR results showed a significant difference in expression levels of GlyR and $GABA_AR$ subunit levels between the SDH and DDH. There was greater expression of $GABA_AR$

α1 and β2 subunits, and GlyR α1 and α2 subunits in the DDH versus the SDH. These data appear to be consistent with the faster kinetics of receptors in this region.

Effects of cannabinoids on glycinergic sIPSCs

Analysis of results using the endocannabinoid analogue, methanandamide, revealed that cannabinoids have effects on spontaneous inhibitory events in the SDH and DDH of the spinal cord. Glycinergic spontaneous IPSC frequency was significantly reduced in both the SDH and DDH (*Figure 3.12*). Spontaneous IPSCs are composed of both action potential dependent (spontaneous) and independent (miniature) events. Any agent that prevents the initiation or propagation of action potentials along axons and into nerve terminals will therefore reduce the frequency of IPSC events. The fact that methanadamide reduced sIPSC frequency in my studies is consistent with reports describing a presynaptic action of cannabinoids, which leads to reduced vesicle release and thus an overall decrease in neuronal excitability (Vaughan *et al*., 1999; Howlett, 1985; Mackie & Hille, 1992; Pan *et al.*, 1996; Ong & Mackie, 1999b). Further, my results support immunohistochemical investigations which suggest that the CB_1 receptor is expressed on intrinsic spinal neurons (Farquhar-Smith *et al*. 2000), and other presynaptic locations such as sensory afferents and descending inputs to the spinal cord (Salio *et al.*, 2002).

It is likely that in my experiments, methanandamide suppressed both excitatory and inhibitory synaptic transmission in the SDH and DDH by decreasing the probability of release of glutamate from primary afferent terminals, which in turn reduced the release of glycine and GABA from interneurons. This finding has also been reported in the RVM, where the antinociceptive actions of cannabinoids were found to be via

presynaptic inhibition of GABAergic neurotransmission (Vaughan *et al*., 1999). At first, this seems to be in contradiction with the antinociceptive role of cannabinoids, because it has been shown previously that glycinergic and GABAergic antagonists produce hyperalgesia and tactile allodynia (Yaksh, 1989; Torsney & MacDermott, 2006). Therefore, one would expect that an increase in inhibitory signaling would be required to have such antinociceptive effects. But in this case, it is the ***net effect*** of the cannabinoid on both excitatory and inhibitory neurons that determines dorsal horn output. This perhaps emphasizes that there is still a long way to go before we can hope to understand the effects of modifying specific circuits in the pain pathway. We simply do not know enough about the various interneuronal populations in the dorsal horn (Graham *et al*., 2007).

It has also been suggested that TRPV1 receptor activation plays a partial role in the antinociceptive effect of AEA at the spinal level, and that cannabinoid and TRPV1 receptor coactivation can give rise to both pronociceptive and antinociceptive effects, depending upon the levels of pro- and antinociceptive ligands present (Horvath *et al*., 2008). This may explain, at least partially, the observed reduction in inhibitory synaptic activity during my studies.

Effects of cannabinoids on GABAergic sIPSCs

Experiments in the SDH showed that $GABA_A$ergic sIPSC amplitude and frequency were significantly decreased after the addition of methAEA *(Figure 3.13)*. This is in agreement with many studies describing cannabinoid effects on a phenomenon known as depolarisation-induced suppression of inhibition, or DSI, in other parts of the nervous system (Freund *et al.*, 2003; Chevaleyre *et al.*, 2006). DSI involves a unique, slow,

Ca^{2+}-dependent type of retrograde signaling (Llano *et al.*, 1991; Pitler & Alger, 1992). It has been shown that a train of postsynaptic action potentials, or prolonged postsynaptic depolarisation, can induce a transient suppression of spontaneous or evoked GABAergic IPSPs or IPSCs, recorded in the postsynaptic neuron (Alger & Pitler, 1995). Early studies in hippocampal pyramidal neurons and cerebellar Purkinje neurons showed that DSI requires a large increase in intracellular Ca^{2+} concentration in the postsynaptic cell, resulting in the release of retrograde messengers that act on the presynaptic terminals, thereby reducing the probability of GABA release. Endocannabinoids were subsequently found to be these retrograde messengers (Kreitzer & Regehr, 2001a, b; Ohno-Shosaku *et al.*, 2001; Wilson & Nicoll, 2001).

DSI can be initiated or blocked by manipulating conditions on the postsynaptic side of the synaptic cleft, and involves voltage-gated Ca^{2+} channels, or Ca^{2+} release from intracellular stores (Llano *et al.*, 1991; Pitler & Alger, 1992, 1994; Lenz *et al.*, 1998). DSI does not involve changes in postsynaptic $GABA_A$ receptor sensitivity, since the response to iontophoretically applied GABA does not change, nor does the amplitude of mIPSCs (Freund *et al.*, 2003).

Despite the postsynaptic site of initiation, numerous experiments have shown that DSI is expressed presynaptically, as a reduction in GABA release (Alger *et al.*, 1996). Direct evidence of an inhibitory G protein-mediated presynaptic action, has been provided by Pitler and Alger (Pitler & Alger, 1994), who showed that DSI was pertussis toxin-sensitive, further supporting a role for the GPCR cannabinoid receptors in this phenomenon.

Interestingly in my studies, methAEA had no effect on amplitude, decay time or frequency of $GABA_A$ergic sIPSCs in the DDH *(Figure 3.13)*. One explanation may involve the differential laminar distribution of $GABA_A$ receptor subunits in the spinal cord. The differential expression of $GABA_A$-receptor subtypes between the SDH and DDH may directly affect the ability of the SDH to modulate nociceptive communication between primary afferents and projection neurons, as proposed by Melzack and Wall in their 'gate theory' (Melzack & Wall, 1965; Wall, 1980). Furthermore, the presence of distinct $GABA_AR$ subtypes suggest that GABAergic transmission could be modulated differentially at these two spinal levels by specific pharmacological agents such as cannabinoids.

Effects of cannabinoids on glycinergic mIPSCs

My experiments showed that methAEA reduces the frequency of glycinergic mIPSCs in the SDH and DDH (*Figure 3.10*). This is in agreement with the literature, which shows that cannabinoids are released postsynaptically and act retrogradely at presynaptic terminals leading to an overall reduction of neurotransmitter release and cellular inhibition (Twitchell *et al*., 1997; Katona *et al*., 1999; Schlicker & Kathmann, 2001; Vaughan & Christie, 2005).

Because two recent reports have suggested that cannabinoids can directly modulate GlyRs (Lozovaya *et al*., 2005; Hejazi *et al*., 2006), I undertook a series of experiments to test this theory by observing the effects of methAEA on glycinergic mIPSCs in both the SDH and DDH. The two previous studies support direct effects, but disagree on the actual effect cannabinoids have on GlyRs. The major disadvantage of these studies is that they were being undertaken in somewhat artificial systems. For example, Lozovaya

et al. (2005) used isolated neurons, whereas Hejazi *et al*. (2006) used both dissociated neurons and Xenopus oocytes transfected with recombinant GlyRs. My studies examined whether CB_1 agonists directly modulate GlyRs by using the more 'physiologically intact' spinal cord slice preparation. The effects of methAEA on glycinergic mIPSCs were made in both the SDH and DDH because recent work suggests that the type of GlyR differs in the two regions (Harvey *et al*., 2004). MethAEA decreased the frequency but not amplitude nor decay time of these events. Thus, I saw no evidence of direct allosteric modulation of synaptically located GlyRs by cannabinoids, in either the SDH or DDH of the mouse spinal cord.

The reasons for the differences between studies could be two-fold. Firstly, my recordings were made from native synapses, where the dynamic state of GlyRs is likely to be different from that in recombinant systems. For example, factors such as the compliment of cellular machinery, the makeup of GlyR subtypes, and the turnover of receptors in the neuronal membrane would obviously differ between the two systems. Secondly, it has recently been reported that direct effects of cannabinoids on recombinant glycine receptors is subunit-specific, and concentration dependent (Yang *et al*., 2008). This would have major implications for comparing effects of bath-applied compounds in an *in vitro* spinal cord preparation with those applied to a recombinant cell culture system. It is most unlikely that the recombinant model would contain all of the physiologically relevant machinery present in the intact preparation. Thus, effective cannabinoid concentrations will vary between these model systems, and subunit expression would also differ. This makes it difficult to extrapolate conclusions from reduced preparations to intact synapses.

Effects of cannabinoids on $GABA_A$ergic mIPSCs

I also tested for direct effects of cannabinoids on $GABA_A$ergic mIPSCs in the SDH and DDH (*Figure 3.11*). My experiments showed a reduction in frequency of mIPSC events. This has also been reported in endogenous cannabinoid-mediated DSI experiments in the cerebellum, although the exact mechanisms underlying these cannabinoid-mediated effects on mIPSCs is unknown (Diana *et al*., 2002). In addition, I also observed a previously unreported, subtle, but significant slowing in mIPSC rise time in both regions. This is perhaps not surprising, as $GABA_A$Rs have been shown to be modulated by a multitude of exogenous and endogenous substances. For example, the benzodiazepines (Haefely *et al*., 1975), gaseous and intravenous anaesthetics (Lin *et al*., 1992; Lin *et al*., 1993), ethanol and other alcohols (Soldo *et al*., 1994), and neurosteroids (Harrison & Simmonds, 1984; Majewska *et al*., 1986) can all positively modulate the $GABA_A$R responses to GABA via allosteric actions on the receptor complex. Further, there are a number of discrete binding sites for Zn^{2+} on $GABA_A$Rs, which can lead to potent subtype-specific inhibition of $GABA_A$R function (Hosie *et al*., 2003). Therefore, it is possible that cannabinoids may prove to be yet another modulatory agent of $GABA_A$R-mediated signaling.

Functional implications for pain processing

It has been shown that suppression of inhibitory signaling in the SDH can lead to hypersensitivity, whereas this same suppression in the DDH leads to tactile allodynia (Torsney & MacDermott, 2006; Yaksh, 1989; Reeve *et al*., 1998). My results showed that differential inhibitory signaling properties exist in the dorsal horn of the spinal cord. When combined with the observed effects that methAEA had on these properties, it reinforces the notion that ***both*** regions of the dorsal horn play roles in nociceptive processing, with neither region more important than the other. Previous work has shown that the SDH and DDH receive different inputs, project to unique targets and possess intrinsic variations in connectivity. I now propose that differences also exist in the inhibitory control mechanisms within each region. These results show a distinct dominance of glycinergic signaling in the DDH and significant differences in the kinetics of both glycinergic and GABAergic events in the SDH and DDH. This provides a mechanism for selectively modifying inhibition in the two regions, and suggests that these two regions of the dorsal horn may process distinct forms of pain differently.

CHAPTER 4

Summary, Future Directions & Conclusions

Summary

The over-arching aim of this thesis was to examine several aspects of cannabinoid signaling that may play a role in spinal cord pain processing mechanisms. In the first series of experiments I assessed dimerization of CB_1 and $5HT_{2A}$ receptors using recombinant, cell culture, and fluorescent resonance energy (FRET) techniques.

The major findings from these studies were:

1. Cannabinoid CB_1 receptors are capable of forming homodimers.
2. Serotonergic $5HT_{2A}$ receptors are capable of forming homodimers.
3. Cannabinoid CB_1 and serotonergic $5HT_{2A}$ receptors can form heterodimers with one another.

Because both spinal cannabinoid CB_1 and serotonergic $5HT_2$ receptors have been implicated in pain and analgesia pathways in the nervous system, this bodes well for the development of analgesic compounds that take advantage of the synergy that may exist between these two signaling systems. Indeed, it has been shown that many receptors can change dimerization state in response to ligand (drug) binding (Woolf & Linderman, 2004). This means drug designers need to consider receptor dimerization, or they can harness dimerization to control cellular responses. For example, creating drugs that promote homo- or heterodimerization would lead to therapies that target receptor organization, internalization and subsequent signaling.

My next series of experiments examined inhibitory mechanisms within the spinal cord dorsal horn of the mouse and the effects of the endocannabinoid, methanandamide, on inhibitory synaptic transmission in SDH and DDH neurons. The use of an *in vitro* spinal cord slice preparation and the whole cell patch clamp technique allowed me to determine whether cannabinoids have a direct effect on glycine and/or $GABA_A$

receptors in a more physiologically relevant environment, rather than recombinant and cell culture systems previously employed.

The major findings from these studies were:

1. Neurons in the SDH are smaller than neurons in the DDH. This is in agreement with histological data.
2. At the neuronal level, $GABA_A$Rs seem to play a more widespread role in fast inhibitory synaptic transmission in both the SDH and DDH whereas the role for glycine appears more prominent in the DDH.
3. I found no evidence for a ***direct*** effect of methAEA on glycine receptors in either SDH or DDH neurons, but rather, it may have ***direct*** effects or modulatory actions on $GABA_A$Rs in both regions.

My final series of experiments investigated the subunit expression of glycine and $GABA_A$ receptors and the cannabinoid CB_1 receptor using real-time RT-PCR (qPCR).

The major findings from these studies were:

1. The Glyα1 subunit gene is highly expressed in both SDH and DDH along with Glyβ. Expression levels of Glyα1 and Glyα2 genes were higher in the DDH. Interestingly, I found higher expression levels of the Glyα3 subunit gene in the DDH versus SDH.
2. The GABAβ3 subunit gene is highly expressed in the SDH, with GABAα1, GABAα5, and GABAβ2 exhibiting similar expression levels in the DDH. The GABAα1 and GABAβ2 subunit genes exhibited higher expression levels in the DDH versus SDH.

3. Expression of the CB_1 receptor gene was higher in the DDH versus SDH.

Inhibitory neurotransmission mediated by the neurotransmitters glycine and GABA in the spinal cord dorsal horn has been shown to be important in both acute and chronic pain states. Similarly, cannabinoids have been shown to influence pain and analgesia. Because the ultimate aim of basic biomedical research is to translate findings to the clinic it is useful to briefly conclude by considering my findings in the context of new therapeutics that might be developed for antinociception and analgesia.

The glycinergic system

One of the main factors driving the work in this thesis was the discovery in 2004 of a unique form of the GlyR (containing α3 subunits) in the spinal cord. Previously, the GlyR was largely ignored as a pain target because the receptor exists primarily in one form (containing α and β subunits) and is widely distributed in spinal cord and brainstem nuclei. Thus, being able to selectively target the unique α3 subunit-containing population of GlyRs should prove promising in the treatment of pain. Unfortunately, there is currently no way to selectively target α3-containing GlyRs. However, experiments studying the α3 GlyR variant using chimeric receptors and eukaryotic expression vectors in human cell lines are underway (Zeilhofer - personal communication). Such studies are needed to discover lead compounds that can modify the function of the unique α3 GlyR. Of course these compounds will ultimately need to be tested in spinal cord slices and in vivo. Further, compounds that selectively potentiate the function of α3 GlyRs or block the PGE_2 pathway may present a promising approach to pain therapy in the future (Zeilhofer, 2005). Finally, I also suggest that future work on the glycinergic system and pain should consider the

neuronal populations in the spinal cord that actually express GlyRs. It is easy to forget that the SDH especially contains multiple neuronal types and that most experiments on SDH neurons simply average results obtained in a large sample of neurons. This may prove important, because even though my data show that glycinergic inhibitory drive is low "overall" in the SDH, this does not preclude the possibility that it is crucially important in a subset of SDH neurons, which themselves may be an integral part of the pain processing machinery. It would be interesting to know which (or if) one neuron type expresses the α3 GlyR in highest concentrations and its role in spinal cord circuitry. Future targeting of fluorescently labelled neurons of known phenotype (excitatory or inhibitory IN or projection neurons; *Figure 3.2*) engineered via transgenic techniques will help address this problem.

The GABAergic system

Unlike the glycinergic systems, the GABAergic system has long been used as a therapeutic target. This is primarily due to the existence of multiple receptor types and the concentration of certain types in specific brain regions. This approach has worked well for some conditions, such as anxiety, but $GABA_A$ergic drugs have not been used extensively for pain therapy. The control and treatment of pain in the future may also be based upon medications that can take advantage of $GABA_A$ receptor heterogeneity in the spinal cord dorsal horn (Zeilhofer and Zeilhofer, 2008). This would require the development of subtype-specific receptor ligands which act selectively at different levels of the spinal cord, producing effective analgesia without the undesirable central side effects. Obviously the study of these two inhibitory systems (glycine and GABA) are not mutually exclusive, and it may be that a combination of drugs that target both

the glycinergic and GABAergic systems in the spinal cord proves beneficial for the treatment of pain in the future.

The Cannabinoid system

Cannabinoids and central or neuropathic pain

Cannabinoids have been shown to prevent two hallmarks of neuropathic pain, namely allodynia (pain from non-noxious stimuli) and hyperalgesia (increased sensitivity to noxious stimuli) (Herzberg *et al.*, 1997; Richardson *et al.*, 1998c; Martin *et al.*, 1999). If neuropathic pain involves an increase in endocannabinoid release, drugs interfering with their inactivation could prove more useful than CB_1 agonists. Additionally, new ligands that recognize different dynamic states of the CB_1 receptor, may be useful in activating the endocannabinoid system, producing analgesia without the undesirable central side effects. In essence, the complexity of the cannabinoid system may actually provide more targets for drug therapies aimed at ultimately increasing CB_1 receptor activation.

Cannabinoids and peripheral pain

It has been shown that cannabinoid receptor agonists can alleviate pain by acting at peripheral CB_1 receptors (Agarwal *et al*., 2007; Calignano *et al.*, 1998; Richardson *et al.*, 1998c). This fact inspires the notion that nociceptive signals could be modulated at the first point of pain processing (ie. the peripheral nociceptor). It also theoretically enables the synthesis of a peripherally-acting drug, which could control peripheral pain without the unwanted psychotropic CNS side effects that normally accompany the administration of CB_1 agonists.

Conclusions

Our knowledge of the mechanisms of pain has increased exponentially over the last two decades, but sadly the discovery of new pharmacological agents to treat pain has been limited. Local anaesthetics and non-steroidal anti-inflammatory drugs (NSAIDs), can produce a reasonable level of analgesia following acute injury, but treatments for neuropathic pain are limited and have proved disappointing. The recent focus on spinal inhibitory mechanisms and their critical role in the pain pathways represents a promising new avenue of enquiry. It is hoped that recent findings at the basic science level of analysis on the glycinergic and $GABA_A$ergic systems may enable new pharmacological approaches to pain management.

Acknowledgements

This work was supported by the National Health and Medical Research Council of Australia (Grants 276403 and 401244), The Hunter Medical Research Institute, and The University of Newcastle, Australia.

REFERENCES

Agarwal N, Pacher P, Tegeder I, Amaya F, Constantin CE, Brenner GJ, Rubino T, Michalski CW, Marsicano G, Monory K, Mackie K, Marian C, Batkai S, Parolaro D, Fischer MJ, Reeh P, Kunos G, Kress M, Lutz B, Woolf CJ & Kuner R. (2007). Cannabinoids mediate analgesia largely via peripheral type 1 cannabinoid receptors in nociceptors. *Nat Neurosci* **10,** 870-879.

Akagi H, Hirai K & Hishinuma F. (1991). Cloning of a glycine receptor subtype expressed in rat brain and spinal cord during a specific period of neuronal development. *FEBS letters* **281,** 160-166.

Alger BE & Pitler TA. (1995). Retrograde signaling at GABAA-receptor synapses in the mammalian CNS. *Trends Neurosci* **18,** 333-340.

Alger BE, Pitler TA, Wagner JJ, Martin LA, Morishita W, Kirov SA & Lenz RA. (1996). Retrograde signalling in depolarization-induced suppression of inhibition in rat hippocampal CA1 cells. *J Physiol* **496 (Pt 1),** 197-209.

Andreasson S, Allebeck P, Engstrom A & Rydberg U. (1987). Cannabis and schizophrenia. A longitudinal study of Swedish conscripts. *Lancet* **2,** 1483-1486.

Andreasson S, Allebeck P, Engstrom A & Rydberg U. (1988). Cannabis and schizophrenia. *Lancet* **1,** 1000-1001.

Andreasson S, Allebeck P & Rydberg U. (1989). Schizophrenia in users and nonusers of cannabis. A longitudinal study in Stockholm County. *Acta Psychiatr Scand* **79,** 505-510.

Angers S, Salahpour A & Bouvier M. (2001). Biochemical and biophysical demonstration of GPCR oligomerization in mammalian cells. *Life Sci* **68,** 2243-2250.

Apkarian AV, Bushnell MC, Treede RD & Zubieta JK. (2005). Human brain mechanisms of pain perception and regulation in health and disease. *EJP (London, England)* **9,** 463-484.

Arora RC & Meltzer HY. (1991). Serotonin2 (5-HT2) receptor binding in the frontal cortex of schizophrenic patients. *J Neural Transm* **85,** 19-29.

Arseneault L, Cannon M, Witton J & Murray RM. (2004). Causal association between cannabis and psychosis: examination of the evidence. *Br J Psychiatry* **184,** 110-117.

Baccei ML & Fitzgerald M. (2004). Development of GABAergic and glycinergic transmission in the neonatal rat dorsal horn. *J Neurosci* **24,** 4749-4757.

Barann M, Molderings G, Bruss M, Bonisch H, Urban BW & Gothert M. (2002). Direct inhibition by cannabinoids of human 5-HT3A receptors: probable involvement of an allosteric modulatory site. *BJP* **137,** 589-596.

Becker CM, Hoch W & Betz H. (1988). Glycine receptor heterogeneity in rat spinal cord during postnatal development. *The EMBO journal* **7,** 3717-3726.

Becker CM, Schmieden V, Tarroni P, Strasser U & Betz H. (1992). Isoform-selective deficit of glycine receptors in the mouse mutant spastic. *Neuron* **8,** 283-289.

Begg M, Pacher P, Batkai S, Osei-Hyiaman D, Offertaler L, Mo FM, Liu J & Kunos G. (2005). Evidence for novel cannabinoid receptors. *Pharmacol Ther* **106,** 133-145.

Bekkers JM & Stevens CF. (1989). NMDA and non-NMDA receptors are co-localized at individual excitatory synapses in cultured rat hippocampus. *Nature* **341,** 230-233.

Beltramo M, Stella N, Calignano A, Lin SY, Makriyannis A & Piomelli D. (1997). Functional role of high-affinity anandamide transport, as revealed by selective inhibition. *Science (New York, NY* **277,** 1094-1097.

Bersani G, Orlandi V, Kotzalidis GD & Pancheri P. (2002). Cannabis and schizophrenia: impact on onset, course, psychopathology and outcomes. *Eur Arch Psychiatry Clin Neurosci* **252,** 86-92.

Beveridge NJ, Tooney PA, Carroll AP, Gardiner E, Bowden N, Scott RJ, Tran N, Dedova I & Cairns MJ. (2008). Dysregulation of miRNA 181b in the temporal cortex in schizophrenia. *Hum Mol Gen* **17,** 1156-1168.

Bisogno T, Melck D, Bobrov M, Gretskaya NM, Bezuglov VV, De Petrocellis L & Di Marzo V. (2000). N-acyl-dopamines: novel synthetic CB(1) cannabinoid-receptor ligands and inhibitors of anandamide inactivation with cannabimimetic activity in vitro and in vivo. *Biochem J* **351 Pt 3,** 817-824.

Bisogno T, Sepe N, Melck D, Maurelli S, De Petrocellis L & Di Marzo V. (1997). Biosynthesis, release and degradation of the novel endogenous cannabimimetic metabolite 2-arachidonoylglycerol in mouse neuroblastoma cells. *Biochem J* **322 (Pt 2),** 671-677.

Bohlhalter S, Weinmann O, Mohler H & Fritschy JM. (1996). Laminar compartmentalization of GABAA-receptor subtypes in the spinal cord: an immunohistochemical study. *J Neurosci* **16,** 283-297.

Boute N, Jockers R & Issad T. (2002). The use of resonance energy transfer in high-throughput screening: BRET versus FRET. *Trends Pharmacol Sci* **23,** 351-354.

Bouvier M. (2001). Oligomerization of G-protein-coupled transmitter receptors. *Nat Rev Neurosci* **2,** 274-286.

Breit A, Lagace M & Bouvier M. (2004). Hetero-oligomerization between beta2- and beta3-adrenergic receptors generates a beta-adrenergic signaling unit with distinct functional properties. *J Biol Chem* **279,** 28756-28765.

Breivogel CS, Griffin G, Di Marzo V & Martin BR. (2001). Evidence for a new G protein-coupled cannabinoid receptor in mouse brain. *Mol Pharmacol* **60,** 155-163.

Breivogel CS, Sim LJ & Childers SR. (1997). Regional differences in cannabinoid receptor/G-protein coupling in rat brain. *J Pharmacol Exp Ther* **282,** 1632-1642.

Bridges D, Ahmad K & Rice AS. (2001). The synthetic cannabinoid WIN55,212-2 attenuates hyperalgesia and allodynia in a rat model of neuropathic pain. *BJ*P **133,** 586-594.

Brown AG. (1982). The dorsal horn of the spinal cord. *Q J Exp Physiol (Cambridge, England)* **67,** 193-212.

Brown SP, Brenowitz SD & Regehr WG. (2003). Brief presynaptic bursts evoke synapse-specific retrograde inhibition mediated by endogenous cannabinoids. *Nat Neurosci* **6,** 1048-1057.

Burgess PR & Perl ER. (1973). Cutaneous mechanoreceptors and nociceptors. *In: Handbook of Sensory Physiology Somatosensory System* **2,** 30-78.

Burnet PW, Eastwood SL & Harrison PJ. (1996). 5-HT1A and 5-HT2A receptor mRNAs and binding site densities are differentially altered in schizophrenia. *Neuropsychopharmacology* **15,** 442-455.

Burt DR. (2005). Alpha subunit position and GABA receptor function. *Sci STKE* **2005,** pe5.

Cadas H, Schinelli S & Piomelli D. (1996). Membrane localization of N-acylphosphatidylethanolamine in central neurons: studies with exogenous phospholipases. *J Lipid Mediat Cell Signal* **14,** 63-70.

Calignano A, La Rana G, Giuffrida A & Piomelli D. (1998). Control of pain initiation by endogenous cannabinoids. *Nature* **394,** 277-281.

Callister RJ & Walmsley B. (1996). Amplitude and time course of evoked and spontaneous synaptic currents in rat submandibular ganglion cells. *The J Physiol* **490 (Pt 1),** 149-157.

Carlisle SJ, Marciano-Cabral F, Staab A, Ludwick C & Cabral GA. (2002). Differential expression of the CB2 cannabinoid receptor by rodent macrophages and macrophage-like cells in relation to cell activation. *Int Immunopharmacol* **2,** 69-82.

Carrier EJ, Kearn CS, Barkmeier AJ, Breese NM, Yang W, Nithipatikom K, Pfister SL, Campbell WB & Hillard CJ. (2004). Cultured rat microglial cells synthesize the endocannabinoid 2-arachidonylglycerol, which increases proliferation via a CB2 receptor-dependent mechanism. *Mol Pharmacol* **65,** 999-1007.

Carrillo JJ, Pediani J & Milligan G. (2003). Dimers of class A G protein-coupled receptors function via agonist-mediated trans-activation of associated G proteins. *J Biol Chem* **278,** 42578-42587.

Cheer JF, Cadogan AK, Marsden CA, Fone KC & Kendall DA. (1999). Modification of 5-HT2 receptor mediated behaviour in the rat by oleamide and the role of cannabinoid receptors. *Neuropharmacology* **38,** 533-541.

Chemin J, Monteil A, Perez-Reyes E, Nargeot J & Lory P. (2001). Direct inhibition of T-type calcium channels by the endogenous cannabinoid anandamide. *The EMBO journal* **20,** 7033-7040.

Chery N & de Koninck Y. (1999). Junctional versus extrajunctional glycine and GABA(A) receptor-mediated IPSCs in identified lamina I neurons of the adult rat spinal cord. *J Neurosci* **19,** 7342-7355.

Chevaleyre V, Takahashi KA & Castillo PE. (2006). Endocannabinoid-mediated synaptic plasticity in the CNS. *Annu Rev Neurosci* **29,** 37-76.

Childers SR & Deadwyler SA. (1996). Role of cyclic AMP in the actions of cannabinoid receptors. *Biochem Pharmacol* **52,** 819-827.

Christensen BN & Perl ER. (1970). Spinal neurons specifically excited by noxious or thermal stimuli: marginal zone of the dorsal horn. *J Neurophysiol* **33,** 293-307.

Cichewicz DL. (2004). Synergistic interactions between cannabinoid and opioid analgesics. *Life Sci* **74,** 1317-1324.

Clements JD & Bekkers JM. (1997). Detection of spontaneous synaptic events with an optimally scaled template. *Biophys J* **73,** 220-229.

Cohen C, Kodas E & Griebel G. (2005). CB1 receptor antagonists for the treatment of nicotine addiction. *Pharmacol Biochem Behav* **81,** 387-395.

Collins AL, Ma D, Whitehead PL, Martin ER, Wright HH, Abramson RK, Hussman JP, Haines JL, Cuccaro ML, Gilbert JR & Pericak-Vance MA. (2006). Investigation of autism and GABA receptor subunit genes in multiple ethnic groups. *Neurogenetics* **7,** 167-174.

Couve A, Filippov AK, Connolly CN, Bettler B, Brown DA & Moss SJ. (1998). Intracellular retention of recombinant GABAB receptors. *J Biol Chem* **273,** 26361-26367.

Craig AD. (1995). Distribution of brainstem projections from spinal lamina I neurons in the cat and the monkey. *J Comp Neurol* **361,** 225-248.

Cravatt BF, Giang DK, Mayfield SP, Boger DL, Lerner RA & Gilula NB. (1996). Molecular characterization of an enzyme that degrades neuromodulatory fatty-acid amides. *Nature* **384,** 83-87.

Cronin JN, Bradbury EJ & Lidierth M. (2004). Laminar distribution of GABAA- and glycine-receptor mediated tonic inhibition in the dorsal horn of the rat lumbar spinal cord: effects of picrotoxin and strychnine on expression of Fos-like immunoreactivity. *Pain* **112,** 156-163.

Curtis DR, Hosli L & Johnston GA. (1968a). A pharmacological study of the depression of spinal neurones by glycine and related amino acids. *Exp Brain Res* **6,** 1-18.

Curtis DR, Hosli L & Johnston GA. (1968b). Inhibitory effect of glycine and similar amino acids on spinal neurons. *Helvetica physiologica et pharmacologica acta* **26,** CR 205-206.

Curtis DR, Hosli L, Johnston GA & Johnston IH. (1968c). The hyperpolarization of spinal motoneurones by glycine and related amino acids. *Exp Brain Res* **5,** 235-258.

Danzebrink RM & Gebhart GF. (1991). Evidence that spinal 5-HT1, 5-HT2 and 5-HT3 receptor subtypes modulate responses to noxious colorectal distension in the rat. *Brain res* **538,** 64-75.

de Fonseca FR, Del Arco I, Bermudez-Silva FJ, Bilbao A, Cippitelli A & Navarro M. (2005). The endocannabinoid system: physiology and pharmacology. *Alcohol Alcsm* **40,** 2-14.

de Haan L, Booij J, Lavalaye J, van Amelsvoort T & Linszen D. (2006). Occupancy of dopamine D2 receptors by antipsychotic drugs is related to nicotine addiction in young patients with schizophrenia. *Psychopharmacology* **183,** 500-505.

Dean B, Sundram S, Bradbury R, Scarr E & Copolov D. (2001). Studies on [3H]CP-55940 binding in the human central nervous system: regional specific changes in density of cannabinoid-1 receptors associated with schizophrenia and cannabis use. *Neuroscience* **103,** 9-15.

Degenhardt L, Hall W & Lynskey M. (2003). Testing hypotheses about the relationship between cannabis use and psychosis. *Drug Alcohol Depend* **71,** 37-48.

Derocq JM, Segui M, Marchand J, Le Fur G & Casellas P. (1995). Cannabinoids enhance human B-cell growth at low nanomolar concentrations. *FEBS letters* **369,** 177-182.

Devane WA, Dysarz FA, 3rd, Johnson MR, Melvin LS & Howlett AC. (1988). Determination and characterization of a cannabinoid receptor in rat brain. *Mol Pharmacol* **34,** 605-613.

Devane WA, Hanus L, Breuer A, Pertwee RG, Stevenson LA, Griffin G, Gibson D, Mandelbaum A, Etinger A & Mechoulam R. (1992). Isolation and structure of a brain constituent that binds to the cannabinoid receptor. *Science (New York, NY* **258,** 1946-1949.

Devlin MG & Christopoulos A. (2002). Modulation of cannabinoid agonist binding by 5-HT in the rat cerebellum. *J Neurochem* **80,** 1095-1102.

Di Marzo V, Blumberg PM & Szallasi A. (2002). Endovanilloid signaling in pain. *Curr Opin Neurobiol* **12,** 372-379.

Di Marzo V, Breivogel CS, Tao Q, Bridgen DT, Razdan RK, Zimmer AM, Zimmer A & Martin BR. (2000). Levels, metabolism, and pharmacological activity of anandamide in CB(1) cannabinoid receptor knockout mice: evidence for non-CB(1), non-CB(2) receptor-mediated actions of anandamide in mouse brain. *J Neurochem* **75,** 2434-2444.

Diana MA, Levenes C, Mackie K & Marty A. (2002). Short-term retrograde inhibition of GABAergic synaptic currents in rat Purkinje cells is mediated by endogenous cannabinoids. *J Neurosci* **22,** 200-208.

D'Mello R & Dickenson AH. (2008). Spinal cord mechanisms of pain. *Br J Anaesth* **101,** 8-16.

Eidne KA, Kroeger KM & Hanyaloglu AC. (2002). Applications of novel resonance energy transfer techniques to study dynamic hormone receptor interactions in living cells. *Trends Endocrinol Metab* **13,** 415-421.

Endlich K, Kuhn R & Steinhausen M. (1993). Visualization of serotonin effects on renal vessels of rats. *Kidney Int* **43,** 314-323.

Facci L, Dal Toso R, Romanello S, Buriani A, Skaper SD & Leon A. (1995). Mast cells express a peripheral cannabinoid receptor with differential sensitivity to anandamide and palmitoylethanolamide. *PNAS* **92,** 3376-3380.

Fan P. (1995). Cannabinoid agonists inhibit the activation of 5-HT3 receptors in rat nodose ganglion neurons. *J Neurophysiol* **73,** 907-910.

Farquhar-Smith WP, Egertova M, Bradbury EJ, McMahon SB, Rice AS & Elphick MR. (2000). Cannabinoid CB(1) receptor expression in rat spinal cord. *Mol Cell Neurosci* **15,** 510-521.

Farquhar-Smith WP & Rice AS. (2001). Administration of endocannabinoids prevents a referred hyperalgesia associated with inflammation of the urinary bladder. *Anesthesiology* **94,** 507-513; discussion 506A.

Felder CC, Joyce KE, Briley EM, Glass M, Mackie KP, Fahey KJ, Cullinan GJ, Hunden DC, Johnson DW, Chaney MO, Koppel GA & Brownstein M. (1998). LY320135, a novel cannabinoid CB1 receptor antagonist, unmasks coupling of

the CB1 receptor to stimulation of cAMP accumulation. *J Pharmacol Exp Ther* **284,** 291-297.

Fezza F, Bisogno T, Minassi A, Appendino G, Mechoulam R & Di Marzo V. (2002). Noladin ether, a putative novel endocannabinoid: inactivation mechanisms and a sensitive method for its quantification in rat tissues. *FEBS letters* **513,** 294-298.

Fisyunov A, Tsintsadze V, Min R, Burnashev N & Lozovaya N. (2006). Cannabinoids modulate the P-type high-voltage-activated calcium currents in purkinje neurons. *J Neurophysiol* **96,** 1267-1277.

Foord SM, Bonner TI, Neubig RR, Rosser EM, Pin JP, Davenport AP, Spedding M & Harmar AJ. (2005). International Union of Pharmacology. XLVI. G protein-coupled receptor list. *Pharmacological reviews* **57,** 279-288.

Foster T. (1959). 10th Spiers Memorial Lecture. Transfer mechanisms of electronic excitation. *Discussions of the Faraday Society* **27,** 7-17.

Frankhauser M. (2002). [Haskish as medication; on the significance of cannabis sativa in western medicine]. *Veroff Schweiz Ges Gesch Pharm* **23,** 1-329.

Franklin KBJ & Paxinos G. (1997). Mouse Brain in Stereotaxic Coordinates, Third Edition. *San Diego, CA: Academic Press*.

Freund TF, Katona I & Piomelli D. (2003). Role of endogenous cannabinoids in synaptic signaling. *Physiol Rev* **83,** 1017-1066.

Galiegue S, Mary S, Marchand J, Dussossoy D, Carriere D, Carayon P, Bouaboula M, Shire D, Le Fur G & Casellas P. (1995). Expression of central and peripheral cannabinoid receptors in human immune tissues and leukocyte subpopulations. *Eur J Biochem* **232,** 54-61.

Gao BX & Ziskind-Conhaim L. (1995). Development of glycine- and GABA-gated currents in rat spinal motoneurons. *J Neurophysiol* **74,** 113-121.

Gaoni Y & Mechoulam RJ. (1964). Isolation structure and partial synthesis of an active constituent of hashish. *J Am Chem Soc* **86,** 1646-1647.

Gebremedhin D, Lange AR, Campbell WB, Hillard CJ & Harder DR. (1999). Cannabinoid CB1 receptor of cat cerebral arterial muscle functions to inhibit L-type Ca2+ channel current. *Am J Physiol* **276,** H2085-2093.

George SR, O'Dowd BF & Lee SP. (2002). G-protein-coupled receptor oligomerization and its potential for drug discovery. *Nat Rev Drug Discovery* **1,** 808-820.

Gether U & Kobilka BK. (1998). G protein-coupled receptors. II. Mechanism of agonist activation. *J Biol Chem* **273,** 17979-17982.

Gilbert PE. (1981). A comparison of THC, nantradol, nabilone, and morphine in the chronic spinal dog. *J Clin Pharmacol* **21,** 311S-319S.

Gilman AG. (1987). G proteins: transducers of receptor-generated signals. *Annu Rev Biochem* **56,** 615-649.

Glass M, Dragunow M & Faull RL. (1997). Cannabinoid receptors in the human brain: a detailed anatomical and quantitative autoradiographic study in the fetal, neonatal and adult human brain. *Neuroscience* **77,** 299-318.

Glass M & Felder CC. (1997). Concurrent stimulation of cannabinoid CB1 and dopamine D2 receptors augments cAMP accumulation in striatal neurons: evidence for a Gs linkage to the CB1 receptor. *J Neurosci* **17,** 5327-5333.

Gong JP, Onaivi ES, Ishiguro H, Liu QR, Tagliaferro PA, Brusco A & Uhl GR. (2006). Cannabinoid CB2 receptors: immunohistochemical localization in rat brain. *Brain Res* **1071,** 10-23.

Goudet C, Kniazeff J, Hlavackova V, Malhaire F, Maurel D, Acher F, Blahos J, Prezeau L & Pin JP. (2005). Asymmetric functioning of dimeric metabotropic glutamate receptors disclosed by positive allosteric modulators. *J Biol Chem* **280,** 24380-24385.

Graham BA, Brichta AM & Callister RJ. (2007). Pinch-current injection defines two discharge profiles in mouse superficial dorsal horn neurones, in vitro. *The J Physiol* **578,** 787-798.

Graham BA, Schofield PR, Sah P & Callister RJ. (2003). Altered inhibitory synaptic transmission in superficial dorsal horn neurones in spastic and oscillator mice. *J Physiol* **551,** 905-916.

Graham BA, Schofield PR, Sah P, Margrie TW & Callister RJ. (2006). Distinct physiological mechanisms underlie altered glycinergic synaptic transmission in the murine mutants spastic, spasmodic, and oscillator. *J Neurosci* **26,** 4880-4890.

Griffin G, Wray EJ, Tao Q, McAllister SD, Rorrer WK, Aung MM, Martin BR & Abood ME. (1999). Evaluation of the cannabinoid CB2 receptor-selective antagonist, SR144528: further evidence for cannabinoid CB2 receptor absence in the rat central nervous system. *Eur J Pharmacol* **377,** 117-125.

Grinspoon L. (1999). The future of medical marijuana. *Forsch Komplementarmed/Research in Complementary Medicine* **6 Suppl 3,** 40-43.

Grudzinska J, Schemm R, Haeger S, Nicke A, Schmalzing G, Betz H & Laube B. (2005). The beta subunit determines the ligand binding properties of synaptic glycine receptors. *Neuron* **45,** 727-739.

Guo W, Shi L, Filizola M, Weinstein H & Javitch JA. (2005). Crosstalk in G protein-coupled receptors: changes at the transmembrane homodimer interface determine activation. *PNAS* **102,** 17495-17500.

Guo W, Shi L & Javitch JA. (2003). The fourth transmembrane segment forms the interface of the dopamine D2 receptor homodimer. *J Biol Chem* **278,** 4385-4388.

Haefely W, Kulcsar A & Mohler H. (1975). Possible involvement of GABA in the central actions of benzodiazepines. *Psychopharmacol Bull* **11,** 58-59.

Hajos N, Katona I, Naiem SS, MacKie K, Ledent C, Mody I & Freund TF. (2000). Cannabinoids inhibit hippocampal GABAergic transmission and network oscillations. *Eur J Neurosci* **12,** 3239-3249.

Hajos N, Ledent C & Freund TF. (2001). Novel cannabinoid-sensitive receptor mediates inhibition of glutamatergic synaptic transmission in the hippocampus. *Neuroscience* **106,** 1-4.

Harrison NL & Simmonds MA. (1984). Modulation of the GABA receptor complex by a steroid anaesthetic. *Brain Res* **323,** 287-292.

Harvey RJ, Depner UB, Wassle H, Ahmadi S, Heindl C, Reinold H, Smart TG, Harvey K, Schutz B, Abo-Salem OM, Zimmer A, Poisbeau P, Welzl H, Wolfer DP, Betz H, Zeilhofer HU & Muller U. (2004). GlyR alpha3: an essential target for spinal PGE2-mediated inflammatory pain sensitization. *Science* **304,** 884-887.

Hebert TE, Moffett S, Morello JP, Loisel TP, Bichet DG, Barret C & Bouvier M. (1996). A peptide derived from a beta2-adrenergic receptor transmembrane domain inhibits both receptor dimerization and activation. *J Biol Chem* **271,** 16384-16392.

Hejazi N, Zhou C, Oz M, Sun H, Ye JH & Zhang L. (2006). Delta9-tetrahydrocannabinol and endogenous cannabinoid anandamide directly potentiate the function of glycine receptors. *Mol Pharmacol* **69,** 991-997.

Henneman E, Somjen G & Carpenter DO. (1965). Excitability and inhibitability of motoneurons of different sizes. *J Neurophysiol* **28,** 599-620.

Herkenham M, Lynn AB, Johnson MR, Melvin LS, de Costa BR & Rice KC. (1991). Characterization and localization of cannabinoid receptors in rat brain: a quantitative in vitro autoradiographic study. *J Neurosci* **11,** 563-583.

Herkenham M, Lynn AB, Little MD, Johnson MR, Melvin LS, de Costa BR & Rice KC. (1990). Cannabinoid receptor localization in brain. *PNAS* **87,** 1932-1936.

Hermann H, Marsicano G & Lutz B. (2002). Coexpression of the cannabinoid receptor type 1 with dopamine and serotonin receptors in distinct neuronal subpopulations of the adult mouse forebrain. *Neuroscience* **109,** 451-460.

Herrick-Davis K, Grinde E, Harrigan TJ & Mazurkiewicz JE. (2005). Inhibition of serotonin 5-hydroxytryptamine2c receptor function through heterodimerization: receptor dimers bind two molecules of ligand and one G-protein. *J Biol Chem* **280,** 40144-40151.

Herrick-Davis K, Grinde E & Mazurkiewicz JE. (2004). Biochemical and biophysical characterization of serotonin 5-HT2C receptor homodimers on the plasma membrane of living cells. *Biochemistry* **43,** 13963-13971.

Herrick-Davis K, Weaver BA, Grinde E & Mazurkiewicz JE. (2006). Serotonin 5-HT2c receptor homodimer biogenesis in the endoplasmic reticulum: Real-time visualization with confocal fluorescence resonance energy transfer. *J Biol Chem*

Herzberg U, Eliav E, Bennett GJ & Kopin IJ. (1997). The analgesic effects of R(+)-WIN 55,212-2 mesylate, a high affinity cannabinoid agonist, in a rat model of neuropathic pain. *Neurosci Lett* **221,** 157-160.

Hillard CJ & Campbell WB. (1997). Biochemistry and pharmacology of arachidonylethanolamide, a putative endogenous cannabinoid. *J Lipid Res* **38,** 2383-2398.

Hillard CJ, Edgemond WS, Jarrahian A & Campbell WB. (1997). Accumulation of N-arachidonoylethanolamine (anandamide) into cerebellar granule cells occurs via facilitated diffusion. *J Neurochem* **69,** 631-638.

Hillard CJ, Manna S, Greenberg MJ, DiCamelli R, Ross RA, Stevenson LA, Murphy V, Pertwee RG & Campbell WB. (1999). Synthesis and characterization of potent and selective agonists of the neuronal cannabinoid receptor (CB1). *J Pharmacol Exp Ther* **289,** 1427-1433.

Hillard CJ, Wilkison DM, Edgemond WS & Campbell WB. (1995). Characterization of the kinetics and distribution of N-arachidonylethanolamine (anandamide) hydrolysis by rat brain. *Biochimica et biophysica acta* **1257,** 249-256.

Hlavackova V, Goudet C, Kniazeff J, Zikova A, Maurel D, Vol C, Trojanova J, Prezeau L, Pin JP & Blahos J. (2005). Evidence for a single heptahelical domain being turned on upon activation of a dimeric GPCR. *The EMBO journal* **24,** 499-509.

Hochman S. (2007). Primer: Spinal Cord. *Curr Biol* **17,** R950-955.

Hogestatt ED, Jonsson BA, Ermund A, Andersson DA, Bjork H, Alexander JP, Cravatt BF, Basbaum AI & Zygmunt PM. (2005). Conversion of acetaminophen to the bioactive N-acylphenolamine AM404 via fatty acid amide hydrolase-dependent arachidonic acid conjugation in the nervous system. *J Biol Chem* **280,** 31405-31412.

Hohmann AG & Herkenham M. (1998). Regulation of cannabinoid and mu opioid receptors in rat lumbar spinal cord following neonatal capsaicin treatment. *Neurosci Lett* **252,** 13-16.

Hohmann AG, Suplita RL, Bolton NM, Neely MH, Fegley D, Mangieri R, Krey JF, Walker JM, Holmes PV, Crystal JD, Duranti A, Tontini A, Mor M, Tarzia G & Piomelli D. (2005). An endocannabinoid mechanism for stress-induced analgesia. *Nature* **435,** 1108-1112.

Hohmann AG, Tsou K & Walker JM. (1998). Cannabinoid modulation of wide dynamic range neurons in the lumbar dorsal horn of the rat by spinally administered WIN55,212-2. *Neurosci Lett* **257,** 119-122.

Hohmann AG, Tsou K & Walker JM. (1999). Cannabinoid suppression of noxious heat-evoked activity in wide dynamic range neurons in the lumbar dorsal horn of the rat. *J Neurophysiol* **81,** 575-583.

Honda M, Uchida K, Tanabe M & Ono H. (2006). Fluvoxamine, a selective serotonin reuptake inhibitor, exerts its antiallodynic effects on neuropathic pain in mice via 5-HT2A/2C receptors. *Neuropharmacology* **51,** 866-872.

Horvath G, Kekesi G, Nagy E & Benedek G. (2008). The role of TRPV1 receptors in the antinociceptive effect of anandamide at spinal level. *Pain* **134,** 277-284.

Hosie AM, Dunne EL, Harvey RJ & Smart TG. (2003). Zinc-mediated inhibition of GABA(A) receptors: discrete binding sites underlie subtype specificity. *Nat Neurosci* **6,** 362-369.

Hou JP. (1977). The development of Chinese herbal medicine and the Pen-ts'ao. *Comp Med East West* **5,** 117-122.

Houser SJ, Eads M, Embrey JP & Welch SP. (2000). Dynorphin B and spinal analgesia: induction of antinociception by the cannabinoids CP55,940, Delta(9)-THC and anandamide. *Brain Res* **857,** 337-342.

Howlett AC. (1985). Cannabinoid inhibition of adenylate cyclase. Biochemistry of the response in neuroblastoma cell membranes. *Mol Pharmacol* **27,** 429-436.

Howlett AC. (2002). The cannabinoid receptors. *Prostaglandins Other Lipid Mediat* **68-69,** 619-631.

Howlett AC, Bidaut-Russell M, Devane WA, Melvin LS, Johnson MR & Herkenham M. (1990). The cannabinoid receptor: biochemical, anatomical and behavioral characterization. *Trends Neurosci* **13,** 420-423.

Ibrahim MM, Deng H, Zvonok A, Cockayne DA, Kwan J, Mata HP, Vanderah TW, Lai J, Porreca F, Makriyannis A & Malan TP, Jr. (2003). Activation of CB2 cannabinoid receptors by AM1241 inhibits experimental neuropathic pain: pain inhibition by receptors not present in the CNS. *PNAS* **100,** 10529-10533.

Inquimbert P, Rodeau JL & Schlichter R. (2007). Differential contribution of GABAergic and glycinergic components to inhibitory synaptic transmission in lamina II and laminae III-IV of the young rat spinal cord. *Eur J Neurosci* **26,** 2940-2949.

Isokawa M & Alger BE. (2005). Retrograde endocannabinoid regulation of GABAergic inhibition in the rat dentate gyrus granule cell. *J Physiol* **567,** 1001-1010.

Isokawa M & Alger BE. (2006). Ryanodine receptor regulates endogenous cannabinoid mobilization in the hippocampus. *J Neurophysiol* **95,** 3001-3011.

Jaggar SI, Hasnie FS, Sellaturay S & Rice AS. (1998). The anti-hyperalgesic actions of the cannabinoid anandamide and the putative CB2 receptor agonist palmitoylethanolamide in visceral and somatic inflammatory pain. *Pain* **76,** 189-199.

Jennings EA, Vaughan CW, Roberts LA & Christie MJ. (2003). The actions of anandamide on rat superficial medullary dorsal horn neurons in vitro. *J Physiol* **548,** 121-129.

Jentsch JD, Verrico CD, Le D & Roth RH. (1998). Repeated exposure to delta 9-tetrahydrocannabinol reduces prefrontal cortical dopamine metabolism in the rat. *Neurosci Lett* **246,** 169-172.

Jordan BA, Cvejic S & Devi LA. (2000). Opioids and their complicated receptor complexes. *Neuropsychopharmacology* **23,** S5-S18.

Jordan BA & Devi LA. (1999). G-protein-coupled receptor heterodimerization modulates receptor function. *Nature* **399,** 697-700.

Jordan BA, Trapaidze N, Gomes I, Nivarthi R & Devi LA. (2001). Oligomerization of opioid receptors with beta 2-adrenergic receptors: a role in trafficking and mitogen-activated protein kinase activation. *PNAS* **98,** 343-348.

Kamiya T, Saitoh O, Yoshioka K & Nakata H. (2003). Oligomerization of adenosine A2A and dopamine D2 receptors in living cells. *Biochem Biophys Res Commun* **306,** 544-549.

Kapur S, Zipursky RB & Remington G. (1999). Clinical and theoretical implications of 5-HT2 and D2 receptor occupancy of clozapine, risperidone, and olanzapine in schizophrenia. *Am J Psychiatry* **156,** 286-293.

Karim F, Roerig SC & Saphier D. (1996). Role of 5-hydroxytryptamine3 (5-HT3) antagonists in the prevention of emesis caused by anticancer therapy. *Biochem Pharmacol* **52,** 685-692.

Karnik SS & Khorana HG. (1990). Assembly of functional rhodopsin requires a disulfide bond between cysteine residues 110 and 187. *J Biol Chem* **265,** 17520-17524.

Katona I, Sperlagh B, Sik A, Kafalvi A, Vizi ES, Mackie K & Freund TF. (1999). Presynaptically located CB1 cannabinoid receptors regulate GABA release from axon terminals of specific hippocampal interneurons. *J Neurosci* **19,** 4544-4558.

Katz B. (1969). *The Release of Neural Transmitter Substances*. University Press, Liverpool.

Kearn CS, Blake-Palmer K, Daniel E, Mackie K & Glass M. (2005). Concurrent stimulation of cannabinoid CB1 and dopamine D2 receptors enhances

heterodimer formation: a mechanism for receptor cross-talk? *Mol Pharmacol* **67,** 1697-1704.

Klop EM, Mouton LJ, Kuipers R & Holstege G. (2005). Neurons in the lateral sacral cord of the cat project to periaqueductal grey, but not to thalamus. *Eur J Neurosci* **21,** 2159-2166.

Kobayashi Y. (1998). Distribution and morphology of spinothalamic tract neurons in the rat. *Anat Embryol* **197,** 51-67.

Kota P, Reeves PJ, Rajbhandary UL & Khorana HG. (2006). Opsin is present as dimers in COS1 cells: identification of amino acids at the dimeric interface. *PNAS* **103,** 3054-3059.

Krebs MO, Goldberger C & Dervaux A. (2005). Cannabis use and schizophrenia. *Am J Psychiatry* **162,** 401-402; author reply 402.

Kreitzer AC & Regehr WG. (2001a). Cerebellar depolarization-induced suppression of inhibition is mediated by endogenous cannabinoids. *J Neurosci* **21,** RC174.

Kreitzer AC & Regehr WG. (2001b). Retrograde inhibition of presynaptic calcium influx by endogenous cannabinoids at excitatory synapses onto Purkinje cells. *Neuron* **29,** 717-727.

Krnjevic K & Schwartz S. (1967). The action of gamma-aminobutyric acid on cortical neurones. *Exp Brain Res* **3,** 320-336.

Kroeger KM, Pfleger KD & Eidne KA. (2003). G-protein coupled receptor oligomerization in neuroendocrine pathways. *Front Neuroendocrinol* **24,** 254-278.

Kuhse J, Schmieden V & Betz H. (1990). A single amino acid exchange alters the pharmacology of neonatal rat glycine receptor subunit. *Neuron* **5,** 867-873.

Kuner R, Kohr G, Grunewald S, Eisenhardt G, Bach A & Kornau HC. (1999). Role of heteromer formation in GABAB receptor function. *Science* **283,** 74-77.

Lam PM, McDonald J & Lambert DG. (2005). Characterization and comparison of recombinant human and rat TRPV1 receptors: effects of exo- and endocannabinoids. *Br J Anaesth* **94,** 649-656.

Lauckner JE, Jensen JB, Chen HY, Lu HC, Hille B & Mackie K. (2008). GPR55 is a cannabinoid receptor that increases intracellular calcium and inhibits M current. *PNAS* **19,** 2699-2704

Laurie DJ, Wisden W & Seeburg PH. (1992). The distribution of thirteen GABAA receptor subunit mRNAs in the rat brain. III. Embryonic and postnatal development. *J Neurosci* **12,** 4151-4172.

Legendre P. (2001). The glycinergic inhibitory synapse. *Cell Mol Life Sci* **58,** 760-793.

Lenz RA, Wagner JJ & Alger BE. (1998). N- and L-type calcium channel involvement in depolarization-induced suppression of inhibition in rat hippocampal CA1 cells. *J Physiol* **512 (Pt 1),** 61-73.

Leroy S, Griffon N, Bourdel MC, Olie JP, Poirier MF & Krebs MO. (2001). Schizophrenia and the cannabinoid receptor type 1 (CB1): association study using a single-base polymorphism in coding exon 1. *Am J Med Genet* **105,** 749-752.

Li HL. (1974). An archeological and historical account of Cannabis in China. *Econ Bot* **28,** 437-448.

Liang Y, Fotiadis D, Filipek S, Saperstein DA, Palczewski K & Engel A. (2003). Organization of the G protein-coupled receptors rhodopsin and opsin in native membranes. *J Biol Chem* **278,** 21655-21662.

Lichtman AH & Martin BR. (1991). Cannabinoid-induced antinociception is mediated by a spinal alpha 2-noradrenergic mechanism. *Brain Res* **559,** 309-314.

Light AR & Kavookjian AM. (1988). Morphology and ultrastructure of physiologically identified substantia gelatinosa (lamina II) neurons with axons that terminate in deeper dorsal horn laminae (III-V). *J Comp Neurol* **267,** 172-189.

Light AR & Perl ER. (1979a). Reexamination of the dorsal root projection to the spinal dorsal horn including observations on the differential termination of coarse and fine fibers. *J Comp Neurol* **186,** 117-131.

Light AR & Perl ER. (1979b). Spinal termination of functionally identified primary afferent neurons with slowly conducting myelinated fibers. *J Comp Neurol* **186,** 133-150.

Ligresti A, Morera E, Van Der Stelt M, Monory K, Lutz B, Ortar G & Di Marzo V. (2004). Further evidence for the existence of a specific process for the membrane transport of anandamide. *Biochem J* **380,** 265-272.

Lin LH, Chen LL, Zirrolli JA & Harris RA. (1992). General anesthetics potentiate gamma-aminobutyric acid actions on gamma-aminobutyric acidA receptors expressed by Xenopus oocytes: lack of involvement of intracellular calcium. *J Pharmacol Exp Ther* **263,** 569-578.

Lin LH, Whiting P & Harris RA. (1993). Molecular determinants of general anesthetic action: role of GABAA receptor structure. *J Neurochem* **60,** 1548-1553.

Llano I, Leresche N & Marty A. (1991). Calcium entry increases the sensitivity of cerebellar Purkinje cells to applied GABA and decreases inhibitory synaptic currents. *Neuron* **6,** 565-574.

Loeser JD & Treede RD. (2008). The Kyoto protocol of IASP Basic Pain Terminology. *Pain*.

Lozovaya N, Yatsenko N, Beketov A, Tsintsadze T & Burnashev N. (2005). Glycine Receptors in CNS Neurons as a Target for Nonretrograde Action of Cannabinoids. *J Neurosci* **25,** 7499-7506.

Lu Q, Straiker A & Maguire G. (2000). Expression of CB2 cannabinoid receptor mRNA in adult rat retina. *Vis Neurosci* **17,** 91-95.

Lu Y & Perl ER. (2003). A specific inhibitory pathway between substantia gelatinosa neurons receiving direct C-fiber input. *J Neurosci* **23,** 8752-8758.

Lu Y & Perl ER. (2005). Modular organization of excitatory circuits between neurons of the spinal superficial dorsal horn (laminae I and II). *J Neurosci* **25,** 3900-3907.

Lynch JW. (2004). Molecular structure and function of the glycine receptor chloride channel. *Physiol Rev* **84,** 1051-1095.

Mackie K & Hille B. (1992). Cannabinoids inhibit N-type calcium channels in neuroblastoma-glioma cells. *PNAS* **89,** 3825-3829.

Mackie K, Lai Y, Westenbroek R & Mitchell R. (1995). Cannabinoids activate an inwardly rectifying potassium conductance and inhibit Q-type calcium currents in AtT20 cells transfected with rat brain cannabinoid receptor. *J Neurosci* **15,** 6552-6561.

Mackie K & Stella N. (2006). Cannabinoid receptors and endocannabinoids: evidence for new players. *AAPS* **8,** E298-306.

Mackie M, Hughes DI, Maxwell DJ, Tillakaratne NJ & Todd AJ. (2003). Distribution and colocalisation of glutamate decarboxylase isoforms in the rat spinal cord. *Neuroscience* **119,** 461-472.

Maingret F, Patel AJ, Lazdunski M & Honore E. (2001). The endocannabinoid anandamide is a direct and selective blocker of the background K(+) channel TASK-1. *The EMBO journal* **20,** 47-54.

Majewska MD, Harrison NL, Schwartz RD, Barker JL & Paul SM. (1986). Steroid hormone metabolites are barbiturate-like modulators of the GABA receptor. *Science* **232,** 1004-1007.

Malan TP, Jr., Ibrahim MM, Deng H, Liu Q, Mata HP, Vanderah T, Porreca F & Makriyannis A. (2001). CB2 cannabinoid receptor-mediated peripheral antinociception. *Pain* **93,** 239-245.

Malinowska B, Kwolek G & Gothert M. (2001). Anandamide and methanandamide induce both vanilloid VR1- and cannabinoid CB1 receptor-mediated changes in heart rate and blood pressure in anaesthetized rats. *Naunyn Schmiedebergs Arch Pharmacol* **364,** 562-569.

Mallet C, Daulhac L, Bonnefont J, Ledent C, Etienne M, Chapuy E, Libert F & Eschalier A. (2008). Endocannabinoid and serotonergic systems are needed for acetaminophen-induced analgesia. *Pain*.

Marshall FH. (2001). Heterodimerization of G-protein-coupled receptors in the CNS. *Curr Opin Pharmacol* **1,** 40-44.

Martin BR & Lichtman AH. (1998). Cannabinoid transmission and pain perception. *Neurobiol Dis* **5,** 447-461.

Martin WJ, Hohmann AG & Walker JM. (1996). Suppression of noxious stimulus-evoked activity in the ventral posterolateral nucleus of the thalamus by a cannabinoid agonist: correlation between electrophysiological and antinociceptive effects. *J Neurosci* **16,** 6601-6611.

Martin WJ, Loo CM & Basbaum AI. (1999). Spinal cannabinoids are anti-allodynic in rats with persistent inflammation. *Pain* **82,** 199-205.

Martin WJ, Tsou K & Walker JM. (1998). Cannabinoid receptor-mediated inhibition of the rat tail-flick reflex after microinjection into the rostral ventromedial medulla. *Neurosci Lett* **242,** 33-36.

Matsuda LA, Lolait SJ, Brownstein MJ, Young AC & Bonner TI. (1990). Structure of a cannabinoid receptor and functional expression of the cloned cDNA. *Nature* **346,** 561-564.

Matz MV, Lukyanov KA & Lukyanov SA. (2002). Family of the green fluorescent protein: journey to the end of the rainbow. *Bioessays* **24,** 953-959.

Maudsley S, Martin B & Luttrell LM. (2005). The origins of diversity and specificity in g protein-coupled receptor signaling. *J Pharmacol Exp Ther* **314,** 485-494.

McPartland JM & Glass M. (2003). Functional mapping of cannabinoid receptor homologs in mammals, other vertebrates, and invertebrates. *Gene* **312,** 297-303.

Mechoulam R, Ben-Shabat S, Hanus L, Ligumsky M, Kaminski NE, Schatz AR, Gopher A, Almog S, Martin BR, Compton DR & et al. (1995). Identification of an endogenous 2-monoglyceride, present in canine gut, that binds to cannabinoid receptors. *Biochem Pharmacol* **50,** 83-90.

Mechoulam R & Gaoni Y. (1965). A Total Synthesis of Dl-Delta-1-Tetrahydrocannabinol, the Active Constituent of Hashish. *J Am Chem Soc* **87,** 3273-3275.

Meltzer HY. (1989). Clinical studies on the mechanism of action of clozapine: the dopamine-serotonin hypothesis of schizophrenia. *Psychopharmacology* **99 Suppl,** S18-27.

Melzack R & Wall PD. (1962). On the nature of cutaneous sensory mechanisms. *Brain* **85,** 331-356.

Melzack R & Wall PD. (1965). Pain mechanisms: a new theory. *Science* **150,** 971-979.

Mercier JF, Salahpour A, Angers S, Breit A & Bouvier M. (2002). Quantitative assessment of beta 1- and beta 2-adrenergic receptor homo- and heterodimerization by bioluminescence resonance energy transfer. *J Biol Chem* **277,** 44925-44931.

Mikuriya TH & Aldrich MR. (1988). Cannabis 1988. Old drug, new dangers. The potency question. *J Psychoactive Drugs* **20,** 47-55.

Millan MJ. (2002). Descending control of pain. *Prog Neurobiol* **66,** 355-474.

Milligan G, Ramsay D, Pascal G & Carrillo JJ. (2003). GPCR dimerisation. *Life Sci* **74,** 181-188.

Molander C, Xu Q & Grant G. (1984). The cytoarchitectonic organization of the spinal cord in the rat. I. The lower thoracic and lumbosacral cord. *J Comp Neurol* **230,** 133-141.

Monhemius R, Azami J, Green DL & Roberts MH. (2001). CB1 receptor mediated analgesia from the Nucleus Reticularis Gigantocellularis pars alpha is activated in an animal model of neuropathic pain. *Brain Res* **908,** 67-74.

Morise H, Shimomura O, Johnson FH & Winant J. (1974). Intermolecular energy transfer in the bioluminescent system of Aequorea. *Biochemistry* **13,** 2656-2662.

Morisset V & Urban L. (2001). Cannabinoid-induced presynaptic inhibition of glutamatergic EPSCs in substantia gelatinosa neurons of the rat spinal cord. *J Neurophysiol* **86,** 40-48.

Muller F, Heinke B & Sandkuhler J. (2003). Reduction of glycine receptor-mediated miniature inhibitory postsynaptic currents in rat spinal lamina I neurons after peripheral inflammation. *Neuroscience* **122,** 799-805.

Munro S, Thomas KL & Abu-Shaar M. (1993). Molecular characterization of a peripheral receptor for cannabinoids. *Nature* **365,** 61-65.

Murray RM & Lewis SW. (1987). Is schizophrenia a neurodevelopmental disorder? *Br Med J (Clin Res Ed)* **295,** 681-682.

Needham LK & Rozengurt E. (1998). Galpha12 and Galpha13 stimulate Rho-dependent tyrosine phosphorylation of focal adhesion kinase, paxillin, and p130 Crk-associated substrate. *J Biol Chem* **273,** 14626-14632.

Ng GY, George SR, Zastawny RL, Caron M, Bouvier M, Dennis M & O'Dowd BF. (1993). Human serotonin1B receptor expression in Sf9 cells: phosphorylation, palmitoylation, and adenylyl cyclase inhibition. *Biochemistry* **32,** 11727-11733.

Obata H, Saito S, Sasaki M, Ishizaki K & Goto F. (2001). Antiallodynic effect of intrathecally administered 5-HT(2) agonists in rats with nerve ligation. *Pain* **90,** 173-179.

Ohno-Shosaku T, Maejima T & Kano M. (2001). Endogenous cannabinoids mediate retrograde signals from depolarized postsynaptic neurons to presynaptic terminals. *Neuron* **29,** 729-738.

Okamoto Y, Morishita J, Tsuboi K, Tonai T & Ueda N. (2004). Molecular characterization of a phospholipase D generating anandamide and its congeners. *J Biol Chem* **279,** 5298-5305.

Olney JW & Farber NB. (1995). Glutamate receptor dysfunction and schizophrenia. *Arch Gen Psychiatry* **52,** 998-1007.

Onaivi ES, Ishiguro H, Gong JP, Patel S, Perchuk A, Meozzi PA, Myers L, Mora Z, Tagliaferro P, Gardner E, Brusco A, Akinshola BE, Liu QR, Hope B, Iwasaki S, Arinami T, Teasenfitz L & Uhl GR. (2006). Discovery of the presence and functional expression of cannabinoid CB2 receptors in brain. *Ann NY Acad Sci* **1074,** 514-536.

Ong WY & Mackie K. (1999a). A light and electron microscopic study of the CB1 cannabinoid receptor in primate brain. *Neuroscience* **92,** 1177-1191.

Ong WY & Mackie K. (1999b). A light and electron microscopic study of the CB1 cannabinoid receptor in the primate spinal cord. *J Neurocytol* **28,** 39-45.

Overton MC, Chinault SL & Blumer KJ. (2003). Oligomerization, biogenesis, and signaling is promoted by a glycophorin A-like dimerization motif in transmembrane domain 1 of a yeast G protein-coupled receptor. *J Biol Chem* **278,** 49369-49377.

Palazzo E, de Novellis V, Petrosino S, Marabese I, Vita D, Giordano C, Di Marzo V, Mangoni GS, Rossi F & Maione S. (2006). Neuropathic pain and the endocannabinoid system in the dorsal raphe: pharmacological treatment and interactions with the serotonergic system. *Eur J Neurosci* **24,** 2011-2020.

Pan X, Ikeda SR & Lewis DL. (1996). Rat brain cannabinoid receptor modulates N-type Ca2+ channels in a neuronal expression system. *Mol Pharmacol* **49,** 707-714.

Perez DM & Karnik SS. (2005). Multiple signaling states of G-protein-coupled receptors. *Pharmacol Rev* **57,** 147-161.

Persohn E, Malherbe P & Richards JG. (1991). In situ hybridization histochemistry reveals a diversity of GABAA receptor subunit mRNAs in neurons of the rat spinal cord and dorsal root ganglia. *Neuroscience* **42,** 497-507.

Pettit DA, Harrison MP, Olson JM, Spencer RF & Cabral GA. (1998). Immunohistochemical localization of the neural cannabinoid receptor in rat brain. *J Neurosci Res* **51,** 391-402.

Pfeiffer M, Koch T, Schroder H, Laugsch M, Hollt V & Schulz S. (2002). Heterodimerization of somatostatin and opioid receptors cross-modulates phosphorylation, internalization, and desensitization. *J Biol Chem* **277,** 19762-19772.

Piomelli D. (2003). The molecular logic of endocannabinoid signalling. *Nat Rev Neurosci* **4,** 873-884.

Pistis M, Perra S, Pillolla G, Melis M, Gessa GL & Muntoni AL. (2004). Cannabinoids modulate neuronal firing in the rat basolateral amygdala: evidence for CB1- and non-CB1-mediated actions. *Neuropharmacology* **46,** 115-125.

Pitler TA & Alger BE. (1992). Postsynaptic spike firing reduces synaptic GABAA responses in hippocampal pyramidal cells. *J Neurosci* **12,** 4122-4132.

Pitler TA & Alger BE. (1994). Depolarization-induced suppression of GABAergic inhibition in rat hippocampal pyramidal cells: G protein involvement in a presynaptic mechanism. *Neuron* **13,** 1447-1455.

Polgar E, Gray S, Riddell JS & Todd AJ. (2004). Lack of evidence for significant neuronal loss in laminae I-III of the spinal dorsal horn of the rat in the chronic constriction injury model. *Pain* **111,** 144-150.

Poling JS, Rogawski MA, Salem N, Jr. & Vicini S. (1996). Anandamide, an endogenous cannabinoid, inhibits Shaker-related voltage-gated K+ channels. *Neuropharmacology* **35,** 983-991.

Pope HG, Jr., Gruber AJ, Hudson JI, Cohane G, Huestis MA & Yurgelun-Todd D. (2003). Early-onset cannabis use and cognitive deficits: what is the nature of the association? *Drug Alcohol Depend* **69,** 303-310.

Porter AC, Sauer JM, Knierman MD, Becker GW, Berna MJ, Bao J, Nomikos GG, Carter P, Bymaster FP, Leese AB & Felder CC. (2002). Characterization of a novel endocannabinoid, virodhamine, with antagonist activity at the CB1 receptor. *J Pharmacol Exp Ther* **301,** 1020-1024.

Prasher DC, Eckenrode VK, Ward WW, Prendergast FG & Cormier MJ. (1992). Primary structure of the Aequorea victoria green-fluorescent protein. *Gene* **111,** 229-233.

Pugh G, Jr., Abood ME & Welch SP. (1995). Antisense oligodeoxynucleotides to the kappa-1 receptor block the antinociceptive effects of delta 9-THC in the spinal cord. *Brain research* **689,** 157-158.

Pugh G, Jr., Smith PB, Dombrowski DS & Welch SP. (1996). The role of endogenous opioids in enhancing the antinociception produced by the combination of delta 9-tetrahydrocannabinol and morphine in the spinal cord. *J Pharmacol Exp Ther* **279,** 608-616.

Radhakrishnan R, King EW, Dickman JK, Herold CA, Johnston NF, Spurgin ML & Sluka KA. (2003). Spinal 5-HT(2) and 5-HT(3) receptors mediate low, but not high, frequency TENS-induced antihyperalgesia in rats. *Pain* **105,** 205-213.

Ramsay D, Kellett E, McVey M, Rees S & Milligan G. (2002). Homo- and hetero-oligomeric interactions between G-protein-coupled receptors in living cells monitored by two variants of bioluminescence resonance energy transfer (BRET): hetero-oligomers between receptor subtypes form more efficiently than between less closely related sequences. *Biochem J* **365,** 429-440.

Reche I, Fuentes JA & Ruiz-Gayo M. (1996). A role for central cannabinoid and opioid systems in peripheral delta 9-tetrahydrocannabinol-induced analgesia in mice. *Eur J Pharmacol* **301,** 75-81.

Reche I, Ruiz-Gayo M & Fuentes JA. (1998). Inhibition of opioid-degrading enzymes potentiates delta9-tetrahydrocannabinol-induced antinociception in mice. *Neuropharmacology* **37,** 215-222.

Rexed B. (1952). The cytoarchitectonic organization of the spinal cord in the cat. *The J Comp Neurol* **96,** 414-495.

Rexed B. (1954). A cytoarchitectonic atlas of the spinal cord in the cat. *J Comp Neurol* **100,** 297-379.

Ribeiro-Da-Silva A & Coimbra A. (1980). Neuronal uptake of [3H]GABA and [3H]glycine in laminae I-III (substantia gelatinosa Rolandi) of the rat spinal cord. An autoradiographic study. *Brain Res* **188,** 449-464.

Richardson JD, Aanonsen L & Hargreaves KM. (1998a). Antihyperalgesic effects of spinal cannabinoids. *Eur J Pharmacol* **345,** 145-153.

Richardson JD, Aanonsen L & Hargreaves KM. (1998b). Hypoactivity of the spinal cannabinoid system results in NMDA-dependent hyperalgesia. *J Neurosci* **18,** 451-457.

Richardson JD, Kilo S & Hargreaves KM. (1998c). Cannabinoids reduce hyperalgesia and inflammation via interaction with peripheral CB1 receptors. *Pain* **75,** 111-119.

Rios C, Gomes I & Devi LA. (2006). mu opioid and CB1 cannabinoid receptor interactions: reciprocal inhibition of receptor signaling and neuritogenesis. *BJP* **148,** 387-395.

Rios CD, Jordan BA, Gomes I & Devi LA. (2001). G-protein-coupled receptor dimerization: modulation of receptor function. *Pharmacol Ther* **92,** 71-87.

Robinson HP, Sahara Y & Kawai N. (1991). Nonstationary fluctuation analysis and direct resolution of single channel currents at postsynaptic sites. *Biophys J* **59,** 295-304.

Rosner B & Glynn RJ. (2008). Power and Sample Size Estimation for the Wilcoxon Rank Sum Test with Application to Comparisons of C Statistics from Alternative Prediction Models. *Biometrics* **65,** 188-197.

Roth BL, Berry SA, Kroeze WK, Willins DL & Kristiansen K. (1998). Serotonin 5-HT2A receptors: molecular biology and mechanisms of regulation. *Crit Rev Neurobiol* **12,** 319-338.

Rouach N & Nicoll RA. (2003). Endocannabinoids contribute to short-term but not long-term mGluR-induced depression in the hippocampus. *Eur J Neurosci* **18,** 1017-1020.

Sagar DR, Kelly S, Millns PJ, O'Shaughnessey CT, Kendall DA & Chapman V. (2005). Inhibitory effects of CB1 and CB2 receptor agonists on responses of DRG neurons and dorsal horn neurons in neuropathic rats. *Eur J Neurosci* **22,** 371-379.

Salio C, Fischer J, Franzoni MF & Conrath M. (2002). Pre- and postsynaptic localizations of the CB1 cannabinoid receptor in the dorsal horn of the rat spinal cord. *Neuroscience* **110,** 755-764.

Salio C, Fischer J, Franzoni MF, Mackie K, Kaneko T & Conrath M. (2001). CB1-cannabinoid and mu-opioid receptor co-localization on postsynaptic target in the rat dorsal horn. *Neuroreport* **12,** 3689-3692.

Schlicker E & Kathmann M. (2001). Modulation of transmitter release via presynaptic cannabinoid receptors. *Trends Pharmacol Sci* **22,** 565-572.

Schmid PC, Zuzarte-Augustin ML & Schmid HH. (1985). Properties of rat liver N-acylethanolamine amidohydrolase. *J Biol Chem* **260,** 14145-14149.

Schneider SP. (1992). Functional properties and axon terminations of interneurons in laminae III-V of the mammalian spinal dorsal horn in vitro. *J Neurophysiol* **68,** 1746-1759.

Schneider SP. (2008). Local circuit connections between hamster laminae III and IV dorsal horn neurons. *J Neurophysiol* **99,** 1306-1318.

Scott DA, Wright CE & Angus JA. (2004). Evidence that CB-1 and CB-2 cannabinoid receptors mediate antinociception in neuropathic pain in the rat. *Pain* **109,** 124-131.

Selvin PR. (2000). The renaissance of fluorescence resonance energy transfer. *Nature Struct Biol* **7,** 730-734.

Shen M, Piser TM, Seybold VS & Thayer SA. (1996). Cannabinoid receptor agonists inhibit glutamatergic synaptic transmission in rat hippocampal cultures. *J Neurosci* **16,** 4322-4334.

Simon MI, Strathmann MP & Gautam N. (1991). Diversity of G proteins in signal transduction. *Science* **252,** 802-808.

Simpson K, Spencer CM & McClellan KJ. (2000). Tropisetron: an update of its use in the prevention of chemotherapy-induced nausea and vomiting. *Drugs* **59,** 1297-1315.

Singer JH & Berger AJ. (1999). Contribution of single-channel properties to the time course and amplitude variance of quantal glycine currents recorded in rat motoneurons. *J Neurophysiol* **81,** 1608-1616.

Singer JH, Talley EM, Bayliss DA & Berger AJ. (1998). Development of glycinergic synaptic transmission to rat brain stem motoneurons. *J Neurophysiol* **80,** 2608-2620.

Sivilotti L & Woolf CJ. (1994). The contribution of GABAA and glycine receptors to central sensitization: disinhibition and touch-evoked allodynia in the spinal cord. *J Neurophysiol* **72,** 169-179.

Smith PB & Martin BR. (1992). Spinal mechanisms of delta 9-tetrahydrocannabinol-induced analgesia. *Brain Res* **578,** 8-12.

Smith PB, Welch SP & Martin BR. (1994). Interactions between delta 9-tetrahydrocannabinol and kappa opioids in mice. *J Pharmacol Exp Ther* **268,** 1381-1387.

Snyder SH. (1976). The dopamine hypothesis of schizophrenia: focus on the dopamine receptor. *Am J Psychiatry* **133,** 197-202.

Soldo BL, Proctor WR & Dunwiddie TV. (1994). Ethanol differentially modulates GABAA receptor-mediated chloride currents in hippocampal, cortical, and septal neurons in rat brain slices. *Synapse* **18,** 94-103.

Solomon RE & Gebhart GF. (1988). Mechanisms of effects of intrathecal serotonin on nociception and blood pressure in rats. *J Pharmacol Exp Ther* **245,** 905-912.

Spike RC, Puskar Z, Andrew D & Todd AJ. (2003). A quantitative and morphological study of projection neurons in lamina I of the rat lumbar spinal cord. *Eur J Neurosci* **18,** 2433-2448.

Stanasila L, Perez JB, Vogel H & Cotecchia S. (2003). Oligomerization of the alpha 1a- and alpha 1b-adrenergic receptor subtypes. Potential implications in receptor internalization. *J Biol Chem* **278,** 40239-40251.

Stockmeier CA, DiCarlo JJ, Zhang Y, Thompson P & Meltzer HY. (1993). Characterization of typical and atypical antipsychotic drugs based on in vivo occupancy of serotonin2 and dopamine2 receptors. *J Pharmacol Exp Ther* **266,** 1374-1384.

Straiker A & Mackie K. (2005). Depolarization-induced suppression of excitation in murine autaptic hippocampal neurones. *J Physiol* **569,** 501-517.

Sugiura T, Kondo S, Sukagawa A, Nakane S, Shinoda A, Itoh K, Yamashita A & Waku K. (1995). 2-Arachidonoylglycerol: a possible endogenous cannabinoid receptor ligand in brain. *Biochem Biophys Res Commun* **215,** 89-97.

Sugiura Y, Lee CL & Perl ER. (1986). Central projections of identified, unmyelinated (C) afferent fibers innervating mammalian skin. *Science* **234,** 358-361.

Takahashi H, Higuchi M & Suhara T. (2006). The role of extrastriatal dopamine D2 receptors in schizophrenia. *Biol Psychiatry* **59,** 919-928.

Terrillon S & Bouvier M. (2004). Roles of G-protein-coupled receptor dimerization. *EMBO reports* **5,** 30-34.

Terrillon S, Durroux T, Mouillac B, Breit A, Ayoub MA, Taulan M, Jockers R, Barberis C & Bouvier M. (2003). Oxytocin and vasopressin V1a and V2 receptors form constitutive homo- and heterodimers during biosynthesis. *Mol Endocrinol* **17,** 677-691.

Todd AJ & Spike RC. (1993). The localization of classical transmitters and neuropeptides within neurons in laminae I-III of the mammalian spinal dorsal horn. *Prog Neurobiol* **41,** 609-645.

Todd AJ & Sullivan AC. (1990). Light microscope study of the coexistence of GABA-like and glycine-like immunoreactivities in the spinal cord of the rat. *J Comp Neurol* **296,** 496-505.

Torsney C & MacDermott AB. (2006). Disinhibition opens the gate to pathological pain signaling in superficial neurokinin 1 receptor-expressing neurons in rat spinal cord. *J Neurosci* **26,** 1833-1843.

Tracey I, Becerra L, Chang I, Breiter H, Jenkins L, Borsook D & Gonzalez RG. (2000). Noxious hot and cold stimulation produce common patterns of brain activation in humans: a functional magnetic resonance imaging study. *Neurosci Lett* **288,** 159-162.

Tramer MR, Carroll D, Campbell FA, Reynolds DJ, Moore RA & McQuay HJ. (2001). Cannabinoids for control of chemotherapy induced nausea and vomiting: quantitative systematic review. *Br Med J* **323,** 16-21.

Traynelis SF, Silver RA & Cull-Candy SG. (1993). Estimated conductance of glutamate receptor channels activated during EPSCs at the cerebellar mossy fiber-granule cell synapse. *Neuron* **11,** 279-289.

Tsai SJ. (2005). Adenosine A2a receptor/dopamine D2 receptor hetero-oligomerization: a hypothesis that may explain behavioral sensitization to psychostimulants and schizophrenia. *Med Hypotheses* **64,** 197-200.

Tsou K, Brown S, Sanudo-Pena MC, Mackie K & Walker JM. (1998). Immunohistochemical distribution of cannabinoid CB1 receptors in the rat central nervous system. *Neuroscience* **83,** 393-411.

Tsou K, Lowitz KA, Hohmann AG, Martin WJ, Hathaway CB, Bereiter DA & Walker JM. (1996). Suppression of noxious stimulus-evoked expression of Fos protein-like immunoreactivity in rat spinal cord by a selective cannabinoid agonist. *Neuroscience* **70,** 791-798.

Tuckett RP & Wei JY. (1987a). Response to an itch-producing substance in cat. I. Cutaneous receptor populations with myelinated axons. *Brain Res* **413,** 87-94.

Tuckett RP & Wei JY. (1987b). Response to an itch-producing substance in cat. II. Cutaneous receptor populations with unmyelinated axons. *Brain Res* **413,** 95-103.

Twitchell W, Brown S & Mackie K. (1997). Cannabinoids inhibit N- and P/Q-type calcium channels in cultured rat hippocampal neurons. *J Neurophysiol* **78,** 43-50.

Vallbo AB, Olausson H & Wessberg J. (1999). Unmyelinated afferents constitute a second system coding tactile stimuli of the human hairy skin. *J Neurophysiol* **81,** 2753-2763.

van der Stelt M, Fox SH, Hill M, Crossman AR, Petrosino S, Di Marzo V & Brotchie JM. (2005). A role for endocannabinoids in the generation of parkinsonism and levodopa-induced dyskinesia in MPTP-lesioned non-human primate models of Parkinson's disease. *Faseb J* **19,** 1140-1142.

Van Gaal LF, Rissanen AM, Scheen AJ, Ziegler O & Rossner S. (2005). Effects of the cannabinoid-1 receptor blocker rimonabant on weight reduction and cardiovascular risk factors in overweight patients: 1-year experience from the RIO-Europe study. *Lancet* **365,** 1389-1397.

van Os J, Bak M, Hanssen M, Bijl RV, de Graaf R & Verdoux H. (2002). Cannabis use and psychosis: a longitudinal population-based study. *Am J Epidemiol* **156,** 319-327.

Van Steenwinckel J, Brisorgueil MJ, Fischer J, Verge D, Gingrich JA, Bourgoin S, Hamon M, Bernard R & Conrath M. (2008). Role of spinal serotonin 5-HT2A receptor in 2',3'-dideoxycytidine-induced neuropathic pain in the rat and the mouse. *Pain* **137,** 66-80.

Vaughan CW. (2006). Stressed-out endogenous cannabinoids relieve pain. *Trends Pharmacol Sci* **27,** 69-71.

Vaughan CW & Christie MJ. (2005). Retrograde signalling by endocannabinoids. *Handb Exp Pharmacol***,** 367-383.

Vaughan CW, McGregor IS & Christie MJ. (1999). Cannabinoid receptor activation inhibits GABAergic neurotransmission in rostral ventromedial medulla neurons in vitro. *Br J Pharmacol* **127,** 935-940.

Voog O, Alstergren P, Leibur E, Kallikorm R & Kopp S. (2000). Immediate effects of the serotonin antagonist granisetron on temporomandibular joint pain in patients with systemic inflammatory disorders. *Life Sci* **68,** 591-602.

Wager-Miller J, Westenbroek R & Mackie K. (2002). Dimerization of G protein-coupled receptors: CB1 cannabinoid receptors as an example. *Chem Phys Lipids* **121,** 83-89.

Wall PD. (1980). The role of substantia gelatinosa as a gate control. *Res Publ Assoc Res Nerv Ment Dis* **58,** 205-231.

Walsh MA, Graham BA, Brichta AM & Callister RJ. (2009). Evidence for a critical period in the development of excitability and potassium currents in mouse lumbar superficial dorsal horn neurons. *J Neurophys*. **101,** 1800-1812.

Ware MA, Doyle CR, Woods R, Lynch ME & Clark AJ. (2003). Cannabis use for chronic non-cancer pain: results of a prospective survey. *Pain* **102,** 211-216.

Welch SP. (1993). Blockade of cannabinoid-induced antinociception by norbinaltorphimine, but not N,N-diallyl-tyrosine-Aib-phenylalanine-leucine, ICI 174,864 or naloxone in mice. *J Pharmacol Exp Ther* **265,** 633-640.

Welch SP, Huffman JW & Lowe J. (1998). Differential blockade of the antinociceptive effects of centrally administered cannabinoids by SR141716A. *J Pharmacol Exp Ther* **286,** 1301-1308.

Werman R, Davidoff RA & Aprison MH. (1967). Inhibition of motoneurones by iontophoresis of glycine. *Nature* **214,** 681-683.

White JH, Wise A, Main MJ, Green A, Fraser NJ, Disney GH, Barnes AA, Emson P, Foord SM & Marshall FH. (1998). Heterodimerization is required for the formation of a functional GABA(B) receptor. *Nature* **396,** 679-682.

Wilcoxon F. (1945). Individual Comparisons by Ranking Methods. *Biometrics Bulletin* **1,** 80-83.

Willins DL, Berry SA, Alsayegh L, Backstrom JR, Sanders-Bush E, Friedman L & Roth BL. (1999). Clozapine and other 5-hydroxytryptamine-2A receptor antagonists alter the subcellular distribution of 5-hydroxytryptamine-2A receptors in vitro and in vivo. *Neuroscience* **91,** 599-606.

Willis WD & Coggeshall RE. (2004a). Sensory Mechanisms of the Spinal Cord. *Kluwer Academic, New York*.

Willis WD & Coggeshall RE. (2004b). Sensory Mechanisms of the Spinal Cord. Primary Afferent Neurons and the Spinal Dorsal Horn (3rd ed.). 19-90.

Willis WD, Jr., Zhang X, Honda CN & Giesler GJ, Jr. (2001). Projections from the marginal zone and deep dorsal horn to the ventrobasal nuclei of the primate thalamus. *Pain* **92,** 267-276.

Wilson RI & Nicoll RA. (2001). Endogenous cannabinoids mediate retrograde signalling at hippocampal synapses. *Nature* **410,** 588-592.

Wisden W, Gundlach AL, Barnard EA, Seeburg PH & Hunt SP. (1991). Distribution of GABAA receptor subunit mRNAs in rat lumbar spinal cord. *Brain Res Mol Brain Res* **10,** 179-183.

Woolf PJ & Linderman JJ. (2004). An algebra of dimerization and its implications for G-protein coupled receptor signaling. *J Theor Biol* **229,** 157-168.

Wotherspoon G, Fox A, McIntyre P, Colley S, Bevan S & Winter J. (2005). Peripheral nerve injury induces cannabinoid receptor 2 protein expression in rat sensory neurons. *Neuroscience* **135,** 235-245.

Yaksh TL. (1989). Behavioral and autonomic correlates of the tactile evoked allodynia produced by spinal glycine inhibition: effects of modulatory receptor systems and excitatory amino acid antagonists. *Pain* **37,** 111-123.

Yang Z, Aubrey KR, Alroy I, Harvey RJ, Vandenberg RJ & Lynch JW. (2008). Subunit-specific modulation of glycine receptors by cannabinoids and N-arachidonyl-glycine. *Biochem Pharmacol* **76,** 1014-1023.

Zavitsanou K, Garrick T & Huang XF. (2004). Selective antagonist [3H]SR141716A binding to cannabinoid CB1 receptors is increased in the anterior cingulate cortex in schizophrenia. *Prog Neuropsychopharmacol Biol Psych* **28,** 355-360.

Zeilhofer HU. (2005). The glycinergic control of spinal pain processing. *Cell Mol Life Sci* **62,** 2027-2035.

Zeilhofer HU, Studler B, Arabadzisz D, Schweizer C, Ahmadi S, Layh B, Bosl MR & Fritschy JM. (2005). Glycinergic neurons expressing enhanced green fluorescent protein in bacterial artificial chromosome transgenic mice. *J Comp Neurol* **482,** 123-141.

Zeilhofer HU & Zeilhofer UB. (2008). Spinal dis-inhibition in inflammatory pain. *Neurosci Lett* **437,** 170-174.

Zhang J, Hoffert C, Vu HK, Groblewski T, Ahmad S & O'Donnell D. (2003). Induction of CB2 receptor expression in the rat spinal cord of neuropathic but not inflammatory chronic pain models. *Eur J Neurosci* **17,** 2750-2754.

Zuardi AW. (2006). History of cannabis as a medicine: a review. *Rev Bras Psiquiatr* **28,** 153-157.

Zygmunt PM, Petersson J, Andersson DA, Chuang H, Sorgard M, Di Marzo V, Julius D & Hogestatt ED. (1999). Vanilloid receptors on sensory nerves mediate the vasodilator action of anandamide. *Nature* **400,** 452-457.